

Diss. ETH No. 13825

**Highways Through the Soil**  
**Properties of Preferential Flow Paths and**  
**Transport of Reactive Compounds**

Dissertation, submitted to the  
SWISS FEDERAL INSTITUTE OF TECHNOLOGY ZÜRICH  
for the degree of  
DOCTOR OF NATURAL SCIENCES

presented by

MAYA BUNDT

Dipl. Geoök., University of Bayreuth (Germany)  
born January 25, 1971 in San Francisco, USA

accepted on the recommendation of

Prof. Dr. Hannes Flühler, examiner

Dr. Peter Blaser, co-examiner

Prof. Dr. Martin Kaupenjohann, co-examiner

## Table of Contents

List of Figures .....	ii
List of Tables .....	iv
Preface .....	v
Acknowledgments .....	vi
Summary .....	vii
Zusammenfassung .....	ix
<b>1 General Introduction .....</b>	<b>1</b>
<i>1.1 Preferential flow .....</i>	<i>1</i>
<i>1.2 Properties of preferential flow paths .....</i>	<i>2</i>
Persistence.....	2
Relevance for plant uptake.....	3
Soil organic matter, sorption, and microbial characteristics .....	4
<i>1.3 Wood ash application to forests.....</i>	<i>5</i>
<i>1.4 Scope of the thesis.....</i>	<i>7</i>
<i>1.5 References.....</i>	<i>8</i>
<b>2 Impact of preferential flow on radionuclide distribution in soil.....</b>	<b>11</b>
<b>3 Abundance of <sup>13</sup>C &amp; <sup>15</sup>N, and C &amp; N dynamics in flow paths and matrix of a forest soil .....</b>	<b>31</b>
<b>4 Preferential flow paths: biological "hot spots" in soils.....</b>	<b>53</b>
<b>5 Sorption characteristics of preferential flow paths and transport of reactive solutes after wood ash application.....</b>	<b>77</b>
<b>6 Forest fertilization with wood ash: impact on the distribution and storage of organic contaminants .....</b>	<b>101</b>
<b>7 Synthesis .....</b>	<b>123</b>
<i>7.1 Persistence.....</i>	<i>123</i>
<i>7.2 Soil organic matter .....</i>	<i>124</i>
<i>7.3 Physico-chemical characteristics .....</i>	<i>125</i>
<i>7.4 Sorption.....</i>	<i>125</i>
<i>7.5 Microbial characteristics.....</i>	<i>126</i>
<i>7.6 Relevance for plant uptake.....</i>	<i>126</i>
<i>7.7 Effects of wood ash application.....</i>	<i>127</i>
<i>7.8 Future research and some open questions.....</i>	<i>128</i>
Curriculum Vitae .....	129

## List of Figures

### 1 General Introduction

Figure 1.1: Processes occurring within a macropore..... 3

### 2 Impact of preferential flow on radionuclide distribution in soil

Figure 2.1: Soil profile with stained preferential flow paths. .... 18

Figure 2.2: Grass  $^{137}\text{Cs}$  activities calculated with a transfer model..... 25

### 3 Abundance of $^{13}\text{C}$ & $^{15}\text{N}$ , and C & N dynamics in flow paths and matrix of a forest soil

Figure 3.1: Experimental setup and digitized image of soil profile..... 35

Figure 3.2: The  $\delta^{13}\text{C}$  values of the needles, forest floor..... 39

Figure 3.3: Isotopic compositions ( $^{13}\text{C}$ ) vs. percent elemental mass..... 40

Figure 3.4: The  $\delta^{15}\text{N}$  values of the needles, forest floor..... 42

Figure 3.5: Isotopic compositions ( $^{15}\text{N}$ ) vs. percent elemental mass..... 43

Figure 3.6: Progression of  $\delta^{15}\text{N}$  values in soil and fine roots. .... 44

Figure 3.7: The  $\delta^{13}\text{C}$  vs.  $\delta^{15}\text{N}$  compositions of leaf litter, fine roots..... 46

### 4 Preferential flow paths: biological "hot spots" in soils

Figure 4.1: Photo of a soil profile, depth profile of  $C_{\text{mic}}$ , DNA..... 63

Figure 4.2: Mean  $C_{\text{mic}}$  concentration in preferential flow paths..... 64

Figure 4.3: Correlation between  $C_{\text{mic}}$ , DNA and cell counts. .... 65

Figure 4.4: Photos of agarose-gels with genetic fingerprints. .... 66

### 5 Sorption characteristics of preferential flow paths and transport of reactive solutes after wood ash application

Figure 5.1: Location of the study site and experimental setup. .... 81

Figure 5.2: Sorption isotherms for Cu and Sr..... 86

Figure 5.3: Effective cation exchange capacity and base saturation. .... 88

Figure 5.4: Sr concentrations in preferential flow paths and matrix. .... 89

Figure 5.5:	Exchangeable Ca concentrations.....	91
Figure 5.6:	Exchangeable Al concentrations. ....	92
Figure 5.7:	Organically bound Pb concentrations. ....	93
Figure 5.8:	Concentrations of Ca, Al, and DOC in the soil solution. ....	94

## **6 Forest fertilization with wood ash: impact on the distribution and storage of organic contaminants**

Figure 6.1:	Location and layout of the experimental site. ....	105
Figure 6.2:	PAH spectra of the Oa horizon and of the wood ash. ....	112
Figure 6.3:	Correlation between the input rates and increase of storage.....	113
Figure 6.4:	PCB spectra of the Oe horizon and of the wood ash.....	115
Figure 6.5:	Relationship between $\log K_{ow}$ and the concentration ratio. ....	118

## List of Tables

### **2 Impact of preferential flow on radionuclide distribution in soil**

Table 2.1:	Soil characteristics of the experimental site.....	14
Table 2.2:	Radionuclide inventories of the experimental site.....	17
Table 2.3:	Activities of radionuclides and root biomass.....	20

### **3 Abundance of $^{13}\text{C}$ & $^{15}\text{N}$ , and C & N dynamics in flow paths and matrix of a forest soil**

Table 3.1:	Properties of preferential flow paths and soil matrix.....	34
------------	--	----

### **4 Preferential flow paths: biological "hot spots" in soils**

Table 4.1:	Physical and chemical properties.....	57
Table 4.2:	PCR primers and amplification conditions.....	60

### **5 Sorption characteristics of preferential flow paths and transport of reactive solutes after wood ash application**

Table 5.1:	Physical and chemical properties.....	80
Table 5.2:	Chemical properties of the used wood ash.....	82

### **6 Forest fertilization with wood ash: impact on the distribution and storage of organic contaminants**

Table 6.1:	Soil properties at the study site.....	104
Table 6.2:	Concentrations $C_{\text{org}}$ , $\Sigma 20$ PAHs, $\Sigma 14$ PCBs.....	109
Table 6.3:	Storage, input with wood ash, and increase of PAHs and PCBs.....	110
Table 6.4:	Concentrations of PAHs and PCBs in preferential flow paths.....	116

## Preface

The basic idea of my Ph.D.-thesis is that soils must not be considered as a homogeneous continuum. Different processes affect different regions of the soil, leading to heterogeneities. One of the key factors is the water flow through the soil, because it is the transport vehicle for dissolved elements, complexes, particles, and even microorganisms. Flow heterogeneities in the unsaturated zone such as preferential flow influence solute resident times and the bioavailability of solutes.

The studies presented here were conducted within the HARWA-project. This acronym means in German HolzAsche Recycling im WALd and translates to wood ash recycling in forests. The project was initiated at the Swiss Federal Institute for Forest, Snow, and Landscape Research (WSL) in 1997. The background is the action plan "Energy 2000" that was passed by the Swiss parliament in 1991, saying that the energy produced by combustion of wood should be doubled by the year 2000. The use of the renewable energy source shall help to reduce the CO<sub>2</sub>-load of the atmosphere.

The combustion of wood to produce energy leads to relatively large quantities of wood ash. Up to the present day, the ash must be disposed of in waste disposal sites, although it generally has a high nutrient value. In the proper sense of recycling, it would be sensible to bring the wood ash back to the forests. However, in Switzerland it is not allowed to apply any kind of fertilizer, calcareous materials or other additives to forests. In order to acquire the necessary information for a possible change of the law, the Swiss Federal Agency for the Environment, Forests, and Landscape (BUWAL) commissioned the investigation of environmental risks and benefits of wood ash application in forests to the WSL. Several research groups participated in this project, the soil ecology group of WSL being one of them.

In risk assessment studies of a forest ecosystem, the soil plays an important role, because it acts as receiver, storage, and transport compartment to a variable extend.

The effect of wood ash to the forest soil has already been investigated in various countries. I took a closer look at the fundamentally different regions in the soil that would receive different fractions of the elements imported with the wood ash. Thus, I studied the preferential flow paths in the soil.

## Acknowledgments

Many people contributed directly or indirectly to this thesis.

Thank you, Peter Blaser, for giving me the opportunity to work in your group at the WSL and for always supporting me in every possible way. You trusted me to go into the right direction. Thank you, Hannes Flühler, for integrating me as an “external” into your soil physics group at the ITO and for providing me with an additional office space, unlimited use of the resources of the ITO, ideas, contacts and a positive image of a teacher/professor. Thank you, Martin Kaupenjohann, for readily taking over the job as a co-examiner. Thank you, Frank Hagedorn, for patiently listening to talk about preferential flow paths for more than three years and for still being open for discussions. Thank you also for all the support you gave me. I thank all the people, who appear as co-authors on the papers included in this dissertation thesis, and who worked together with me on the different parts of my project: Achim Albrecht, Peter Blaser, Frank Hagedorn, Hannes Flühler, Pascal Froidevaux, Maya Jaeggi, Martin Krauss, Manuel Pesaro, Franco Widmer, Wolfgang Wilcke, Josef Zeyer, and Stefan Zimmermann. This teamwork made my thesis to something very special. I could not have conducted the labor intensive field experiments without the help of Jörg Leuenberger, whom I want to thank for his dedication, helpfulness and reliability. Also, I thank all the people, who came out to the forest in Unterehrendingen to help during one or more of my sampling campings, or who helped in the laboratory: Meinrad Abegg, Philipp Aeby, Achim Albrecht, Michael Burkhardt, Dani Christen, Christof Düggelein, Amy Fischer, Paul Gähwiller, Jeannette Hollinger, Roger Köchli, Sigrid Kretzschmar, Sabina Pfister, Sabine Meier, Mark Thür, and Hannes Wydler. Many thanks to all of you! I also thank the soil ecology group at the WSL and the soil physics group at ITÖ for always being open to questions, Dani Christen and Beat Peter for being helpful in the laboratory and Stefan and Ute Zimmermann for patiently sharing the offices with me. The central lab of the WSL analyzed many 1000 samples for me, and I want to thank the lab-crew for that. Last but not least I want to acknowledge the people being responsible for the HARWA-project and the Swiss Federal Agency for the Environment, Forests, and Landscape (BUWAL) for financing me during the three years of my thesis.

## Summary

Although heterogeneous water flow and solute transport is a widespread phenomenon, little is known about the chemical and biological properties of the preferential flow paths. This thesis aimed at characterizing preferential flow paths in a forest soil and at assessing the effects of a massive disturbance: an experimental wood ash application of  $8 \text{ Mg ha}^{-1}$  onto the soil surface in a forest in Unterehrendingen, Switzerland, in May 1998. Wood ash application to forests is tested as a soil amendment to replace elements exported with tree harvest and as a cheap option for disposal. We conducted dye tracer experiments to stain the preferential flow paths in the soil and sampled soil material from preferential flow paths and from the soil matrix.

The activities of the atmospherically deposited radionuclides  $^{137}\text{Cs}$ ,  $^{210}\text{Pb}$ ,  $^{239,240}\text{Pu}$ ,  $^{238}\text{Pu}$ , and  $^{241}\text{Am}$  were higher in the preferential flow paths than in the matrix by factors of up to 3.5. Despite their different deposition histories, the enrichment in preferential flow paths was similar for all radionuclides. This indicates a temporal stability of preferential flow paths for more than 40 years. Furthermore, the enrichment of radionuclides in the preferential flow paths might influence the uptake by plants, because root biomass was also higher in the preferential flow paths. Taking both, radionuclide and root distribution between the two flow regions into account provides a more physical and biological basis for the calculation of plant activities with soil-to-plant transfer models than using the homogeneously mixed bulk soil activities as input parameters.

Preferential flow paths had higher concentrations of soil organic C (SOC) and total N (15 to 75%) and were significantly depleted in  $^{13}\text{C}$  and  $^{15}\text{N}$  relative to the soil matrix. This suggests that SOC is 'younger' in the preferential flow paths. Adding a highly enriched  $^{15}\text{N}$ -tracer homogeneously onto the soil surface showed a higher recovery of  $^{15}\text{N}$  in soil samples and in the fine roots from preferential flow paths than in those from the soil matrix, indicating that N cycling is more rapid in the preferential flow paths.

Distinct differences in physico-chemical properties existed between preferential flow paths and matrix. In preferential flow paths, the effective cation exchange capacity and the base saturation were higher, while the pH was similar in the two flow regions. Also, the sorption capacity for Cu was increased as compared to the matrix, whereas the



sorption capacity for Sr was similar in both flow regions. This points to enhanced sorption of organically bound heavy metals, which potentially counterbalances the enhanced transport of heavy metals by preferential flow.

Microbial biomass was 10 to 90% higher in the preferential flow paths than in the soil matrix, probably due to the better nutrient and substrate supply. Domain-specific genetic fingerprints did not reflect the differences between preferential flow paths and soil matrix, while the single genera *Pseudomonas* did. This indicates that possibly only few populations with a broad acceptance for substrates and aerobic as well as anaerobic growth specifically profit from the favorable conditions in the preferential flow paths.

The impact of the application of 8 Mg wood ash ha<sup>-1</sup> on soil chemical properties was mainly restricted to the uppermost 20 cm of the soil and was negligible in the matrix. Concentrations of exchangeable Ca in the preferential flow paths increased nearly ten-fold during the six months following the wood-ash application, those of organically bound Pb by 50%. The opposite effect was found for exchangeable Al. The results show that in our study only part of the whole soil volume, approximately 50% of 0 to 20 cm depth, participated in transporting and sorbing the elements applied with the wood ash or as tracers.

In the forest soil, the concentrations of 20 polycyclic aromatic hydrocarbons (PAHs) in the organic layer were in the range of moderately polluted soils (sum of 20 PAHs: 0.8 to 1.6 mg kg<sup>-1</sup>), but sum concentrations of 14 polychlorinated biphenyls (PCBs) were high (21 to 48 µg kg<sup>-1</sup>) as compared to other forest soils in Central Europe. In the mineral soil, the preferential flow paths of the A-horizon were enriched with PAHs and PCBs, in particular with higher molecular compounds. The wood ash application increased the PAH concentrations in the organic layer up to a factor of 6 in the Oa horizon. In contrast, PCB concentrations decreased by a third in the Oe-horizon. The decrease was probably caused by re-mobilization of already stored PCBs due to the pH effect of the wood ash.

In conclusion, characteristics of preferential flow paths and rates of soil processes occurring within the preferential flow paths are very different from those of the matrix. This must be considered in models as well as when assessing the impacts of fertilizers or wood ash applications.

## Zusammenfassung

Bis heute ist noch wenig über die chemischen und biologischen Eigenschaften von sogenannten „präferentiellen Fliesswegen“ bekannt, obwohl bevorzugter Wasserfluss in den meisten Böden vorkommt. Das Ziel dieser Dissertation war es, die präferentiellen Fliesswege genauer zu charakterisieren und die Auswirkungen einer massiven Störung durch Holzascheausbringung abzuschätzen. Im Mai 1998 wurden in einem Wald im Schweizer Mittelland 8 Mg Holzasche ha<sup>-1</sup> ausgebracht. Infiltrationsexperimente wurden durchgeführt, bei denen die präferentiellen Fliesswege im Boden mit einem Lebensmittelfarbstoff angefärbt wurden. Auf diese Weise konnte Bodenmaterial von den Fliesswegen und von der Bodenmatrix beprobt werden.

In den präferentiellen Fliesswegen war die Aktivität der atmosphärisch eingetragenen Radionuklide <sup>137</sup>Cs, <sup>210</sup>Pb, <sup>239,240</sup>Pu, <sup>238</sup>Pu und <sup>241</sup>Am bis zu einem Faktor von 3,5 erhöht. Obwohl sich ihre Depositionsgeschichte stark voneinander unterscheidet, war die Verteilung der unterschiedlichen Radionuklide zwischen Fliesswegen und Matrix ähnlich. Dieses Ergebnis deutet auf eine zeitliche Persistenz der Fliesswege von mindestens 40 Jahren hin. Die Anreicherung der Radionuklide in den Fliesswegen kann die Pflanzenaufnahme dieser Elemente beeinflussen, da auch die Wurzelbiomasse in den Fliesswegen erhöht war. Berücksichtigt man beide Phänomene, lassen sich Transfermodelle auf eine wissenschaftlich besser fundierte Basis stellen.

Die Fliesswege hatten gegenüber der Matrix erhöhte Konzentrationen an organischem Kohlenstoff und totalem Stickstoff (15 bis 75%). Ausserdem waren sie relativ zur Matrix an <sup>13</sup>C und <sup>15</sup>N angereichert. In den Bodenproben und in den Wurzeln aus den präferentiellen Fliesswegen wurde ein höherer Anteil des gleichmässig auf die Bodenoberfläche aufgetragenen <sup>15</sup>N Tracers wiedergefunden. Diese Befunde deuten darauf hin, dass die organische Substanz in den Fliesswegen „jünger“ ist als in der Matrix (bzw. mehr „frische“ organische Substanz hinzukommt) und dass Stickstoff in den Fliesswegen schneller umgesetzt oder ausgewaschen wird.

Zwischen den Fliesswegen und der Matrix bestanden deutliche physico-chemische Unterschiede, z.B. waren sowohl die effektive Kationenaustauschkapazität als auch die effektive Basensättigung in den Fliesswegen signifikant erhöht. Der pH-Wert wies allerdings keinen Unterschied zwischen den Fliessregionen auf, was wahrscheinlich auf die relative Insensitivität dieses Parameters zurückzuführen ist. Die Sorptionskapazität der Fliesswege war für Cu gegenüber der Matrix erhöht, nicht jedoch für Sr. Das deutet auf eine erhöhte Sorption organisch gebundener Schwermetalle in den Fliesswegen hin

und könnte den präferentiellen Transport von Schwermetallen in den Fliesswegen ausgleichen.

Die mikrobielle Biomasse war in den Fliesswegen zwischen 10 und 90% höher als in der Matrix. Dies ist wahrscheinlich auf ihre bessere Nährstoffversorgung zurückzuführen. Mit genetischen Fingerabdrücken konnten jedoch keine Unterschiede auf Stammesebene zwischen den mikrobiellen Populationen in den Fliesswegen und in der Matrix festgestellt werden. Nur die bakterielle Gattung *Pseudomonas* sp zeigte deutliche Unterschiede in der Zusammensetzung ihrer Lebensgemeinschaft zwischen Fliesswegen und Matrix. Wahrscheinlich können sich nur wenige Gattungen mit einer sehr breiten ökologischen Nische spezifisch anpassen und von den guten Lebensbedingungen in den Fliesswegen profitieren.

Die Holzascheausbringung beeinflusste in erster Linie die Fliesswege in den oberen 20 cm des Bodens, während die Matrix relativ unbeeinflusst blieb. Die Konzentrationen austauschbaren Kalziums stiegen in den Fliesswegen um das zehnfache, die Konzentrationen organisch gebundenen Bleis um 50%. Der umgekehrte Effekt wurde für Al beobachtet. In unserer Studie standen nur etwa die Hälfte des Bodens in den oberen 20 cm für den Stofftransport und die Pufferung oder Sorption zur Verfügung.

In der organischen Auflage entsprachen die Konzentrationen an polycyclischen aromatischen Kohlenwasserstoffen (PAKs) denen von mässig belasteten Standorten ( $\Sigma 20$  PAK: 0.8 bis 1.6 mg kg<sup>-1</sup>), während die Konzentrationen an polychlorierten Biphenylen (PCBs) im Vergleich zu anderen mitteleuropäischen Waldböden hoch waren ( $\Sigma 14$  PCB: 21 bis 48 µg kg<sup>-1</sup>). Die präferentiellen Fliesswege wiesen höhere Gehalte an organischen Schadstoffen auf als die Matrix. Nach der Holzascheausbringung erhöhten sich die PAK Konzentrationen in einzelnen Horizonten der organischen Auflage um bis zu einen Faktor von 6, während die PCB Konzentrationen um ein Drittel abnahmen. Diese Abnahme kann wahrscheinlich auf einen Mobilisierungseffekt durch die Erhöhung des pH-Wertes und durch verstärkte Mineralisierung nach der Aschedüngung zurückgeführt werden.

Die präferentiellen Fliesswege und die Bodenmatrix haben sehr unterschiedliche Eigenschaften und Prozessraten. Dies muss sowohl in der Stofftransportmodellierung als auch bei der Abschätzung der maximalen Ausbringungsmengen von Dünger, Kalk oder Holzasche beachtet werden.

# CHAPTER 1

## General Introduction

### 1.1 Preferential flow

The expression “preferential flow” is used for the rapid movement of water and solutes through the soil that bypasses a large portion of the soil matrix. There are several mechanisms causing preferential flow:

-Fast flow through macropores such as earthworm burrows, root channels, and other biopores or through cracks and fissures, generally termed macropore flow (Beven and Germann, 1982; Booltink and Bouma, 1991; Logsdon, 1995; Jacobsen et al., 1997).

-Fingered flow through macroscopically homogeneous soil due to wetting front instabilities initiated by differences in water content, trapped air, water repellency of the solid surfaces, textural boundaries or imposed by inhomogeneous infiltration at the surface (Glass et al., 1989; Selker et al., 1992; Stagnitti et al., 1995; Dekker and Ritsema, 1996).

Preferential flow of water was neglected for a long time, because it was difficult to detect and even more difficult to model. However, in the last 15 to 20 years, efforts have been made to account for this widespread phenomenon. One possibility to investigate preferential flow in soils is to conduct break through experiments at different scales: at the laboratory scale with soil columns, at the larger scale with lysimeters or at the field scale with drainage systems.

However, these experiments led more or less to black-box models, linking a given input function with a measured output. Knowledge about the processes within the soil body itself was rather incomplete. Early in the 1970's and to a larger extend since the 1990's, scientist tried to understand the phenomenon better by visualizing the flow pathways of the water in the soil. Experiments were conducted with different dye tracers that infiltrated with the water during simulated rain events and stained the flow paths (Ehlers, 1975; Corey, 1968; Ghodrati and Jury, 1990; Flury and Flühler, 1994). These

experiments were valuable for understanding the characteristics of preferential flow and generally acknowledging the heterogeneity of water flow in soils. After a series of systematic infiltration studies in arable soils, Flury and Flühler (1994) stated that preferential flow was the rule rather than the exception.

The nature of preferential flow is the fast transport of water, solutes, and particles. The short residence time is important, because it limits the ability of soils to filter strongly sorbing solutes or particles. Surface applied herbicides or fertilizers, heavy metals, radionuclides, or microorganisms may be transported faster and to greater depths than predicted, leading to the risk of groundwater contamination (Jørgensen and Fredericia, 1992; Flury, 1996; Natsch et al., 1996; Jacobsen, et al., 1997).

## 1.2 Properties of preferential flow paths

### *Persistence*

Little is known about the temporal and spatial persistence of preferential flow paths. Beven and German (1982) suggested that root-derived macropores may last for 50 to 100 years. Glass et al. (1989) showed the persistence of preferential flow fingers and Buchter et al. (1995) found invariant flow paths during consecutive breakthrough experiments with large soil columns. However, other studies with large undisturbed soil monoliths reported a meandering of active preferential flow paths with time (de Rooij, 1996). Solute transport and also the prediction of solute movement with transport models is to a great extent dependent on the spatial and temporal occurrence of preferential flow and thus the persistence of preferential flow paths.

If we assume some of these preferential flow paths are reasonably stable in space and time, the rapidly moving water and the simultaneously transported solutes, acids and particles must alter the chemical properties of the preferential flow paths as compared to the soil matrix (Figure 1.1). Thus, the occurrence of gradients between preferential flow paths and the rest of the soil matrix is based on the long-term stability of the preferential flow paths and on an overall higher flow volume through the preferential flow path as compared to the surrounding matrix. The question of the persistence of preferential flow paths is addressed in chapter 2 and 3.

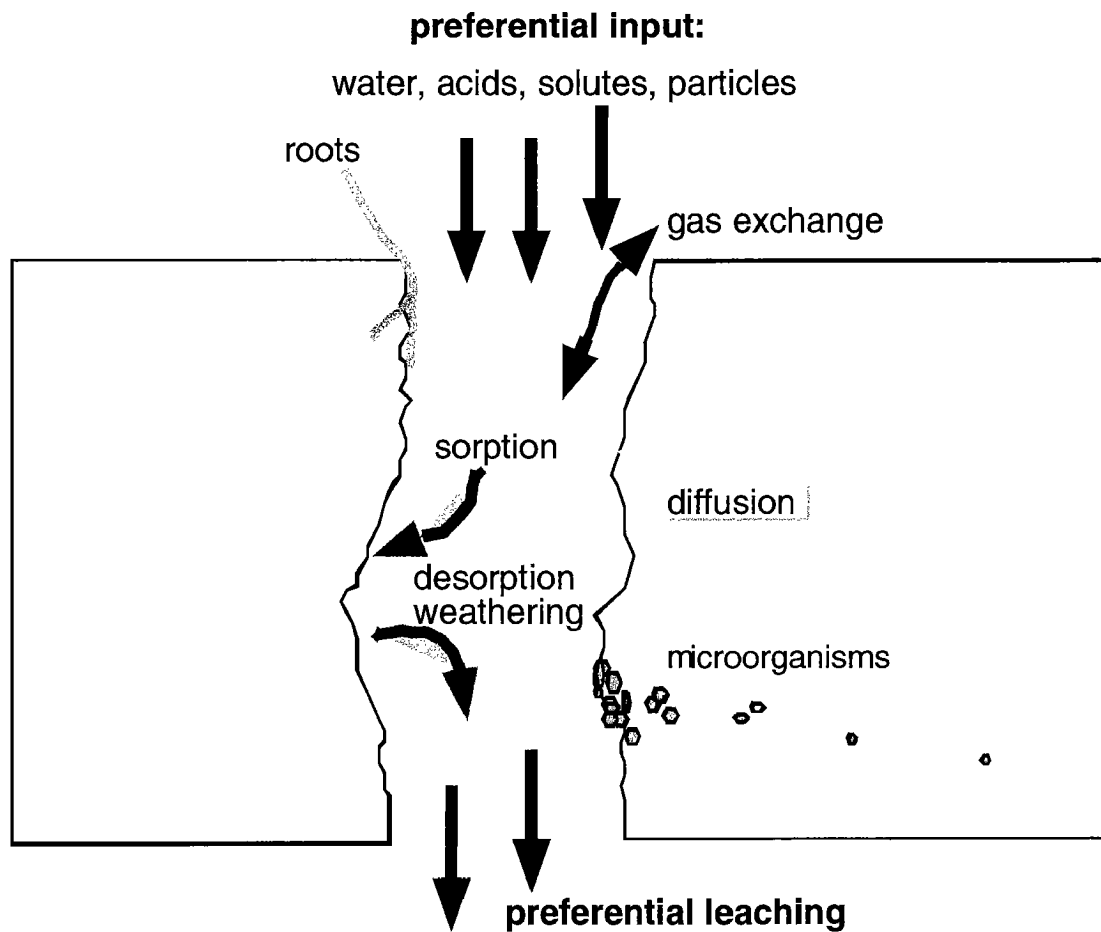


**Figure 1.1:** Processes occurring within a macropore as one realization of a preferential flow path.

### ***Relevance for plant uptake***

The other important process in risk assessment besides nutrient and pollutant leaching to the groundwater is the uptake of potentially harmful substances by plants. Plant uptake is a function of the capability of plants to assimilate the considered compound and of its chemical and physical availability. The physical availability is a critical factor and includes the distribution of the compound in question within the soil and the root distribution. In this regard, I examine not only the vertical distributions of elements and roots, but also their distribution transversal to the main flow direction. In chapter 2, we

describe the distribution of atmospherically deposited radionuclides in the soil. We compare a widely used plant-transfer model with a new approach that includes heterogeneous radionuclide and root distribution.

### *Soil organic matter, sorption, and microbial characteristics*

Several studies have found significant concentrations of pesticides in groundwater in much larger amounts and at earlier times than models predict (Czapar et al., 1992; Elliot et al., 1998). However, other studies observed that (i) the sorption capacity of macropores is higher than the sorption capacity of the matrix, and that (ii) pesticide concentrations in the macropores decrease rapidly due to biodegradation (Stehouwer et al., 1994; Pivetz and Steenhuis, 1995; Mallawatantri et al., 1996).

(i) Sorption of compounds to the solid phase is crucial factor in assessing transport distances and leaching rates. Soil organic matter (SOM) is one of the most important sorbents for heavy metals and organic compounds. Potentially higher SOM concentrations in preferential flow paths may lead to increased sorption and may therefore counterbalance the preferred transport of pollutants. In chapter 3, we investigated the natural  $^{13}\text{C}$  and  $^{15}\text{N}$  abundance as well as SOM concentrations in preferential flow paths and in the soil matrix and the fate of  $^{15}\text{N}$ -double labeled  $\text{NH}_4\text{NO}_3$  in both soil compartments. The aim of this study was to test the hypothesis whether SOM concentrations and the isotopic signatures of preferential flow paths differ from those of the rest of the soil, which would indicate different SOC turnover rates and/ or different inputs into these flow regions.

Other important sorbents like clay minerals or Fe and Mn oxides might also be heterogeneously distributed between the flow regions. Since sorption is such an important parameter in describing reactive transport, chapter 5 deals with sorption characteristics of preferential flow paths and soil matrix.

(ii) Many biological processes are affected by the content and properties of SOM. The rate of biodegradation depends on spatially varying parameters like substrate concentration, availability of nutrients, microbial population and community structure. Therefore, biodegradation cannot be considered uniform with individual soil depths and

macropores, or more generally preferential flow paths, may be important for this process.

In a study with micro suction cups, Hagedorn et al. (1999) identified the position of suction cups relative to preferential flow paths with the dye tracer technique. They found a higher nitrogen turnover in the soil solution from preferential flow paths as compared to the soil solution from the matrix and attributed this to a higher biological activity in these flow regions. Analysis of an agricultural soil and a forest soil indicated that microbial biomass and bacterial numbers were higher in samples immediately adjacent to macropores than from matrix samples (Vinther et al., 1999). However, to my knowledge, nothing is known so far about the microbial community structures in preferential flow paths. In chapter 4 we tested the hypothesis whether preferential flow paths have higher microbial biomass and different community structure than the rest of the soil.

### **1.3 Wood ash application to forests**

Wood ash has been used as soil amendments for centuries. These days, the primary motivation has shifted from using wood ash as a fertilizer in agricultural soils towards the low-priced disposal of wood ash in times of rapidly rising landfill costs. Secondly, recycling of nutrients is a fundamental principle in a sustainable land management that has provided incentives to replace nutrients removed from forest soils by tree harvest and other silvicultural practices. However, the use of wood ash in forests is only suitable if benefits outweigh risks that are coupled to the wood ash application (Noger et al., 1996; Zollner et al., 1997).

Wood ash application to forest soils has been studied widely in many different countries (Vance, 1996). The effects of the application to a forest soil mostly depend on the amount of wood ash used and on the properties of the soil. Generally, an increase in pH and a better supply with neutral cations such as Ca, K, and Mg are the desired effects of the wood ash application to a forest soil (Lerner and Utzinger, 1986; Ohno and Erich, 1990; Kahl et al., 1993; Bramyard and Fransman, 1995). An unwanted effect is the additional loading of the forest soil with heavy metals (Zhan et al., 1996). The high pH and strong reactivity of the wood ash are the reasons for most “side-effect” processes



occurring after wood ash application and are similar to those processes occurring after liming. They reach from a mineralization flush, to an increase of dissolved organic carbon (DOC) concentrations in the soil solution, and to increased nitrate leaching (Raison and McGarity, 1980; Matzner, 1985; Kahl et al., 1996).

In almost all studies, bulk soil samples or soil solution samples are taken to determine the effect of wood ash on soil chemical properties, thus averaging the specific properties over an often unknown volume and disregarding their heterogeneous distribution in the soil. However, heterogeneities might be important if only a small portion of the whole soil volume actually buffers the element load. In chapter 5, we describe the transport of elements after the wood ash application and the distribution of these elements between preferential flow paths and soil matrix.

Little is known about the concentrations of organic contaminants such as polycyclic aromatic hydrocarbons (PAHs) and polychlorinated biphenyls (PCBs) in wood ash and their fate after wood ash application to the soil. Polycyclic aromatic hydrocarbons are among the most intensively studied organic contaminants, because of the carcinogenic and mutagenic nature of some of their members (Baek et al., 1991). They are mainly produced during combustion processes, but to a lesser extent also through organic geochemical reactions or biological processes (Sims and Overcash, 1983; Wilcke et al., 2000). Polychlorinated biphenyls consist of 209 individual congeners of different toxicity. They were industrially produced for their chemical and physical properties like temperature stability, inertness, and low electrical conductivity, and were released to the environment through improper handling. However, combustion processes also lead to the formation of PCBs (Fiedler, 1993). Both groups of contaminants are ubiquitous and are persistent in different ecosystems (Buchert et al., 1982; Sims and Overcash, 1983; Fiedler, 1993). Soils are the most important storage media for PAHs and PCBs (Harrad et al., 1994; Wild and Jones, 1995). A risk analysis of wood ash application in respect to organic contaminants must not only include the loading of the ash with PAHs or PCBs, but also subsequent translocation. In chapter 6, the distribution of organic contaminants in relation to preferential flow paths is investigated and the effects of an experimental application of wood ash to the concentrations of PAHs and PCBs in a forest soil are described.

#### 1.4 Scope of the thesis

The aim of this dissertation thesis was to investigate the biogeochemical aspects of preferential flow and to study the effects of an experimental application of wood ash to a forest soil. The study site was situated in a forest stand in Unterehrendingen, Central Switzerland. We added 8 Mg wood ash ha<sup>-1</sup> to four experimental plots within the forest in May 1998 and collected samples at three different sampling campaigns within one year. We conducted dye tracer experiments to stain the preferential flow paths in the soil. Thus, we were able to sample soil material from the stained “preferential flow paths” and from the unstained “matrix”. These samples were used for biological, physical and chemical analyses.

Data about radionuclides, being deposited during global fall-out, was used to make inferences about the age and persistence of preferential flow paths and to assess their importance for plant uptake (chapter 2). Stable isotope analysis (<sup>13</sup>C and <sup>15</sup>N) in combination with SOM measurements were performed to gain information about the soil organic matter in the preferential flow paths, since SOM is one of the prime sorption sites for heavy metals and organic molecules (chapter 3). In chapter 4, microbial biomass and community structure are investigated in the preferential flow paths and in the soil matrix. The effect of the experimental wood ash application on the distribution of nutrients and heavy metals in preferential flow paths as compared to the soil matrix was studied in chapter 5, and chapter 6 deals with the distribution of organic contaminants (PAHs and PCBs) after the wood ash application.

### 1.5 References

- Baek, S.O., R.A. Field, M.E. Goldstone, P.W. Kirk, J.N. Lester, and R. Perry. 1991. A review of atmospheric polycyclic aromatic hydrocarbons: Sources, fate and behaviour. *Water Air Soil Pollut.* 60: 279-300.
- Beven, K., and P. Germann. 1982. Macropores and water flow in soils. *Water Resour. Res.* 18: 1311-1325.
- Booltink, H.W.G., and J. Bouma. 1991. Physical and morphological characterization of bypass flow in a well-structured clay soil. *Soil Sci. Soc. Am. J.* 55: 1249-1254.
- Bramyard, T., and B. Fransman. 1995. Sylvicultural use of wood ashes- Effects on the nutrient and heavy metal balance in a pine (*Pinus sylvestris* L.) forest soil. *Water Air Soil Pollut.* 85: 1039-1044.
- Buchert, H., S. Bihler, and K. Ballschmiter. 1982. *Fresenius Z. Anal. Chem.* 313: 1-20.
- Buchter, B., C. Hinz, M. Flury, and H. Flüher. 1995. Heterogeneous flow and solute transport in an unsaturated stony soil monolith. *Soil Sci. Soc. Am. J.* 59: 14-21.
- Corey, J.C. 1968. Evaluation of dyes for tracing water movement in acid soils. *Soil Sci.* 106: 182-187.
- Czapar, C.F., R. Horton, and R.S. Fawcett. 1992. Herbicide and tracer movement in soil columns containing an artificial macropore. *J. Environ. Qual.* 21: 110-115.
- de Rooij, G.H. 1996. Preferential flow in water-repellent sandy soils. Model development and lysimeter experiments. Ph.D-thesis. pp: 229. Agricultural University Wageningen, Wageningen.
- Dekker, L.W., and C.J. Ritsema. 1996. Preferential flow paths in a water repellent clay soil with grass cover. *Water Resour. Res.* 32: 1239-1249.
- Ehlers, W. 1975. Observations on earthworm channels and infiltration on tilled and untilles Loess soil. *Soil Sci.* 119: 242-249.
- Elliot, J.A., A.J. Cessna, K.B. Best, W. Nicholaichuk, and L.C. Tollefson. 1998. Leaching and preferential flow of Clopyralid under irrigation: field observations and simulating modeling. *J. Environ. Qual.* 27: 124-131.
- Fiedler, H. 1993. PCDD/PCDF und PCB: Quellen, Vorkommen in der Umwelt. p. 7-38. *In* Hutzinger, O., and H. Fiedler (eds.) *Organohalogen compounds 16. Proceedings of the conference: Dioxine, PCB, AOX im Klärschlamm: Gesetzliche Grundlagen, Umsetzung, Analytik und Verwertung.* Nürnberg, Germany, Nov. 1993.
- Flury, M. 1996. Experimental evidence of transport of pesticides through field soils- a review. *J. Environ. Qual.* 25: 25-45.

- Flury, M., and H. Flühler. 1994. Susceptibility of soils to preferential flow of water: A field study. *Water Resour. Res.* 30: 1945-1954.
- Ghodrati, M., and W.A. Jury. 1990. A field study using dyes to characterize preferential flow of water. *Soil Sci. Soc. Am. J.* 54: 1558-1563.
- Glass, R.J., T.S. Steenhuis, and J.-Y. Parlange. 1989. Mechanism for finger persistence in homogeneous, unsaturated, porous media: Theory and verification. *Soil Sci.* 148: 60-70.
- Hagedorn, F., J. Mohn, P. Schleppei, and H. Flühler. 1999. The role of rapid flow paths for nitrogen transformation in a forest soil- a field study with micro suction cups. *Soil Sci. Soc. Am. J.* 63: 1915-1923.
- Harrad, S.J., A.P. Sewart, R. Alcock, R. Boumphrey, V. Burnett, R. Duarte-Davidson, C. Halsall, G. Sanders, K. Waterhouse, S.R. Wild, and K.C. Jones. 1994. Polychlorinated biphenyls (PCBs) in the British environment: sinks, sources and temporal trends. *Environ. Pollut.* 85: 131-146.
- Jacobsen, O.H., P. Moldrup, C. Larsen, L. Konnerup, and L.W. Petersen. 1997. Particle transport in macropores of undisturbed soil columns. *J. Hydrol.* 196: 185-203.
- Jørgensen, P.R., and J. Fredericia. 1992. Migration of nutrients, pesticides and heavy metals in fractured clayey till. *Gèotechnique* 42: 67-77.
- Kahl, J.S., I.J. Fernandez, and L.E. Rustad. 1993. Chemical changes in soils and soil solutions resulting from application of wood ash to forest soils. *Maine Sludge and Residuals Utilization Foundation. Report 1.* Orono.
- Kahl, J.S., I.J. Fernandez, L.E. Rustad, and J. Peckenham. 1996. Threshold application rates of wood ash to an acidic forest soil. *J. Environ. Qual.* 25: 220-227.
- Lerner, B.R., and J.D. Utzinger. 1986. Wood ash as soil liming material. *Hort. Sci.* 21: 78-78.
- Logsdon, S.D. 1995. Flow mechanisms through continuous and buried macropores. *Soil Sci.* 160: 237-242.
- Mallawatantri, A.P., B.G. McConkey, and D.J. Mulla. 1996. Characterization of pesticide sorption and degradation in macropore linings and soil horizons of Thatuna silt loam. *J. Environ. Qual.* 25: 227-235.
- Matzner, E. 1985. Auswirkungen von Düngung und Kalkung auf den Elementumsatz und die Elementverteilung in zwei Waldökosystemen im Solling. *Allg. Forst Z.* 43: 1143-1147.
- Natsch, A., C. Keel, J. Troxler, M. Zala, N. von Albertini, and G. Dèfago. 1996. Importance of preferential flow and soil management in vertical transport of a biocontrol strain of *Pseudonomas fluorescens* in structured field soil. *Appl. Environ. Microbiol.* 62: 33-40.

- Noger, D., H. Felber, and E. Pletscher. 1996. Verwertung und Beseitigung von Holzaschen. Bundesamt für Umwelt, Wald und Landschaft. Schriftenreihe Umwelt 269. Bern.
- Ohno, T., and M.S. Erich. 1990. Effects of wood ash application on soil pH and soil test nutrient levels. *Agricult. Ecosys. Environ.* 32: 223-239.
- Pivetz, B.E., and T.S. Steenhuis. 1995. Soil matrix and macropore biodegradation of 2,4-D. *J. Environ. Qual.* 24: 564-570.
- Raison, R.J., and J.W. McGarity. 1980. Some effects of plant ash on the chemical properties of soils and aqueous suspensions. *Plant Soil* 55: 339-352.
- Selker, J.S., T.S. Steenhuis, and J.-Y. Parlange. 1992. Wetting front instability in homogeneous sandy soils under continuous infiltration. *Soil Sci. Soc. Am. J.* 56: 1346-1350.
- Sims, R.C., and M.R. Overcash. 1983. Fate of polynuclear aromatic compounds (PNAs) in soil-plant systems. *Res. Rev.* 88: 1-68.
- Stagnitti, F., J.-Y. Parlange, T.S. Steenhuis, J. Boll, B. Pivetz, and D.A. Barry. 1995. Transport of moisture and solutes in the unsaturated zone by preferential flow. *In* V. P. Singh (ed.) *Secondary Transport of moisture and solutes in the unsaturated zone by preferential flow*. Kluwer Academic Publishers. Amsterdam.
- Stehouwer, R.C., W.A. Dick, and S.J. Traina. 1994. Sorption and retention of herbicides in vertically oriented earthworm and artificial burrows. *J. Environ. Qual.* 23: 286-292.
- Vance, E.D. 1996. Land application of wood-fired and combination boiler ashes: An overview. *J. Environ. Qual.* 25: 937-944.
- Vinther, F.P., F. Eiland, A.-M. Lind, and L. Elsgaard. 1999. Microbial biomass and numbers of denitrifiers related to macropore channels in agricultural and forest soils. *Soil Biol. Biochem.* 31: 603-611.
- Wilcke, W., W. Amelung, C. Martius, V.B. Garcia, and W. Zech. 2000. Biological sources of Polycyclic Aromatic Hydrocarbons (PAHs) in the Amazonian rain forest. *J. Plant Nutr. Soil Sci.* 163: 27-30.
- Wild, S.R., and K.C. Jones. 1995. Polynuclear aromatic hydrocarbons in the United Kingdom environment: A preliminary source inventory and budget. *Environ. Pollut.* 88: 91-108.
- Zhan, G., M.S. Erich, and T. Ohno. 1996. Release of trace elements from wood ash by nitric acid. *Water Air Soil Pollut.* 88: 279-311.
- Zollner, A., N. Remler, and H.-P. Dietrich. 1997. Eigenschaften von Holzaschen und Möglichkeiten der Wiederverwertung im Wald. Bayerische Landesanstalt für Wald und Forstwirtschaft. Report 14. Freising.

## **CHAPTER 2**

# **Impact of preferential flow on radionuclide distribution in soil**

with

**ACHIM ALBRECHT, PASCAL FROIDEVAUX, PETER BLASER AND HANNES FLÜHLER**

Environmental Science and Technology 34: 3895-3899

## 2.1 Abstract

Migration of radionuclides in soils and their transfer to edible plants are usually estimated using volume-averaged bulk concentrations. However, radionuclides might not be homogeneously distributed in soils due to heterogeneous water flow and solute transport. One important cause of heterogeneous transport is preferential flow. The aim of this study was to investigate the spatial distribution of radionuclides in the soil in relation to preferential flow paths and to assess the possible consequences for their transfer from soil to plants. We identified the preferential flow paths in a forest soil by staining them with a blue dye, and we compared radionuclide activity in samples from the stained preferential flow paths with those from the unstained soil matrix. The activities of the atmospherically deposited radionuclides  $^{137}\text{Cs}$ ,  $^{210}\text{Pb}$ ,  $^{239,240}\text{Pu}$ ,  $^{238}\text{Pu}$ , and  $^{241}\text{Am}$  were enriched in the preferential flow paths by a factor of up to 3.5. Despite their different depositional histories, the distribution of the radionuclides between preferential flow paths and matrix was similar. Our findings indicate increased transport of radionuclides through the preferential flow paths, representing a possible risk of groundwater contamination. Furthermore, enrichment of radionuclides in the preferential flow paths might influence the uptake by plants. The heterogeneous radionuclide distribution in the soil and the more intense rooting in the preferential flow paths can be incorporated into soil-to-plant transfer models. Taking the correlated radionuclide and root distribution between the two flow regions into account provides a more physical and biological basis for the calculation of plant activities with transfer models than using the homogeneously mixed bulk soil activities as input parameters.

## 2.2 Introduction

Migration of elements such as radionuclides and their transfer from soil to plants are estimated with bulk soil activities, although it is known that water flow and solute transport in soils is often heterogeneous (Dörr and Münnich, 1991; Müller and Pröhl, 1993; McBride, 1998; Klos et al., 1999; Smith and Elder, 1999). Such heterogeneities, one of them being preferential flow, are the rule rather than the exception (Flury and Flühler, 1994b). Preferential flow is the rapid transport of water and solutes, bypassing a large part of the soil matrix and therefore affecting only a small portion of the whole soil volume. Short-term laboratory and field experiments showed that preferential flow plays an important role for the transport of highly sorbing solutes such as pesticides (Flury, 1996). However, to our knowledge, no long-term field experiments exist that assess the impact of preferential flow on the spatial distribution of sorbing substances. It affects the leaching process of such substances toward the groundwater as well as their accessibility by plant roots.

To analyze the long-term impact of preferential flow on the distribution of different tracers, we take advantage of the fallout of radionuclides with different depositional histories: the single-pulse deposition of  $^{137}\text{Cs}$  in 1986, the continuous deposition of  $^{210}\text{Pb}$ , and the step-input deposition of  $^{239,240}\text{Pu}$ ,  $^{238}\text{Pu}$  and  $^{241}\text{Am}$  in the 1950s and 1960s. The aim of this study was to investigate the spatial distribution of these radionuclides in a soil profile in relation to preferential flow paths and to assess the consequences for the transfer from soil to plants.



## 2.3 Experimental Methods

### 2.3.1 Study site

The study presented here was conducted on four plots of 3 m by 7 m situated on the corners of a well-characterized site of approximately 2 ha in Central Northern Switzerland from April 1998 to May 1999. The site was planted in 1930 with Norway spruce (*Picea abies* (L.) Karst.) as the dominant tree species mixed with beech (*Fagus sylvatica* L.) and some other species. The soil is an acid brown forest soil (Dystric Cambisol (FAO, 1988)). Selected chemical and physical properties are given in Table 2.1.

**Table 2.1:** Soil characteristics (mean of the four plots) of the experimental site.

Depth	pH	C <sub>org</sub>	Bulk density	CEC <sub>eff</sub> <sup>a</sup>	Texture (s/u/c) <sup>b</sup>
[cm]	(CaCl <sub>2</sub> )	[g kg <sup>-1</sup> ]	[g cm <sup>-3</sup> ]	[mmol <sub>c</sub> kg <sup>-1</sup> ]	[g kg <sup>-1</sup> ]
0-9	3.4	26.7	1.13	80.6	360/429/211
9-20	3.7	11.8	1.32	62.5	375/423/202
20-50	3.8	5.9	1.44	62.2	360/421/220
50-100	3.8	3.0	1.56	86.5	294/456/250

<sup>a</sup> Effective cation exchange capacity expressed as the sum of cations, extracted with 1 M NH<sub>4</sub>NO<sub>3</sub> and a soil-solution ratio of 1:25.

<sup>b</sup> s = sand, u = silt, c = clay.

### 2.3.3 Sampling procedure

To determine the total atmospheric deposition of radionuclides we took samples (blocks with the following dimensions: 14 cm width, 25 cm length, and 10 or 20 cm depth, see Table 2) to a depth of 0.6 m at one of the four plots.

To stain the preferential flow paths in the soil we applied 45 mm of a dye solution (deionized water containing 3 g L<sup>-1</sup> Brilliant Blue FCF (CI 42090)) in 6 h with a portable sprinkling device (Flury and Flühler, 1994a; Flury and Flühler, 1994b) at a constant rate that did not cause ponding. This corresponds approximately to a heavy thunderstorm shower. One day after dye application, we opened a trench to 1.2 m depth. A vertical soil profile of 1 m by 1 m was prepared within the irrigated plot, 30 cm away from the plots' border, and photographed. These photos (n=100) were then used to quantify the proportion of the profile area stained with Brilliant Blue. This dye coverage is a measure for the volumetric proportion of preferential flow paths. In delineated depths of 0-9, 9-20, 20-50 and 50-100 cm, samples were taken with a small spatula from the stained regions, representing preferential flow paths, and from the unstained soil matrix. On each of the four plots we sampled five profiles with a separation distance of 10 cm. To determine the root biomass, we used three small cores per depth and flow region (e.g. preferential flow path and matrix) with a volume of 9.07 cm<sup>3</sup> each. The cores were pushed carefully by hand into the soil perpendicular to the exposed face. We repeated the same experimental protocol five times (04/98, 06/98, 10/98, 04/99, 05/99).

### 2.3.4 Analyses

After the soil had been oven dried and sieved (2 mm), <sup>137</sup>Cs and <sup>210</sup>Pb were measured using  $\gamma$ -spectroscopy, and <sup>239,240</sup>Pu, <sup>238</sup>Pu and <sup>241</sup>Am, the latter being a decay product of <sup>241</sup>Pu, were measured using  $\alpha$ -spectroscopy (Horwitz et al., 1995). Since preparation prior to analysis of <sup>239,240</sup>Pu, <sup>238</sup>Pu and <sup>241</sup>Am is excessively time consuming, we only measured a limited set of samples, namely depth-wise mixed samples of the dates 10/98 and 04/99.

Statistical analyses for the  $^{137}\text{Cs}$  and  $^{210}\text{Pb}$  and root biomass data were performed with the software S+ (MathSoft, Seattle, version 5). The differences of the log-transformed activities between the preferential flow path and soil matrix samples were tested using analysis of variance. The statistical model used was a split-plot-model with the plot as the block-factor, the depth and flow region as split-unit-factors, and the time of sampling as the main-unit-factor. The data were log-transformed to approximate a normal distribution of the residuals. The residuals were checked for normality and independence using the normal-probability-plot and the Tukey-Anscombe-plot. For  $^{210}\text{Pb}$  we used a paired  $t$ -test to test the difference between preferential flow paths and matrix within individual depth zones, although we are aware that samples within one plot may be spatially dependent.

## 2.4 Results and Discussion

### 2.4.1 Radionuclide inventory

The total  $^{137}\text{Cs}$  inventory (Table 2) compared well to the sum of the  $^{137}\text{Cs}$  fall-out following the atomic bomb testing in the 1960s ( $\sim 2.7 \text{ kBq m}^{-2}$ ) and the Chernobyl accident in 1986 ( $\sim 6 \text{ kBq m}^{-2}$ , both calculated for May, 1 1986) (Albrecht, 1999). Most of the  $^{137}\text{Cs}$  (69%) can still be found in the uppermost 9 cm. The agreement between measured and published results is also satisfactory for  $^{239,240}\text{Pu}$  with a measured inventory of  $73.4 \text{ Bq m}^{-2}$  and published data of  $81 \pm 18.5 \text{ Bq m}^{-2}$ , (Hardy et al., 1973) and for  $^{241}\text{Am}$  with a measured inventory of  $27.3 \text{ Bq m}^{-2}$  compared to the published inventory of  $31 \pm 7 \text{ Bq m}^{-2}$ , (Bunzl et al., 1992).  $^{210}\text{Pb}$  is an intermediate member of the decay chain of  $^{238}\text{U}$ . Its presence in soil samples relates to the decay of U present in the soil (i.e. supported  $^{210}\text{Pb}$ , analogous to soil background) and to atmospheric deposition of  $^{210}\text{Pb}$  formed from gaseous  $^{222}\text{Rn}$  escaped to the atmosphere (unsupported  $^{210}\text{Pb}$ ). To estimate the portion of supported  $^{210}\text{Pb}$ , we subtract the mean activity of matrix soil samples from a depth below 9 cm (Table 3), assuming virtually no atmospherically derived  $^{210}\text{Pb}$  could have reached the sorbing matrix below the

surface horizon. We chose this method rather than derivation on the basis of the precursor  $^{226}\text{Ra}$  and an assumed  $^{222}\text{Rn}$  loss history. The latter can hardly be quantified as it depends on the soil water content (Appleby and Oldfield, 1992). To test the validity of this simplified procedure, we compared the measured unsupported  $^{210}\text{Pb}$  inventory (Table 2) with a modeled inventory. Knowing the atmospheric deposition rate of  $^{210}\text{Pb}$  ( $P=140 \text{ Bq m}^{-2} \text{ yr}^{-1}$ , (Schuler et al., 1991) for Zürich, located approximately 20 km SE of our site), we can model the  $^{210}\text{Pb}$  inventory (I) with the following equation:

$$I(t) = \frac{P}{\lambda} (1 - e^{-\lambda t}), \quad (1)$$

where  $\lambda$  is the decay constant of  $^{210}\text{Pb}$  ( $0.03108 \text{ a}^{-1}$ ) and  $t$  the time period of deposition and decay. The saturation level of  $4500 \text{ Bq m}^{-2}$ , reached after 100 y, compares well with the measured inventory of  $4100 \pm 200 \text{ Bq m}^{-2}$  (Table 2).

**Table 2.2:** Radionuclide inventories (one plot) of the experimental site.

Depth	$^{137}\text{Cs}$	$^{210}\text{Pb}_{\text{unsupported}}$	$^{239/240}\text{Pu}$	$^{241}\text{Am}$
	(vd [%] <sup>a</sup> )	(vd [%])	(vd [%])	(vd [%])
[cm]		-----[Bq m <sup>-2</sup> ]-----		
0-10	6251 (69)	2144 (52)	43.3 (59)	15.9 (58)
10-20	1846 (20)	436 (10)	17.4 (24)	7.5 (27)
20-40	596 (7)	829 (20)	7.1 (10)	3.1 (11)
40-60	396 (4)	717 (17)	5.6 (8)	0.8 (3)

<sup>a</sup> vd = vertical distribution as percent of the total inventory of the soil profile.

### 2.4.2 Preferential flow paths

An example of water flow heterogeneity is depicted by the dye distribution (Figure 2.1). The proportion of preferential flow paths, expressed as dye coverage, decreases with depth, being 0.69, 0.38, 0.13, and 0.02 in the four different depth zones from top to bottom.

There is a significantly higher root biomass in the preferential flow paths than in the matrix ( $p < 0.001$ ; see also Table 2.1). Roots often show a preference for growing in macroporous interstices rather than in the denser soil matrix or aggregates (Whiteley and Dexter, 1983; Hatano et al., 1987; van Noorwijk et al., 1993; Pierret et al., 1999).

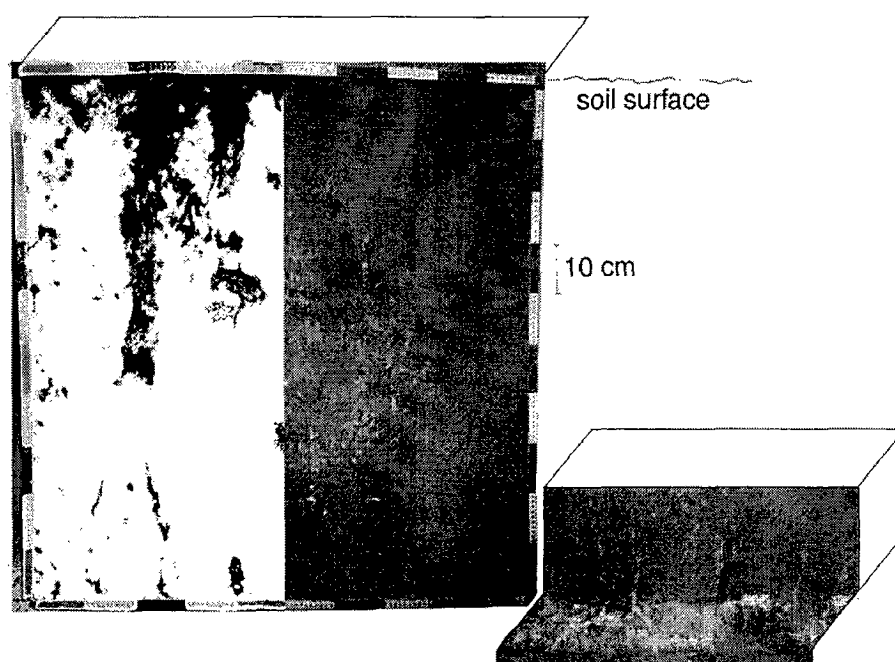


**Figure 2.1:** Soil profile with stained preferential flow paths. The image on the left shows the black and white image of stained flow paths and unstained soil matrix. The image was digitized and processed with the software Adobe Photoshop 5.0. The inset exhibits details from 90 to 100 cm depth and shows the three-dimensionality of flow paths.

### 2.4.3 Radionuclide distribution in relation to preferential flow paths

#### <sup>137</sup>Cs

The <sup>137</sup>Cs activity is significantly higher in the preferential flow paths as compared to the matrix ( $p < 0.001$ ). In 0-9, 9-20, and 20-50 cm depth the <sup>137</sup>Cs activity in the preferential flow paths exceeds that of the matrix by factors of 2.2, 2.4, and 3.5, respectively. The differences in the individual depth zones are statistically significant as well (Table 2.3). From 50-100 cm the <sup>137</sup>Cs activity is close to the detection limit in both matrix and flow-path soil with no statistically significant difference between the two flow regions.

The <sup>137</sup>Cs activities are tracing the recent flow paths and highlight the importance of preferential flow for the spatial distribution of radionuclides and the temporal stability of the observed flow paths over a period of at least 13 y. Most of the <sup>137</sup>Cs originates from the Chernobyl accident on April 28, 1986, and was deposited mainly during a single rainstorm on May 1, 1986 (Santschi et al., 1988). High rainfall intensities are known to promote preferential flow and the transport of rather immobile compounds such as pesticides (Flury, 1996).

#### <sup>210</sup>Pb

The distribution of <sup>210</sup>Pb between preferential flow paths and matrix is almost the same as in case of <sup>137</sup>Cs. The activities of <sup>210</sup>Pb are significantly higher in the preferential flow paths than in the matrix ( $p = 0.001$ ), by a factor of 1.9 in 0-9 cm, 1.3 in 9-20 cm, and 1.3 in 20-50 cm depth (Table 2.3).

**Table 2.3:** Activities of radionuclides and root biomass in stained flow paths and unstained soil matrix.

Depth [cm]	Root biomass <sup>a</sup> [g m <sup>-3</sup> ]	<sup>137</sup> Cs <sup>b</sup> [Bq kg <sup>-1</sup> ]	<sup>210</sup> Pb <sup>c</sup> [Bq kg <sup>-1</sup> ]	<sup>241</sup> Am <sup>d</sup> [Bq kg <sup>-1</sup> ]	m.e. <sup>e</sup>	<sup>239,240</sup> Pu <sup>d</sup> [Bq kg <sup>-1</sup> ]	m.e.	<sup>238</sup> Pu <sup>d</sup> [Bq kg <sup>-1</sup> ]	m.e.
0-9	1654**	82.6**	60.09**	0.33	0.03	0.78	0.04	0.032	0.003
9-20	859*	12.7**	21.22*	0.08	0.01	0.23	0.01	0.008	0.002
20-50	645**	4.4**	18.49*	0.015	0.004	0.02	0.01	<LD	
50-100	n.m. <sup>f</sup>	0.9	20.09	0.006	0.002	0.01	0.01	<LD	
0-9	1022	37.9	32.13	0.27	0.03	0.66	0.03	0.021	0.003
9-20	509	5.3	15.94	0.045	0.01	0.11	0.01	0.003	0.001
20-50	226	1.26	14.64	<LD <sup>g</sup>		<LD		<LD	
50-100	n.m.	0.85	22.32	<LD		<LD		<LD	

\*\* , \* Difference between preferential flow paths and matrix is statistically significant (p<0.01 and p<0.05, respectively).

<sup>a</sup>Fine roots (< 2 mm).

<sup>b</sup><sup>137</sup>Cs activities are decay corrected to 1 March 1998.

<sup>c</sup> Measured <sup>210</sup>Pb (supported and unsupported).

<sup>d</sup> α measurements are decay corrected to the date of measurement (February 1999).

<sup>e</sup> Measurement error.

<sup>f</sup> Not measured.

<sup>g</sup> Limit of detection.

Atmospheric <sup>210</sup>Pb is removed from the atmosphere by dry and wet deposition. This represents a steady input into the soil. Despite temporal variations of the <sup>210</sup>Pb deposition, on time scales of a year or more, the atmospheric flux remains fairly constant (Brunskill and Ludlam, 1988; von Gunten and Moser, 1993). Therefore, the <sup>210</sup>Pb input was continuous and more or less uniform whereas <sup>137</sup>Cs was introduced into the system approximately as a single pulse input. The similarity in their distributions in the soil in relation to the preferential flow paths suggests that the flow paths that were actively

conducting water during the time period of the Chernobyl fallout are largely the same ones that were “active” over the course of years.

#### *<sup>239,240</sup>Pu and <sup>241</sup>Am*

In contrast to <sup>137</sup>Cs and <sup>210</sup>Pb, the activities of <sup>239,240</sup>Pu and <sup>241</sup>Am seem to be only slightly enriched in the preferential flow paths of the topsoil (0-9 cm). In order to compare the various radionuclides, we calculated the activity differences between preferential flow paths and matrix samples and normalized them with the inventory given in Table 2.2. Doing this, the differences between preferential flow paths and the matrix of <sup>239,240</sup>Pu and <sup>241</sup>Am are only slightly smaller than those of <sup>137</sup>Cs and <sup>210</sup>Pb. In 9-20 cm depth, <sup>239,240</sup>Pu and <sup>241</sup>Am activities are markedly larger in the preferential flow paths. At even greater depths, both <sup>239,240</sup>Pu and <sup>241</sup>Am were only detected in flow-path material. The ratio <sup>239,240</sup>Pu/<sup>241</sup>Am is remarkably stable in all samples ( $2.5 \pm 0.2$ ), excluding samples with activities close to the detection limit (Table 2.3). These ratios lie in the same range as those of other samples of Swiss soils obtained in 1999 (Froidevaux, unpublished data). This implies a similar migration rate of Pu and Am.

Plutonium was emitted into the atmosphere as a consequence of atmospheric nuclear bomb tests and the SNAP-9A (Systems for Nuclear Auxiliary Power generator) satellite re-entry in the 1950s and early 1960s (Hardy, et al., 1973). It reached the ground both as dry and wet deposition in a variety of rain events, attached to leaf-litter, and as particles. The importance of the depositional history for radionuclide migration and distribution in the soil is documented by other studies (Bunzl, et al., 1992; Schimmack et al., 1994).

The elevated activities of <sup>137</sup>Cs, <sup>210</sup>Pb, <sup>239,240</sup>Pu, and <sup>241</sup>Am in preferential flow paths highlight the importance of preferential flow for the mobility of strongly sorbing substances and are an expression of the temporal stability of the preferential flow structures. Generally, all radionuclides investigated in this study are rapidly immobilized by soil particles and show a slow transport behavior in soils and sediments once they are adsorbed (Comans et al., 1991; Bunzl, et al., 1992; Schimmack, et al., 1994). Diffusion is



probably negligible. For example, Pu occurs in soils and sediments mainly in the form of tightly bound plutonium dioxide (Graf, 1994), and has a high  $K_d$  ( $> 500 \text{ mL g}^{-1}$ ) (Kersting et al., 1999) and a low diffusion coefficient ( $< 10^{-10} \text{ cm}^2 \text{ s}^{-1}$ ) (Bruesseler and Sholkovitz, 1987). By comparing nuclear weapon-derived cesium in soils between 1977 and 1992, Smith et al. found no vertical mobility during these 15 years (Smith et al., 1997).

The occurrence of radionuclides at greater depths implies an initial mobility during the first hours after deposition, when water flow and thus physical rather than chemical processes control their behavior. After the initial displacement, redistribution between phases and surface reactions become more important. We cannot rule out remobilization and translocation of radionuclides by co-transport with dissolved or colloidal ligands (Essington et al., 1976; Dörr and Münnich, 1991; Silva and Nitsche, 1995; Kersting, et al., 1999; Kretzschmar et al., 1999), but even in case of facilitated transport the main movement of radionuclides would still occur in preferential flow paths. If we assume only an initial mobility of radionuclides immediately after deposition, we can estimate the temporal stability of flow paths to be at least 40 y.

#### **2.4.4 Relevance**

Radionuclides travel more rapidly through the supposedly strongly sorbing soil toward groundwater than expected based on the chromatographic transport concept, therefore providing a risk for the groundwater. Recently, activities of  $^{137}\text{Cs}$  above the tolerance level were found in aquifers around Chernobyl (Ukraine) despite a thick soil layer that should have served as a natural filter (Shestopalov and Bohuslavsky, 2000, oral communication).

The second important pathway from the soil to the human food chain is the uptake by plants. The transfer of elements such as  $^{137}\text{Cs}$  from soil to plants is in most transfer models described by a transfer factor relating plant to soil concentrations. The transfer factor is obtained from greenhouse experiments using well mixed, unstructured soil materials (Ng,

1982). Commonly used transfer models, e.g. the radionuclide dose estimation program ECOSYS, which is the basis of the emergency management systems in Germany, Austria and Switzerland and an integral part of the European real-time dose assessment system, assumes homogeneous uptake from a defined soil volume (Müller and Pröhl, 1993). In the original equation

$$C_{\text{plant}} = C_{\text{soil}} F, \quad (2)$$

the plant concentration  $C_{\text{plant}}$  is expressed in terms of the bulk concentration in the soil and the transfer factor  $F$ . The bulk concentration  $C_{\text{soil}}$  is obtained by mixing the entire radionuclide inventory into the top 10 cm (grassland) or 25 cm (arable land) of the soil. Using the  $^{137}\text{Cs}$  deposition found at our study site and a transfer factor of 0.14 (Ng, 1982) yields a  $^{137}\text{Cs}$  activity in fresh grass of 3.5 Bq kg<sup>-1</sup> for 25cm mixing depth or 8.7 Bq kg<sup>-1</sup> for 10cm mixing depth. Equation 1 yields highly variable results depending on the mixing depth over which we assume homogenous distribution of radionuclides (Figure 2.2, right-hand side).

Knowing the radionuclide and root distribution in the soil, we can estimate the plant concentrations on a more physical and biological basis. Since root biomass is enriched in the preferential flow paths as compared to the soil matrix (Table 2.3), the elevated radionuclide activities in the preferential flow paths represent higher concentrations in the rhizosphere. The following extended equation illustrates, how preferential radionuclide distribution and inhomogeneous rooting can be incorporated into soil-to-plant transfer models:

$$C_{\text{plant}} = \sum_{i=1}^{n_h} \sum_{j=1}^2 C_j(\Delta z_i) \cdot R_j(\Delta z_i) \cdot F_j \quad (3)$$

where  $j = 1$  for preferential flow paths,  $j = 2$  for soil matrix,  $n_h$  refers to the number of soil horizons,  $\Delta z_i$  to the depths of the individual horizons,  $C$  to the radionuclide concentration,  $F$  to the transfer factor, and  $R$  to the relative root density expressed as

$$R_j(\Delta z_i) = \frac{r_j(\Delta z_i) \cdot A_j(\Delta z_i)}{\sum_{i=1}^{n_h} \sum_{j=1}^2 r_j(\Delta z_i) \cdot A_j}, \quad (4)$$

with  $r_j$  and  $A_j$  being the root density and the area of flow region  $j$ . Thus, the root density in the two flow regions (preferential flow paths and matrix) is weighed with the area of the respective flow region to account for the “actual” root distribution in the soil profile (for the distribution of the root densities between preferential flow paths and matrix within the individual soil horizons, see Figure 2.2). The radionuclide activity in plants can be calculated on the basis of eq. 3 with measured root and radionuclide concentrations in the preferential flow path and matrix compartments, the areas of the two compartments (Table 2.3, Figure 2.2) and published transfer factors (in our example they were assumed to be equal for the two compartments). With measured  $^{137}\text{Cs}$  activities of preferential flow paths and matrix and the respective root concentrations, we can estimate the contribution of the two flow regions to the calculated plant activities. By adding the contributions of both flow regions, we calculate the plant activity to be  $6.6 \text{ Bq kg}^{-1}$  (Figure 2.2, left hand side). For the calculation, we included the three depth zones from 0 to 0.5 m. However, since the root biomass is relatively small in 20-50 cm depth and  $^{137}\text{Cs}$  activities are low, the contribution of the root uptake from 20 to 50 cm depth to the total plant activity is smaller than 1%.

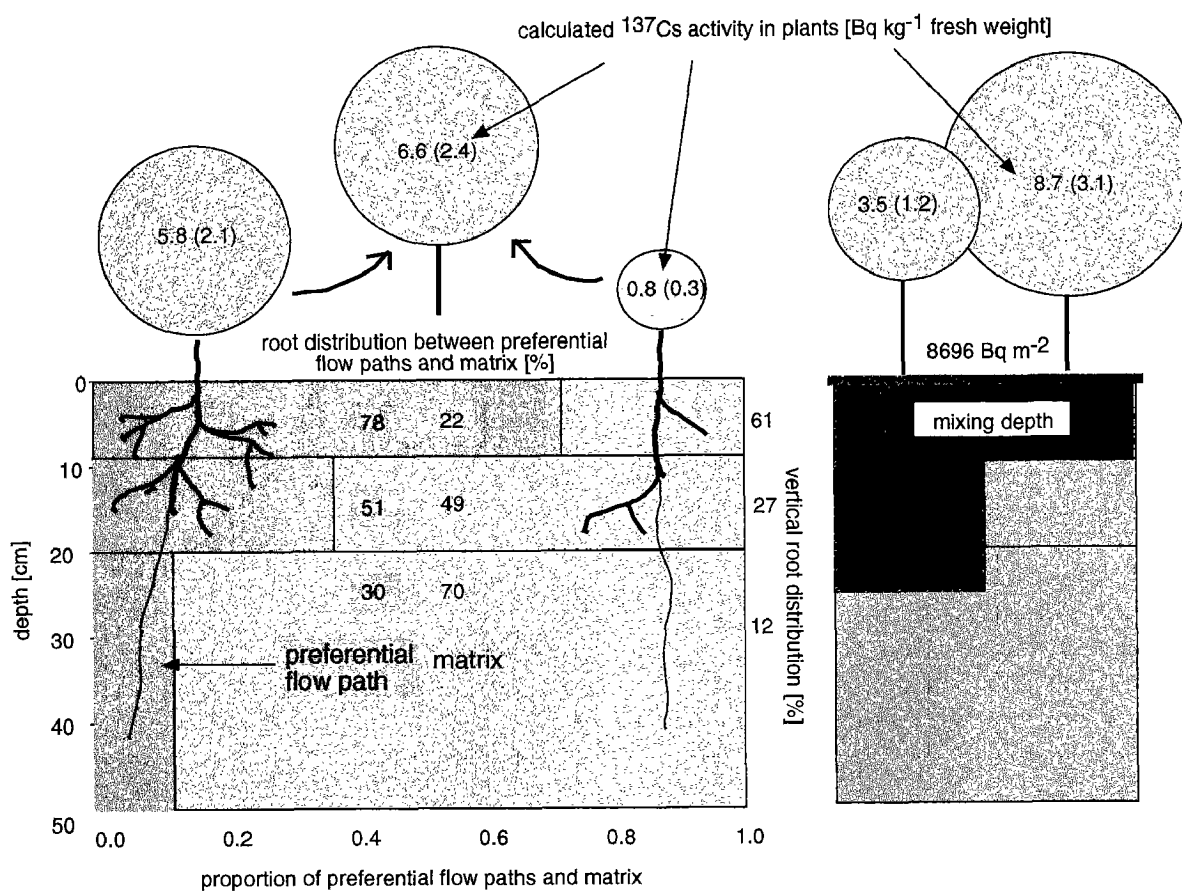


**Figure 2.2:** Grass  $^{137}\text{Cs}$  activities calculated with the commonly used transfer model ECOSYS (eq. 2, right hand side) and with our transfer model including preferential flow and inhomogeneous root distribution (eq. 3, left hand side). ECOSYS calculates the soil  $^{137}\text{Cs}$  activity by mixing the deposition of  $8696 \text{ Bq }^{137}\text{Cs m}^{-2}$  homogeneously to a soil depth of 25 cm and 10 cm, respectively, with a bulk density of  $1.4 \text{ g cm}^{-3}$ . Transfer factors for grass are taken from Ng: 0.14 (Ng, 1982) and Müller and Pröhl: 0.05 (numbers in parenthesis) (Müller and Pröhl, 1993).

This example shows that the substantially different elemental concentrations of preferential flow paths and matrix may be a critical factor for calculating plant concentrations with a transfer model. The differentiation of the flow regions is important, because the root distribution, which is a key factor for plant uptake, is biased toward higher root densities in the preferential flow paths. Taking the correlated radionuclide and root distribution between the two flow regions into account, provides a more physical and biological basis for the calculation of plant activities than mixing the entire deposition homogeneously over an arbitrarily chosen depth. This concept can also be applied to other elements such as heavy metals or nutrients.

## 2.5 References

- Albrecht, A. 1999. Radiocesium and  $^{210}\text{Pb}$  in sediments, soils and surface waters of a high alpine catchment: A mass balance approach to radionuclide migration and storage. *Aquat. Sci.* 61: 1-22.
- Appleby, P.G., and F. Oldfield. 1992. Application of  $^{210}\text{Pb}$  to sedimentation studies. *In* M. Ivanovich, and R.S. Harmon (eds.) *Secondary Application of  $^{210}\text{Pb}$  to sedimentation studies.* Oxford Clarendon Press, Oxford.
- Bruesseler, K.O., and E.R. Sholkovitz. 1987. The geochemistry of fallout plutonium in the North Atlantic: I. A pore water study in shelf, slope and deep-sea sediments. *Geochim. Cosmochim. Acta* 51: 2605-2622.
- Brunskill, G.J., and S.D. Ludlam. 1988. The variation of annual  $^{210}\text{Pb}$  flux to varved sediments of Fayetteville Green Lake, New York from 1885 to 1965. *Verh. Int. Verein. Limnol.* 23: 848-854.
- Bunzl, K., W. Kracke, and W. Schimmak. 1992. Vertical migration of Plutonium-239 + - 240, Americium-241 and Caesium-137 fallout in a forest under spruce. *Analyst* 117: 469-474.
- Comans, R.N.J., M. Haller, and P. De Preter. 1991. Sorption of cesium on illite: Non-equilibrium behaviour and reversibility. *Geochim. Cosmochim. Acta* 55: 433-440.
- Dörr, H., and K.O. Münnich. 1991. Lead and Cesium transport in European forest soils. *Water Air Soil Pollut.* 57-58: 809-818.
- Essington, E.H., E.B. Fowler, R.O. Gilbert, and L.L. Eberhardt. 1976. Plutonium, americium and uranium concentrations in Nevada test site soil profiles. *In* *Secondary Plutonium, americium and uranium concentrations in Nevada test site soil profiles.* International Atomic Energy Agency, Vienna.
- FAO. 1988. *FAO-Unesco Soil map of the world*, Rome.
- Flury, M. 1996. Experimental evidence of transport of pesticides through field soils- A review. *J. Environ. Qual.* 25: 25-45.
- Flury, M., and H. Flühler. 1994a. Brilliant Blue FCF as a dye tracer for solute transport studies- A toxicological overview. *J. Environ. Qual.* 23: 1108-1112.
- Flury, M., and H. Flühler. 1994b. Susceptibility of soils to preferential flow of water: A field study. *Water Resour. Res.* 30: 1945-1954.

- Graf, W.L. 1994. Plutonium and the Rio Grande. Environmental Change and Contamination in the Nuclear Age. Editor. Oxford University Press, New York.
- Hardy, E.P., P.W. Krey, and H.L. Volchok. 1973. Global inventory and distribution of fallout Pu. *Nature* 241: 444-445.
- Hatano, R., K. Iwanaga, H. Okajima, and T. Sakuma. 1987. Relationship between the distribution of macropores and root elongation. *Soil Sci. Plant Nutr.* 34: 535-546.
- Horwitz, E.P., M.L. Dietz, R. Chiarizia, H. Diamond, S.L. Maxwell III, and R.N. Matthew. 1995. Separation and preconcentration of actinides by extraction chromatography using supported liquid anion exchanger: application to the characterization of high-level nuclear waste solutions. *Anal. Chim. Acta* 310: 63-78.
- Kersting, A.B., D.W. Efurud, D.L. Finnegan, D.J. Rokop, D.K. Smith, and J.L. Thompson. 1999. Migration of plutonium in ground water at the Nevada Test Site. *Nature* 397: 56-59.
- Klos, R.A., I. Simón, U. Bergström, A.M. Uijt de Haag, C. Valentin-Ranc, T. Zeevaert, J.A.K. Reid, P. Santucci, J. Titley, and J. Stansby. 1999. Complementary studies: biosphere modelling for dose assessments of radioactive waste repositories. *J. Environ. Radioactivity* 42: 237-254.
- Kretzschmar, R., M. Borkovec, D. Grolimund, and M. Elimelech. 1999. Mobil subsurface colloids and their role in contaminant transport. *Adv. Agron.* 66: 121-194.
- McBride, M.B. 1998. Growing food crops on sludge-amended soils: problems with the U.S. environmental protection agency method of estimating toxic metal transfer. *Environ. Toxicol. Chem.* 17: 2274-2281.
- Müller, H., and G. Pröhl. 1993. ECOSYS-87: A dynamic model for assessing radiological consequences of nuclear accidents. *Health Phys.* 64: 232-252.
- Ng, Y.C. 1982. A review of transfer factors for assessing the dose from radionuclides in agricultural products. *Nuclear safety* 23: 57-71.
- Pierret, A., C.J. Moran, and C.E. Pankhurst. 1999. Differentiation of soil properties related to the spatial association of wheat roots and soil macropores. *Plant Soil* 211: 51-58.
- Santschi, P.H., S. Bollhalder, K. Farrenkothen, A. Lück, S. Zingg and M. Sturm. 1988. Chernobyl radionuclides in the environment: Tracers for the tight coupling of atmospheric, terrestrial, and aquatic geochemical processes. *Environ. Sci. Technol.* 22: 510-516.

- Schimmack, W., K. Bunzl, F. Dietl, and D. Klotz. 1994. Infiltration of radionuclides with low mobility ( $^{137}\text{Cs}$  and  $^{60}\text{Co}$ ) into a forest soil. Effect of irrigation intensity. *J. Environ. Radioact.* 24: 53-63.
- Schuler, C., E. Wieland, P.H. Santschi, M. Sturm, A. Lueck, S. Bollhalder, J. Beer, G. Bonani, H. Hoffmann, M. Suter, and W. Wölfli. 1991. A multitracer radionuclide study in Lake Zürich, Switzerland. 1. Comparison of atmospheric and sedimentary fluxes of  $^7\text{Be}$ ,  $^{10}\text{Be}$ ,  $^{210}\text{Pb}$ ,  $^{210}\text{Po}$ , and  $^{137}\text{Cs}$ . *J. Geophys. Res.* 96: 17051-17065.
- Silva, R.J., and H. Nitsche. 1995. Actinide environmental chemistry. *Radiochim. Acta* 70/71: 377-396.
- Smith, J.T., P.G. Appleby, J. Hilton, and N. Richardson. 1997. Inventories and fluxes of  $^{210}\text{Pb}$ ,  $^{137}\text{Cs}$ , and  $^{241}\text{Am}$  determined from soils of three small catchments in Cumbria, UK. *J. Environ. Radioactivity* 37: 127-142.
- Smith, J.T., and D.G. Elder. 1999. A comparison of models for characterizing the distribution of radionuclides with depth in soils. *Eur. J. Soil Sci.* 50: 295-307.
- van Noorwijk, M., P.C. de Ruiter, K.B. Zwart, J. Bloem, J.C. Moore, H.G. van Faassen, and S.L.G.E. Burgers. 1993. Synlocation of biological activity, roots, cracks and recent organic inputs in a sugar beet field. *Geoderma* 56: 265-276.
- von Gunten, H.R., and R.N. Moser. 1993. How reliable is the  $^{210}\text{Pb}$  dating method? Old and new results from Switzerland. *J. Paleolim.* 9: 161-178.
- Whiteley, G.M., and A.R. Dexter. 1983. Behaviour of roots in cracks between soil peds. *Plant Soil* 74: 153-162.



Seite Leer /  
Blank leaf

## **CHAPTER 3**

# **Abundance of $^{13}\text{C}$ & $^{15}\text{N}$ , and C & N dynamics in flow paths and matrix of a forest soil**

with

**MAYA JÄGGI, PETER BLASER, ROLF SIEGWOLF AND FRANK HAGEDORN**

Submitted to the Soil Science Society of America Journal

### 3.1 Abstract

We used soil organic carbon (SOC), total nitrogen,  $\delta^{13}\text{C}$  and  $\delta^{15}\text{N}$  measurements to test the hypothesis that new C and N inputs primarily affect the preferential flow paths in a forest soil in Central Switzerland. Preferential flow paths in the soil were identified with a dye tracer that was homogeneously applied to the soil surface. In the blue stained preferential flow paths, concentrations of SOC and total N were between 15 and 75% increased as compared to the soil matrix. The total increase of SOC in preferential flow paths ranged between 740 and 960 g C m<sup>-2</sup> in the four individual soil plots. Values of  $\delta^{13}\text{C}$  and  $\delta^{15}\text{N}$  were lowest in the tree leaves and in the forest floor and increased with depth and thus with the degree of decomposition of SOC. In the mineral soil, preferential flow paths were significantly depleted in <sup>13</sup>C between 0.15 and 0.4‰ relative to the soil matrix. The  $\delta^{15}\text{N}$  values increased with depth from -0.9‰ to 4.7‰ in the preferential flow paths and from 0.5‰ to 6‰ in the soil matrix. Adding a highly enriched <sup>15</sup>N-tracer homogeneously onto the soil surface showed a higher recovery of <sup>15</sup>N in soil samples and in the fine roots from preferential flow paths than in those from the soil matrix. Our results suggest that in preferential flow paths, SOC is 'younger' and N cycling is more rapid than in the soil matrix.

### 3.2 Introduction

The natural abundance of the stable isotopes <sup>13</sup>C and <sup>15</sup>N has been widely used to study C and N cycling in forest soils (Nadelhoffer and Fry, 1988; Högberg, 1997). The aim of many of these studies was to gain information about the transformation and turnover of soil organic matter (SOM) and to determine the age of soil organic matter with help of <sup>14</sup>C dating or to assess forest ecosystem health (Gebauer and Schulze, 1991). Since the heavier isotopes are fractionated during biological and chemical processes, they become enriched in the substrate compared to the product. Therefore, the  $\delta^{13}\text{C}$  and  $\delta^{15}\text{N}$  values generally increase with soil depth and degree of decomposition of SOM.

In all of these studies, bulk samples are taken to determine the natural abundance of <sup>13</sup>C and <sup>15</sup>N in soils, although sometimes, different physical or chemical fractions are studied. However, the procedure of taking depth-wise bulk soil samples averages over a certain soil volume and disregards spatial heterogeneity. Heterogeneity is considered in the vertical direction by sampling different soil depths, and in the horizontal direction on larger scales by sampling different plots or compartments of ecosystems. On the intermediate scale of centimeters to meters, however, heterogeneities exist as well. These heterogeneities are not necessarily randomly distributed but are likely associated with soil structure, which is important for microbial processes and nutrient cycling (Parkin, 1993; Hagedorn et al., 1999).

Preferential flow paths are the 'streamtubes' of fast flowing water and solutes that bypass a large portion of the soil matrix. They are also relevant for transport of dissolved organic matter to deeper soil depths (Jardine et al., 1989; Hagedorn et al., 2000). Thus, preferential flow paths may act as transport pathways of 'new' and 'young' soil organic matter into the deeper soil. Furthermore, it was shown that preferential flow paths have an increased microbial biomass as compared to the soil matrix, since locations along flow paths are more exposed to drying and wetting and have a better nutrient supply (Chapter 4). As a consequence, preferential flow paths might be locations with an enhanced turnover of soil organic matter and nutrients.

In this study, we investigated the natural <sup>13</sup>C and <sup>15</sup>N abundance in preferential flow paths and in the soil matrix and studied the fate of <sup>15</sup>N-double labeled  $\text{NH}_4\text{NO}_3$  in both soil compartments. The aim was to test the hypothesis that the isotopic signatures of

preferential flow paths differ from the rest of the soil, which would point to different SOC turnover rates and/ or to different inputs in these flow regions.

### 3.3 Materials and Methods

#### 3.3.1 Study site

The study was conducted on four plots within a 2-ha site in a spruce–beech forest in Unterehrendingen, Central Switzerland (N: 47°30'34"/E: 008°20'50"). The forest was planted in 1930 and was managed by selective thinning. The soil type is a *typic Haplumbrept* (Soil Survey Staff, 1994) and developed on upper sea molasses overlain with end-moraine at one of the four plots. The soil texture is sandy loam, and the soil is reasonably well drained. Selected physical and chemical properties are given in Table 3.1. From 1992 to 1999 the mean annual precipitation was 1120 mm.

**Table 3.1:** Physical and chemical properties of preferential flow paths and soil matrix.

Depth [cm]	Flow region	pH	Sand ----[%]----	Silt	Clay	N <sub>tot</sub> ----[g kg <sup>-1</sup> ]----	C <sub>org</sub>	C/N	Root density [mg l <sup>-1</sup> ]
0-9	flow	3.4	48	34	19	2.18**	34.5**	15.83	1654**
9-20	path	3.7	47	34	19	0.98*	14.5**	14.80	859*
20-50		3.8	44	38	18	0.65*	8.2**	12.61	645**
50-100		3.8	28	45	27	0.47*	4.9**	10.42*	n.d. <sup>a</sup>
0-9	matrix	3.4	41	38	21	1.57	24.3	15.48	1022
9-20		3.6	40	39	21	0.88	12.9	14.66	508
20-50		3.8	40	40	20	0.60	6.4	10.67	226
50-100		3.8	30	44	27	0.34	2.9	8.93	n.d.

\*,\*\* Differences between preferential flow paths and matrix are significant at  $P < 0.05$  and  $P < 0.01$ , respectively.

a: n.d. not determined

### 3.3.2 Identification of preferential flow paths and sampling

We identified preferential flow paths in the soil by applying the food dye Brilliant Blue FCF (CI. 42090) with a field sprinkler. The amount of 45 mm dye solution was homogeneously distributed onto the soil surface during 6 hours (Flury and Flühler, 1994a; Flury and Flühler, 1994b) (Figure 3.1). One day after dye application, we opened a trench of 1.2 m depth. A vertical soil profile of 1 by 1 m was prepared 0.3 m away from the plot's border within the sprinkled area. Photographs were taken that were later used to estimate the dye coverage, corresponding to the volumetric proportion of preferential flow paths. We then defined the following sampling depths: 0-9, 9-20, 20-50 and 50-100 cm.

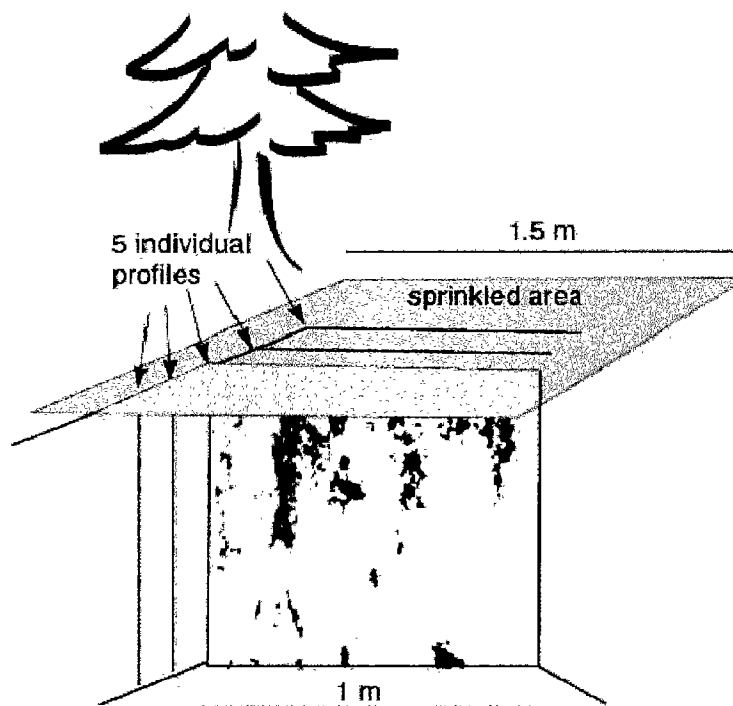


*Figure 3.1: Experimental setup and digitized image of one of the 100 soil profiles with preferential flow paths being visualized by the dye tracer Brilliant Blue.*

In each depth, we took soil samples over the whole horizon with a small spatula along the stained preferential flow paths and from the unstained soil matrix. Root samples were taken with three small cores per depth and flow region (i.e. preferential flow path and matrix) with a volume of  $9.07\text{ cm}^3$  each. Then, we prepared four more profiles with 10 cm spacing to the previous one and repeated the sampling procedure.

The samples of the five profiles were later pooled to obtain one composite sample per depth and flow region for each soil plot. On each plot, the organic layer was sampled according to its horizons. To estimate the natural abundance of <sup>13</sup>C and <sup>15</sup>N, samples were taken from all four plots in April 1998.

Soil solution was collected with zero-tension lysimeters below the forest floor and with suction cups (SoilMoisture Corp., Santa Barbara, California) at 10-15, 20-25, and 75-80 cm depths.

### 3.3.3 <sup>15</sup>N-labelling experiment

To study the fate of deposited N in the soil a <sup>15</sup>N-tracer experiment was conducted. In May 1998, we applied 20.15 mg <sup>15</sup>N m<sup>-2</sup>, which is equivalent to 55 mg double labeled and 99.8% enriched ammonium nitrate (<sup>15</sup>NH<sub>4</sub><sup>15</sup>NO<sub>3</sub>). The tracer was dissolved in distilled water and distributed evenly with a vaporizer over the designated soil plots covering an area of 24 m<sup>2</sup> in total. The samples were taken as described above in June and October 1998 and in May 1999.

### 3.3.4 Sample preparation and analysis

Soil and organic layer samples were oven-dried (50°C), sieved (2 mm), and ground to fine powder prior to analysis. Roots were carefully washed out of the fresh soil, dried and also ground to fine powder. Root samples of all four soil plots were pooled to obtain enough material for the analysis. Soil solution samples were freeze-dried.

Total C and N were determined with a CN auto analyzer (NA 1500, Carlo Erba Instruments, Italy). For the mass-balance calculations, measured SOM values from preferential flow paths were corrected for the C and N added with the experimental Brilliant Blue application. The dye tracer Brilliant Blue had a C content of 56% and a δ<sup>13</sup>C value of -27.5‰, and a N content of 3.3% and a δ<sup>15</sup>N value of -1‰. We used a conservative estimation with measured Brilliant Blue concentrations in 0.5M K<sub>2</sub>SO<sub>4</sub> extracts of the soil samples and an assumed mass recovery of 0.2.

Potentially existing carbonates were removed prior to stable isotope analysis. An amount of 5 g per sample was dissolved in 15 ml distilled water and 25 ml 1 N HCl were added. After 30 min of stirring, when the pH reached 1, we added 1 N KOH until

the pH was between 4 and 5. After vacuum-filtration the sample on the filter paper was dried for 24 h at 65°C and then crushed to a fine powder. For the stable isotope analysis (<sup>13</sup>C and <sup>15</sup>N), the ground soil, organic layer, soil solution and root samples were weighed into small tin capsules. The sample amount for soil varied between 30 to 80 mg for N, 12 to 15 mg for C, and approximately 5 mg for root and organic layer C and N analyses. For the δ<sup>13</sup>C and δ<sup>15</sup>N determination, the samples were combusted in an Elemental Analyzer (EA-1110, Carlo Erba, Italy) which was connected to a continuous flow mass spectrometer (DELTA-S, Finnigan MAT, Germany). The isotopic signatures are expressed in the delta notation:

$$\delta_x = \left( \frac{R_{\text{sample}}}{R_{\text{standard}}} - 1 \right) \cdot 1000 \quad [‰], \quad (1)$$

with δ<sub>x</sub> being the isotope ratio of C or N in delta-units relative to the international standards (Pee Dee Belemnite for C and atmospheric N<sub>2</sub> for N) and R<sub>sample</sub> and R<sub>standard</sub> are the <sup>13</sup>C/<sup>12</sup>C or <sup>15</sup>N/<sup>14</sup>N ratios of the samples and standards, respectively. The external precision was < 0.1‰ for δ<sup>13</sup>C and < 0.15‰ for δ<sup>15</sup>N.

### 3.3.5 Calculations and statistical analysis

The enrichment of SOC in preferential flow paths compared to that in the soil matrix (SOC<sub>e</sub>) was calculated as follows:

$$SOC_e = f_f \cdot V \cdot \rho_s \cdot (C_f - C_m), \quad (2)$$

where f<sub>f</sub> is the areal fraction of preferential flow paths identified in the soil profile; we assume that f approximates the volume fraction of the two flow regions on a total soil volume basis V; ρ<sub>s</sub> is the bulk soil density, and C<sub>f</sub> and C<sub>m</sub> are the SOC concentrations in the preferential flow paths and in the soil matrix, respectively. To account for the C increase by the Brilliant Blue addition, the total amount of added Brilliant Blue C (67 g C m<sup>-2</sup>) was subtracted. The enrichment of fine root C in the preferential flow paths was calculated with the same equation using the concentrations of fine root C in the soil. The drainage was estimated from the difference between rainfall and evapotranspiration, the latter being approximately 550 mm according to Spreafico et al. (1992).



The differences of parameters between preferential flow paths and soil matrix were tested for statistical significance with analysis of variance, or, for single depth zones with the paired t-test. Residuals were tested for normality and for similar variance. In case of non-normality, we preferred the more robust non-parametric Wilcoxon signed-rank test. All calculations were conducted with the software S-plus (version 5.0, MathSoft, Seattle, USA).

## 3.4 Results

### 3.4.1 Flow patterns

An example of the inhomogeneous dye distribution resulting from heterogeneous water flow is given in Figure 3.1. The proportions of stained preferential flow paths at the total soil volume ranged from  $70 \pm 11\%$  in 0-9 cm depth to  $2 \pm 2\%$  at 50 to 100 cm depth.

### 3.4.2 Soil organic carbon

The organic C content of the soil showed a sharp decrease with depth and was at all depths higher in the preferential flow paths than in the matrix (Table 3.1). Soil organic C was increased in preferential flow paths compared to the soil matrix by 42% at 0-9 cm and 12%, 28%, and 69% in the subsequent depths. The experimental addition of Brilliant Blue increased the  $C_{\text{org}}$  content of the preferential flow paths at most by 2.5% in 0-9 cm depth and by  $< 3.5\%$  in 50-100 cm depth. However, for the calculations of the total SOC enrichment we subtracted the Brilliant Blue derived C from the total  $C_{\text{org}}$  concentration. Summing up over the total soil compartment and taking the volume of preferential flow paths into account yields a total SOC accumulation along preferential flow paths of 740 to 960 g C m<sup>-2</sup> in the four plots with a mean accumulation of 860 g C m<sup>-2</sup>.

The needles of the dominant tree species in the forest, Norway spruce, was markedly depleted in  $^{13}\text{C}$  compared to the mineral soil. The mean  $\delta^{13}\text{C}$  value of needles was  $-27.0\text{‰}$  (mean of needles up to four years of age in 1998), single values of fine roots ranged between  $-26.8\text{‰}$  and  $-28.9\text{‰}$  (mean values: Figure 3.2). Fine roots sampled from the matrix were depleted in  $^{13}\text{C}$  as compared to the fine roots from the flow paths ( $P < 0.001$ ). Most depleted in  $^{13}\text{C}$  was the forest floor with  $\delta^{13}\text{C}$  values of  $-28.0$  to  $-28.5\text{‰}$ .

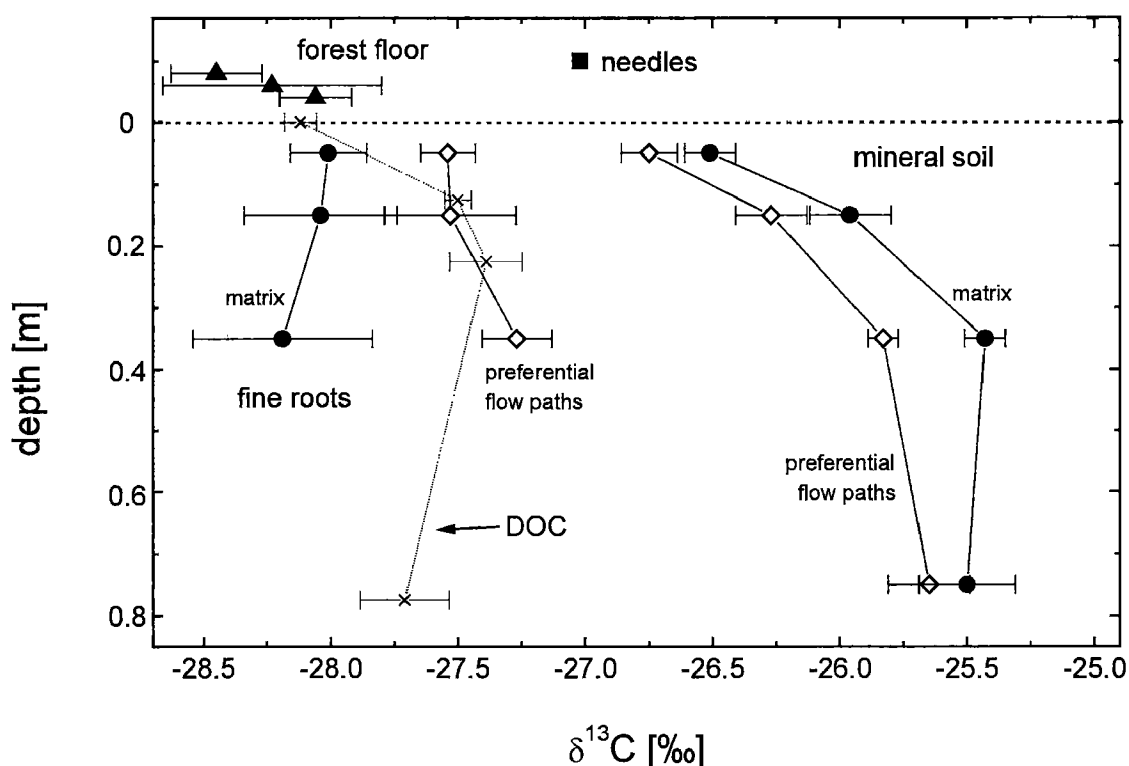


**Figure 3.2:**  $\delta^{13}\text{C}$  values of the needles from Norway spruce, of the forest floor, and of the mineral soil sampled from the preferential flow paths and from the matrix of the fine roots of preferential flow paths and matrix, and of the soil solution. Root isotopic signatures are the mean of 5 sampling dates.

In the mineral soil, the  $\delta^{13}\text{C}$  values increased with depth from  $-26.8\text{‰}$  to  $-25.8\text{‰}$  in the preferential flow paths and from  $-26.5\text{‰}$  to  $-25.4\text{‰}$  in the matrix (Figure 3.2). The SOC of the preferential flow paths was significantly more depleted in  $^{13}\text{C}$  than that of

the matrix soil at all depths ( $P=0.001$ ). This was not caused by the experimental addition of Brilliant Blue, because the fraction of Brilliant Blue derived C was negligible in comparison to the SOC content of the soil (approximately 2.5% in 0-9 cm to 3.5% in 50-100 cm depth). According to a mixing model (Balesdent et al., 1990), the maximal decrease in  $\delta^{13}\text{C}$  due to Brilliant Blue was below 0.05‰.

To estimate the accumulation of SOC with <sup>13</sup>C in the soil profile, an isotopic discrimination factor (i.e. the slope of the regression between  $\delta^{13}\text{C}$  and  $-\ln(\%C)$ ) was calculated. The isotopic discrimination factor was originally derived for mineralization studies and shows the degree of isotopic discrimination during organic matter decomposition (O'Leary, 1981). It can also be applied to soil profiles, where the SOM content usually decreases with depth (Nadelhoffer and Fry, 1988).

The discrimination factor was similar for preferential flow path and soil matrix samples (Figure 3.3). However, the discrimination ratio, i.e. the ratio between  $\delta^{13}\text{C}$  and  $-\ln(\%C)$  of the individual samples, was significantly lower for preferential flow paths than for soil matrix (Wilcoxon signed rank test:  $P=0.004$ ).

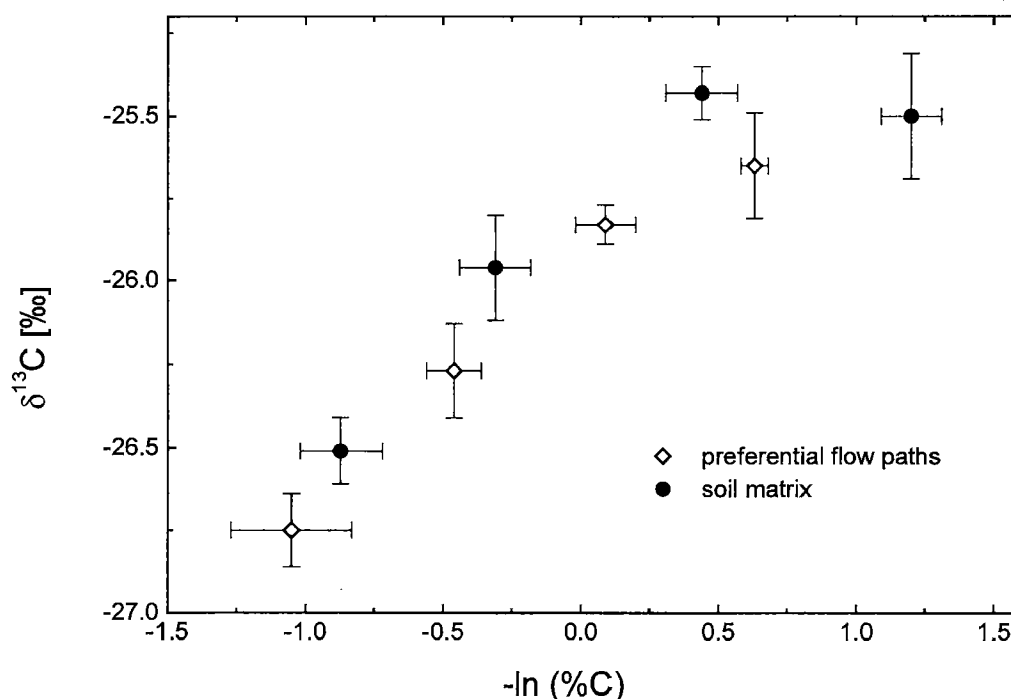


**Figure 3.3:** Isotopic compositions ( $\delta$  values) vs. percent elemental mass in soil from the preferential flow paths and from the matrix ( $n = 4$ ).

In the soil solution the concentrations of DOC decreased from 35 to 45 mg DOC l<sup>-1</sup> in the forest floor to less than 2 mg DOC l<sup>-1</sup> in 75 cm depth (S. Zimmermann, WSL, personal communication). The  $\delta^{13}\text{C}$  signature of dissolved organic carbon (DOC) showed about the same increase with depths as the mineral soil. However, the  $\delta^{13}\text{C}$  values of DOC were about 2‰ more negative than those of the solid organic C at all depths (Figure 3.2).

### 3.4.3 Soil nitrogen

Similar to the C contents, the total N contents in the mineral soil decreased throughout the four sampling depths (Table 3.1). At all depths, the preferential flow paths had significantly higher total N concentrations than the soil matrix ( $P= 0.009$ ). Fine roots from the matrix had higher N contents than fine roots from the preferential flow paths. However, this difference is statistically not significant.

The natural <sup>15</sup>N abundance followed the pattern of <sup>13</sup>C (Figure 3.4). Values of  $\delta^{15}\text{N}$  were lowest in needles with -5.7‰ and ranged from -5.4 to -5.0‰ in the forest floor. Fine roots had  $\delta^{15}\text{N}$  values almost as low as in the forest floor, with the lowest values at 20-50 cm depth. In 0 to 9 cm depth, the fine roots from the matrix were depleted in <sup>15</sup>N as compared to those from the preferential flow paths, but this difference was statistically not significant.

In the mineral soil, the  $\delta^{15}\text{N}$  values increased with depth from -0.9‰ to 4.7‰ in the preferential flow paths and from 0.5‰ to 6‰ in the matrix (Figure 3.4). The depletion of <sup>15</sup>N in preferential flow paths compared to the matrix was significant ( $P<0.001$ ). As with  $\delta^{13}\text{C}$ , the  $\delta^{15}\text{N}$  was not significantly affected by the experimental Brilliant Blue addition. Using the same mixing model as before (Balesdent et al., 1990), the maximal shift in  $\delta$ -values would have been less than 0.04‰ in the topsoil and less than 0.25‰ in the lowest depth. This is substantially lower than the measured difference between preferential flow paths and soil matrix.

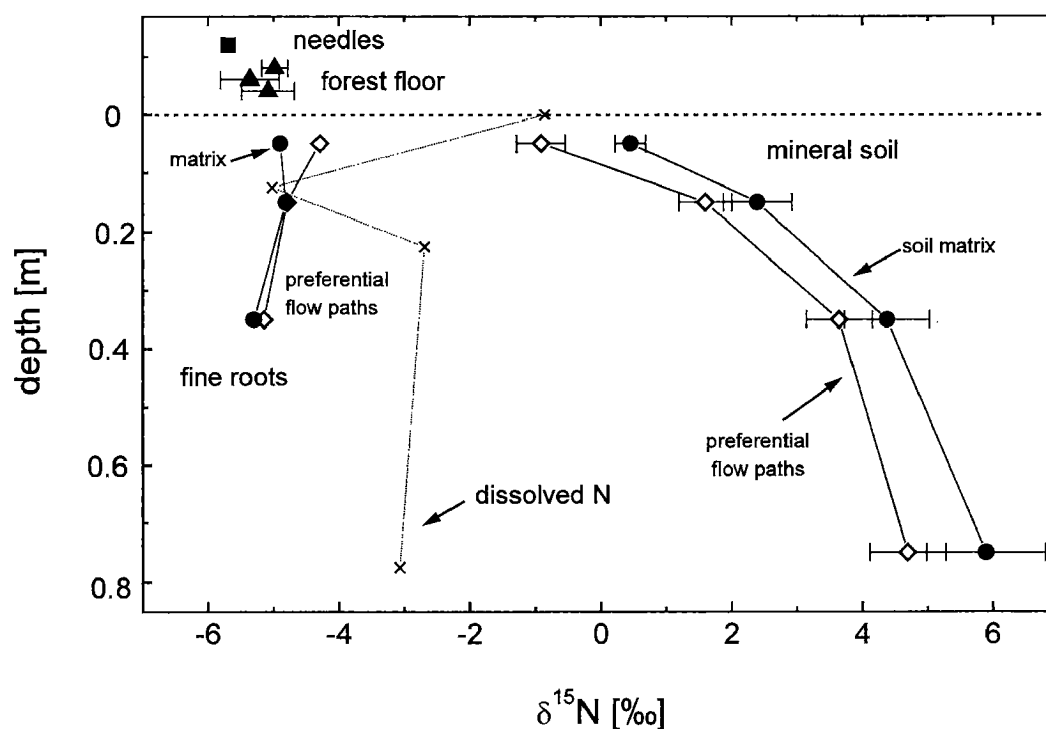


**Figure 3.4:**  $\delta^{15}\text{N}$  values of the needles from Norway spruce, of the forest floor, and of the mineral soil sampled from the preferential flow paths and from the matrix, of the fine roots of preferential flow paths and matrix, and of the soil solution. Root isotopic signatures are the mean of 5 sampling dates.

The  $\delta^{15}\text{N}$  of the soil solution did not follow the signature of the mineral soil. In the topsoil, the N in the soil solution had similar  $\delta^{15}\text{N}$  values as the mineral soil, but was distinctly lower in the deeper soil horizons (Figure 3.4). Assuming a DOC to DON mass ratio of 30 (Currie et al., 1996; Hagedorn et al., 2000), the proportion of nitrate relative to the total dissolved N increased from 75% at the mineral soil surface to 100% in the soil solution below 25 cm depth (S. Zimmermann, WSL, personal communication).

The discrimination factor for  $\delta^{15}\text{N}$  was nearly identical for preferential flow paths and matrix (Figure 3.5). However, the two regression lines were displaced horizontally, which is in accordance with the fact that the individual discrimination ratios for preferential flow paths and matrix differed significantly (Wilcoxon signed rank test:  $P < 0.001$ ).

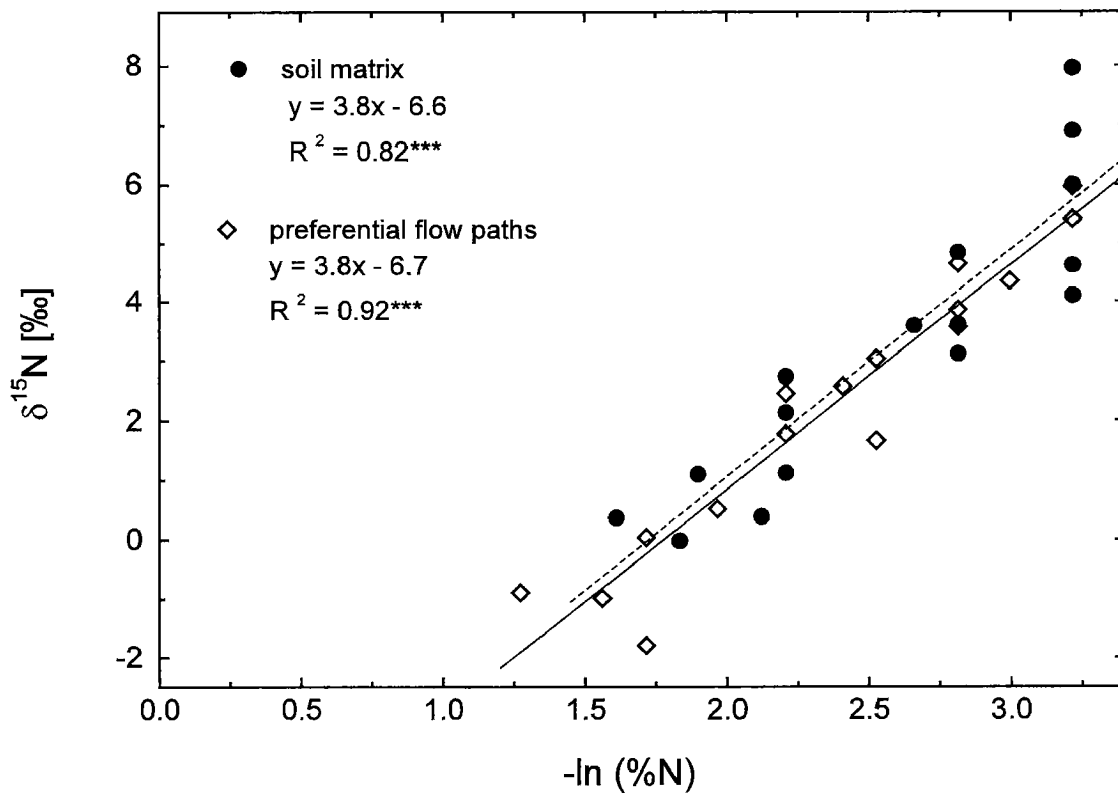


**Figure 3.5:** Isotopic compositions ( $\delta$  values) vs. percent elemental mass in soil from the preferential flow paths and from the matrix. The slope of the respective regression line is called isotopic discrimination factor.

#### 3.4.4 <sup>15</sup>N tracer study

The mean <sup>15</sup>N recovery of the <sup>15</sup>N tracer experiment was  $88\% \pm 24\%$  <sup>15</sup>N after one year, including roots, mineral soil and forest floor. Most of the added <sup>15</sup>N was retained in the forest floor (60%). In the mineral soil,  $\delta^{15}\text{N}$  values rose steeply after the tracer application (Figure 3.6). The increase in  $\delta^{15}\text{N}$  was higher in the preferential flow paths than in the matrix at all depths (ANOVA,  $P=0.011$ ). Subsequently, 6 and 12 months after the <sup>15</sup>N addition, the  $\delta^{15}\text{N}$  remained stable in the flow paths at all depths, but still increased in the soil matrix of 9-20 cm and 20-50 cm depth.

A similar pattern was found for the  $\delta^{15}\text{N}$  of fine roots (Figure 3.6). The amplitude of the changes was about one order of magnitude higher in the fine roots than in the

mineral soil. The temporal changes in  $\delta^{15}\text{N}$  of the fine roots and of the soil were linearly correlated ( $R^2 = 0.95$ ).

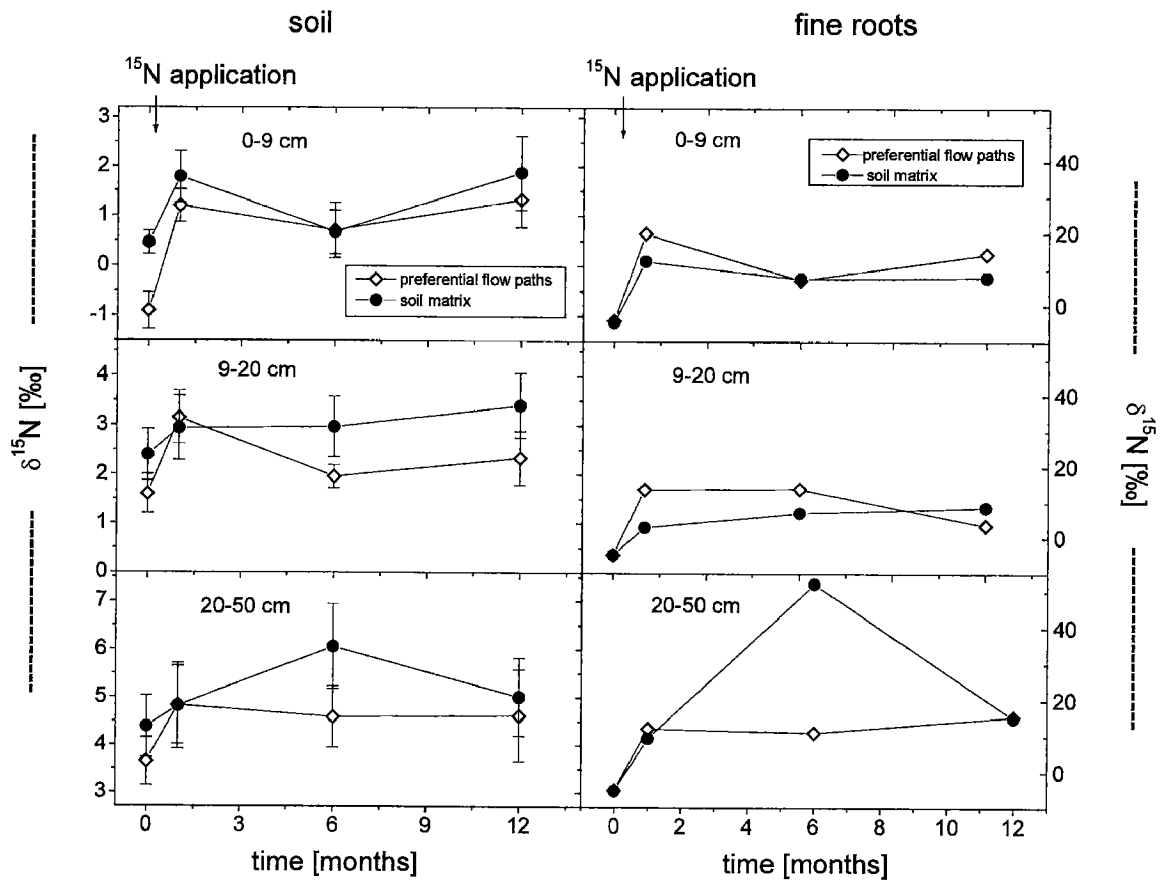


**Figure 3.6:** Progression of  $\delta^{15}\text{N}$  values in soil and fine roots of preferential flow paths and matrix before and 1, 6, and 12 months after  $^{15}\text{N}$  application in 0-9 cm, 9-20 cm, and 20-50 cm depth. For the root  $\delta$  values, root material from four plots was pooled to yield enough material for analysis.

### 3.5 Discussion

#### 3.5.1 Soil organic carbon dynamics

The increase of  $\delta^{13}\text{C}$  and  $\delta^{15}\text{N}$  with soil depth is consistent with the results from other studies in forest soils (O'Brien and Stout, 1978; Huang et al., 1996; Koopmans, et al., 1997). This increase is usually related (i) to the overall depletion of  $^{15}\text{N}$  and  $^{13}\text{C}$  during organic matter decomposition (ii) to the differential preservation of soil organic matter or plant litter components, (iii) to the changes from litter inputs with high  $\delta^{15}\text{N}$  and  $\delta^{13}\text{C}$  values to litter inputs with lower values, and (iv) to the illuviation of  $^{15}\text{N}$  and  $^{13}\text{C}$  enriched dissolved organic matter into lower soil layers (Nadelhoffer and Fry, 1988). Our findings show that within a given horizon,  $\delta^{13}\text{C}$  and  $\delta^{15}\text{N}$  values were not evenly distributed. Preferential flow paths were significantly depleted in  $^{13}\text{C}$  and  $^{15}\text{N}$  compared to the rest of the soil.

Huang et al. (1996) and Bol et al. (1999) found that  $\delta^{13}\text{C}$  values of SOC were closely correlated with  $^{14}\text{C}$  values, indicating that  $\delta^{13}\text{C}$  values increase with the age of SOC. Moreover, it was shown that labile C-pools with high turnover rates (sand-associated and light SOC fractions) are depleted in  $^{13}\text{C}$  compared to recalcitrant C-pools (Balesdent et al., 1988; Bonde et al., 1992). Thus, our findings, that SOC of preferential flow paths was depleted in  $^{13}\text{C}$  relative to the soil matrix strongly suggest that SOC of the preferential flow paths is 'younger' than SOC of the soil matrix. This is supported by the relationship between  $\delta^{15}\text{N}$  and  $\delta^{13}\text{C}$  values (Figure 3.7). All potential input sources of SOC (leaves, forest floor, roots and soil solution) fell into a relatively narrow range of about 2‰ into direction of both x-axis and y-axis. In the mineral soil, the  $\delta$ -values of C and N formed a straight line originating in the middle of the "plant-input cloud" (i.e. sources) and extending towards higher  $\delta^{15}\text{N}$  and  $\delta^{13}\text{C}$  values. The uppermost horizon was closest to the plant-input source of the SOC. Within a given horizon, the values of the preferential flow paths always resembled the source more strongly than those of the corresponding matrix soil. This suggests that SOC of flow paths is 'younger' and less humified.

This might be partly due to a higher input of root-derived C along preferential flow paths as indicated by a higher root biomass with rather negative  $\delta^{13}\text{C}$ -values (Table 3.1,



Figure 3.2). The C-accumulation due to fine roots along preferential flow paths ranged between 20 and 40 g C m<sup>-2</sup> in the individual soil plots (estimated according to equation 3.2). However, little is known about the relative amount of humus formed from roots or litter. Assuming a humification factor for fine roots of 0.5, which is about twice as high as those used in SOC models (Aber et al., 1990; Perruchoud et al., 1999), and a constant input per year, yields a contribution of the increased fine root biomass in the preferential flow paths of about 10 to 20 g C m<sup>-2</sup> y<sup>-1</sup>. This conservative estimate is almost two orders of magnitude lower than the measured SOC accumulation along preferential flow paths of 740 to 960 g C m<sup>-2</sup>.

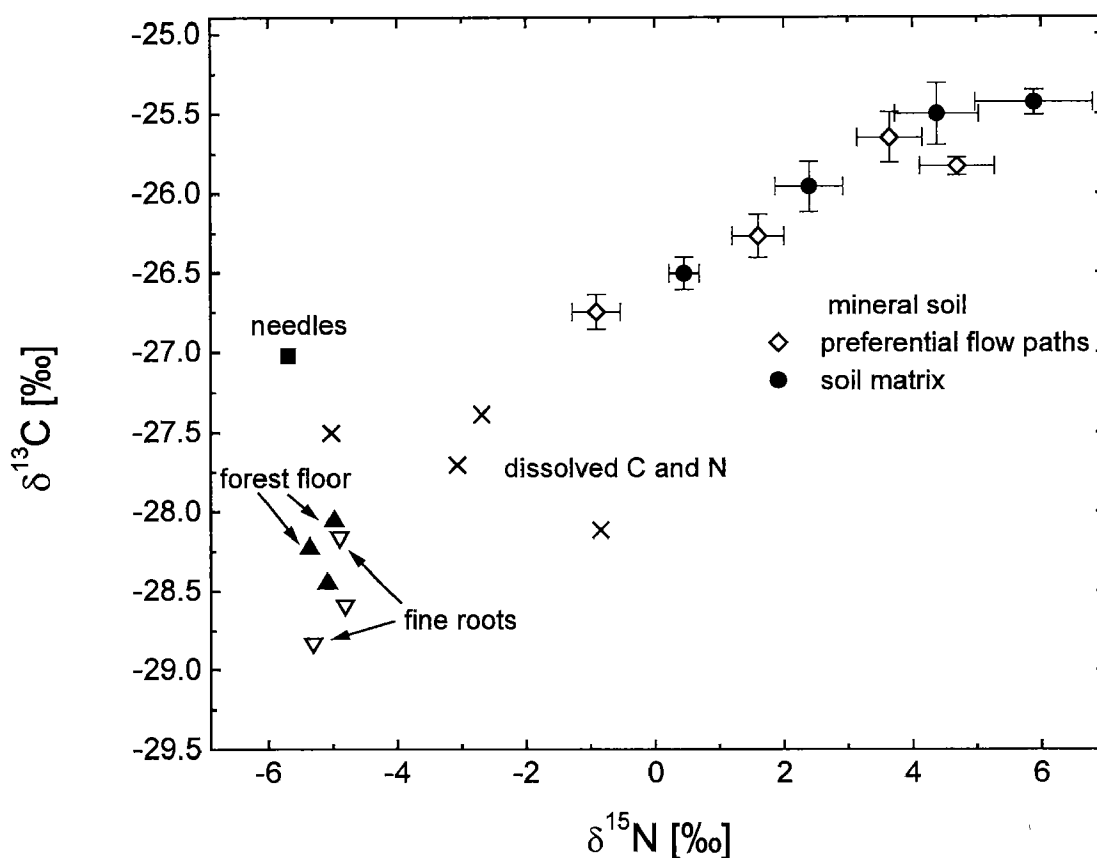


**Figure 3.7:** The  $\delta^{13}\text{C}$  vs.  $\delta^{15}\text{N}$  compositions of leaf litter, fine roots, soil solution, and soil material from preferential flow paths and from the soil matrix.

Increased illuviation of DOC and colloids might add to the inputs of 'young' C even down to the deeper soil depths, because preferential flow paths are preferred pathways

for the transport of solutes and particles (Jardine et al., 1989; Hagedorn et al., 2000). The  $\delta^{13}\text{C}$  values of DOC in the soil solution were close to those of fine roots and between 1 to 2‰ more negative than the mineral soil signature (Figure 3.2). Transport of 'young' C with percolating water was already shown for two Alfisols in Northern Germany by Becker-Heidemann and Scharpenseel (1986) and is thought to be an important mechanism in pedogenesis (Buurman, 1985; Schoenau and Bettany, 1987; Blaser, 1994). In our forest soil almost all DOC that was leached from the forest floor was retained in the mineral soil. The maximal contribution of DOC leaching to the SOC accumulation in preferential flow paths ranged between 15 to 40 g C m<sup>-2</sup>y<sup>-1</sup>. This estimate is based on the following conservative assumptions: that all of the drainage water (400 to 900 mm y<sup>-1</sup> according to the simple water budget) moved through the identified preferential flow paths (1), that all of the DOC was sorbed to the walls of the flow paths (2), and that redistribution of DOC and mineralization of DOC was negligible (3). These values are consistent with the estimated DOC inputs from forest floors into the mineral soil in other temperate forest ecosystems (Guggenberger and Zech, 1993; Currie, et al., 1996). As with the increased fine root production in flow paths, this maximal possible increase of SOC through DOC illuviation is rather small compared to the observed total SOC accumulation along preferential flow paths.

The SOC accumulation in flow paths of 740 to 960 g C m<sup>-2</sup> appears to be high even in comparison with the yearly C-input through litter-fall of about 200 g C m<sup>-2</sup>y<sup>-1</sup> at this forest site (D. Hallenbarter, WSL, personal communication). The remaining mass of forest litter after 3 years of decay usually ranges between 15 and 30% (Melillo et al., 1989; Aber et al., 1990; Magill and Aber, 1998). Measured rates of SOC accumulation after forest establishment, with the maximal C input rate during soil development, range between 10 and 60 g C m<sup>-2</sup>y<sup>-1</sup> (Schlesinger, 1990; Post and Kwon, 2000). Therefore, if all of the 'new' SOC is assumed to accumulate in the preferential flow paths, the C accumulation along preferential flow paths can at most account for 60 g C m<sup>-2</sup>y<sup>-1</sup>. Furthermore, it is unlikely that a stimulated mineralization of SOC in the soil matrix compared to that in the preferential flow paths contributed to the SOC enrichment in flow paths, since microbial biomass was higher along the preferential flow paths (Chapter 4, Bundt et al., 2000b).

Thus, the high SOC accumulation in preferential flow paths strongly suggests that the increase of SOC in the predominant flow regions was a long-lasting process. Summing up over all potential contributors to SOC enrichment such as increased fine root biomass, enhanced DOC illuviation, and preferred incorporation of litter, indicates that SOC accumulation in the identified flow paths lasted for at least 10 years. This rough and conservative estimate is supported by radionuclide data from the same soil samples, which showed that the flow paths persisted for at least 40 years (Bundt et al., 2000a).

### 3.5.2 Nitrogen dynamics

The temporal variations of  $\delta^{15}\text{N}$  after the <sup>15</sup>N labelling were higher in the preferential flow paths than in the matrix (Figure 3.6). The tracer enrichment in the preferential flow paths was even higher than denoted by the  $\delta^{15}\text{N}$  signature, because the total N concentrations were 25% higher in preferential flow paths than in the soil matrix. The low temporal resolution of the <sup>15</sup>N-tracer study can be responsible for the rather small preferential flow path effect. The N transport might have been faster than measured at the first sampling time one month after the <sup>15</sup>N application. In the preferential flow paths, the  $\delta^{15}\text{N}$  values decreased one month after application, suggesting that the tracer front had already passed. In contrast,  $\delta^{15}\text{N}$  values of the soil matrix still rose after one month, which indicates a retarded arrival of the tracer front at locations in the soil matrix. This is consistent with the concept of transport –limited mass transfer between rapid and stagnant flow regions. The faster transport of  $\text{NO}_3^-$  along preferential flow paths is also consistent with the results of a field study with micro suction cups, which showed that the highest  $\text{NO}_3^-$  concentrations in the soil solution of highly conductive zones were reached within hours after an  $\text{NO}_3^-$  application and dropped back to the background concentrations within three days (Hagedorn et al., 1999).

Nevertheless, the significantly higher increase of  $\delta^{15}\text{N}$  in the preferential flow paths as compared to the matrix shows the importance of preferential flow paths for transport of nutrients and for plant nutrition. The latter is particularly important since the concentrations of plant roots in the preferential flow paths were also significantly higher

than in the matrix (Table 3.1). As a result, the initial increase in  $\delta^{15}\text{N}$  of the fine roots in preferential flow paths was more pronounced than in the soil matrix (Figure 3.6).

After the initial increase of  $^{15}\text{N}$ ,  $\delta^{15}\text{N}$  values decreased more in the preferential flow paths than in the soil matrix during the following 11 months. This suggests an enhanced N cycling along preferential flow paths compared to the rest of the soil. However, we cannot distinguish whether this was due to a more pronounced leaching or to root uptake of  $^{15}\text{N}$  or to an increased illuviation of new unlabelled N.

### 3.6 Conclusions

Our results show that within a given soil horizon, SOC concentrations, total N concentrations,  $\delta^{13}\text{C}$  and  $\delta^{15}\text{N}$  values were not evenly distributed. Preferential flow paths, identified with a homogeneously applied dye tracer, had a higher SOC concentration compared to the rest of the soil. A  $^{15}\text{N}$ -addition experiment led to a higher rise and a stronger decrease of the  $\delta^{15}\text{N}$  values in the preferential flow paths than in the soil matrix. This suggests higher turnover rates in the preferential flow paths. Preferential flow paths were significantly depleted in  $^{13}\text{C}$  and  $^{15}\text{N}$  compared to the rest of the soil indicating that SOC from preferential flow paths was 'younger' than SOC from the soil matrix. Potential pathways of SOC accumulation are an accelerated input of root-derived C and an increased illuviation of DOC. The SOC accumulation of 800 to 1000 g C m<sup>-2</sup> in preferential flow paths compared to the soil matrix was much larger than the contribution from these potential sources. This strongly suggests that accumulation of SOC in the identified preferential flow paths lasted for periods of more than 10 years.

The findings of SOC enrichment along preferential flow paths have implications for the transport of reactive solutes through the soil. Sorption of organic pollutants and heavy metals strongly increases with increasing SOC concentrations. Thus, higher SOC concentrations in preferential flow paths may lead to an increased sorption and may therefore counterbalance the preferred transport of pollutants.

### 3.7 References

- Aber, J.D., J.M. Melillo, and C.A. McLaugherty. 1990. Predicting long-term patterns of mass loss, nitrogen dynamics, and soil organic matter formation from initial fine litter chemistry in temperate forest ecosystems. *Can. J. Bot.* 68: 2201-2208.
- Balesdent, J., A. Mariotti, and D. Boisgontier. 1990. Effects of tillage on soil organic carbon mineralization estimated from <sup>13</sup>C abundance in maize fields. *J. Soil Sci.* 41: 587-596.
- Balesdent, J., G.H. Wagner, and A. Mariotti. 1988. Soil organic matter turnover in long-term field experiments as revealed by carbon-13 natural abundance. *Soil Sci. Soc. Am. J.* 52: 118-124.
- Becker-Heidemann, P., and H.-W. Scharpenseel. 1986. Thin layer  $\delta^{13}\text{C}$  and  $\text{D}^{14}\text{C}$  monitoring of "lessive" soil profiles. *Radiocarbon* 28: 383-390.
- Blaser, P. 1994. The role of natural organic matter in the dynamics of metals in forest soils. p. 943-960. *In* Senesi, N. and T.M. Miano (eds.) *The role of natural organic matter in the dynamics of metals in forest soils*. Elsevier, Amsterdam.
- Bol, R.A., D.D. Harkness, Y. Huang, and D.M. Howard. 1999. The influence of soil processes on carbon isotope distribution and turnover in the British uplands. *Europ. J. Soil Sci.* 50: 41-51.
- Bonde, T.A., B.T. Christensen, and C.C. Cerri. 1992. Dynamics of soil organic matter as reflected by natural <sup>13</sup>C abundance in particle size fractions of forested and cultivated Oxisols. *Soil Biol. Biochem.* 24: 275-277.
- Bundt, M., Albrecht, A., Froidevaux, P., Blaser, P., and Flühler, H. 2000a. Impact of preferential flow on radionuclide distribution in soil. *Environ. Sci. Technol.* in press.
- Bundt, M., F. Widmer, P. Blaser, and H. Flühler. 2000b. Präferentieller Wasserfluss-Auswirkungen eines bodenphysikalischen Phänomens auf chemische und biologische Parameter. *Mitt. Dt. Bodenkundl. Gesellsch.* 91: 314-317.
- Buurman, P. 1985. Carbon/sesquioxide ratios in organic complexes and the transition albic-spodic horizon. *J. Soil Sci.* 36: 255-260.
- Currie, W.S., J.D. Aber, W.H. McDowell, R.D. Boone, and A.H. Magill. 1996. Vertical transport of dissolved organic C and N under long-term N amendments in pine and hardwood forest. *Biogeochem.* 35: 471-505.
- Flury, M., and H. Flühler. 1994a. Brilliant Blue FCF as a dye tracer for solute transport studies - A toxicological overview. *J. Environ. Qual.* 23: 1108-1112.
- Flury, M., and H. Flühler. 1994b. Susceptibility of soils to preferential flow of water: A field study. *Water Resour. Res.* 30: 1945-1954.

- Gebauer, G., and E.-D. Schulze. 1991. Carbon and nitrogen isotope ratios in different compartments of a healthy and a declining *Picea abies* forest in the Fichtelgebirge, NE Bavaria. *Oecologia* 87: 198-207.
- Guggenberger, G., and W. Zech. 1993. Dissolved organic carbon controls in acid forest soils of the Fichtelgebirge (Germany) as revealed by distribution patterns and structural composition analyses. *Geoderma* 59: 109-129.
- Hagedorn, F., K. Kaiser, H. Feyen, and P. Schleppei. 2000. Effects of redox conditions and flow processes on the mobility of dissolved organic carbon and nitrogen in a forest soil. *J. Environ. Qual.* 29: 288-297.
- Hagedorn, F., J. Mohn, P. Schleppei, and H. Flühler. 1999. The role of rapid flow paths for nitrogen transformation in a forest soil - a field study with micro suction cups. *Soil Sci. Soc. Am. J.* 63: 1915-1923.
- Högberg, P. 1997. <sup>15</sup>N natural abundance in soil-plant systems. *New Phytol.* 137: 179-203.
- Huang, Y., R. Bol, D.D. Harkness, P. Ineson, and G. Eglinton. 1996. Post-glacial variations in distributions, <sup>13</sup>C and <sup>14</sup>C contents of aliphatic hydrocarbons and bulk organic matter in three types of British acid upland soils. *Org. Geochem.* 24: 273-287.
- Jardine, P.M., G.V. Wilson, R.J. Luxmoore, and J.F. McCarthy. 1989. Transport of inorganic and natural organic tracers through an isolated pedon in a forest watershed. *Soil Sci. Soc. Am. J.* 53: 317-323.
- Koopmans, C.J., D. van Dam, A. Tietema, and J.M. Verstraten. 1997. Natural <sup>15</sup>N abundance in two nitrogen saturated forest ecosystems. *Oecologia* 111: 470-480.
- Magill, H., and J.D. Aber. 1998. Long-term effects of experimental nitrogen additions on foliar litter decay and humus formation in forest ecosystems. *Plant Soil* 203: 301-311.
- Melillo, J.M., J.D. Aber, A.E. Linkins, A. Ricca, B. Fry, and K.J. Nadelhoffer. 1989. Carbon and nitrogen dynamics along the decay continuum: Plant litter to soil organic matter. *Plant Soil* 115: 189-198.
- Nadelhoffer, K.J., and B. Fry. 1988. Controls on natural nitrogen-15 and carbon-13 abundances in forest soil organic matter. *Soil Sci. Soc. Am. J.* 52: 1633-1640.
- O'Brien, B.J., and J.D. Stout. 1978. Movement and turnover of soil organic matter as indicated by carbon isotope measurements. *Soil Biol. Biochem.* 10: 309-317.
- O'Leary, M.H. 1981. Carbon isotope fractionation in plants. *Phytochem.* 20: 553-567.
- Parkin, T.B. 1993. Spacial variability of microbial processes in soil - a review. *J. Environ. Qual.* 22: 409-417.

- Perruchoud, D., F. Joos, A. Fischlin, I. Hajdas, and G. Bonani. 1999. Evaluating timescales of carbon turnover in temperate forest soils with radiocarbon data. *Global Biogeochem. Cycles* 13: 555-573.
- Post, W.M., and K.C. Kwon. 2000. Soil carbon sequestration and land-use change: processes and potential. *Global Change Biol.* 6: 317-327.
- Schlesinger, W.H. 1990. Evidence from chronosequence studies for a low carbon-storage potential of soils. *Nature* 348: 232-234.
- Schoenau, J.J., and J.R. Bettany. 1987. Organic matter leaching as a component of carbon, nitrogen, phosphorus, and sulfur cycles in a forest, grassland, and gleyed soil. *Soil Sci. Soc. Am. J.* 51: 646-651.
- Spreafico, M., R. Weingartner, and C. Leibundgut. 1992. Hydrological atlas of Switzerland. *Landeshydrologie und -geologie*, Bern.

## **CHAPTER 4**

# **Preferential flow paths: biological ‘hot spots’ in soils**

with

FRANCO WIDMER, MANUEL PESARO, JOSEF ZEYER AND PETER BLASER

Soil Biology and Biochemistry, accepted



## 4.1 Abstract

Preferential flow of water in soils is a common phenomenon. Our objective was to investigate whether preferential flow paths have higher microbial biomass and different microbial community structures than the rest of the soil. We stained the preferential flow paths in a forest soil with a food dye and sampled soil material from preferential flow paths and from the soil matrix in 4 depths down to 1 m. Distinct differences in physico-chemical properties between preferential flow paths and soil matrix existed and thus different environmental living conditions for microorganisms. The experimental addition of wood ash increased pH and base saturation in the preferential flow paths to a higher extent than in the soil matrix, highlighting the importance of preferential flow paths for solute input into the mineral soil. The organic C concentrations were approximately 10% to 70% higher in the preferential flow paths than in the matrix. The organic N concentrations were also enriched in the preferential flow paths, as well as the effective cation exchange capacity and the base saturation. Microbial biomass determined with the fumigation-extraction method was 9% to 92% higher in the preferential flow paths than in the soil matrix, probably due to the better nutrient and substrate supply. The DNA concentrations and direct cell counts showed a similar pattern, while domain-specific genetic fingerprints based on small subunit ribosomal RNA genes did not reflect the differences between preferential flow paths and soil matrix. Eukarya and Archaea only showed a depth-dependence and Bacteria showed no changes with flow region or with depths. However, *Pseudomonas* displayed different community structures between preferential flow paths and soil matrix. This indicated that possibly only few communities with a broad acceptance for substrates and aerobic as well as anaerobic growth specifically profit from the favourable conditions in the preferential flow paths.

## 4.2 Introduction

'Hot spots' in soils are zones of increased biological activity. They are described as small, spatially separated soil compartments. Some examples for "hot spots" are soil aggregates (Sexstone et al., 1985) with distinct physicochemical properties, zones with accumulated particulate organic matter (Parkin, 1987; van Noorwijk et al., 1993), or animal manure (Petersen et al., 1996), and the rhizosphere (Joergensen, 2000).

Preferential flow describes the physical phenomenon of rapid transport of water and solutes in soil. It occurs in most soils and is often attributed to macropore flow, either through cracks and fissures or through biopores such as earthworm burrows or root channels (Flury and Flühler, 1994b; Stagnitti et al., 1995). However, preferential flow in soils is not restricted to macropore flow. Non-homogeneous infiltration and wetting front instabilities can also lead to preferential flow (Sollins and Radulovich, 1988; Selker et al., 1992; Edwards et al., 1993). One important characteristic of preferential flow is that solutes bypass a large part of the soil matrix. Thus, strongly sorbing compounds like pesticides or rather immobile nutrients like phosphorus may be more mobile than anticipated and provide a possible hazard for ground and surface waters (Flury, 1996; Stamm et al., 1998). Additionally, sorption and degradation rates of preferential flow paths and soil matrix may be different due to the presence of different microbial populations (Pivetz and Steenhuis, 1995; Mallawatantri et al., 1996). A potential technique to visualise preferential flow in soils is the use of colour dye tracers (Ghodrati and Jury, 1990; Flury and Flühler, 1994b). With this technique, preferential flow paths are stained and become visible after preparing a soil profile.

In a study with micro suction cups Hagedorn et al. (1999) identified the position of suction cups relative to preferential flow paths with the dye tracer technique. They found higher nitrogen turnover in soil solution from preferential flow paths as compared to soil solution from the matrix and attributed this to a higher biological activity in such areas (Hagedorn et al., 1999). Analysis of an agricultural soil and a forest soil indicated that microbial biomass and bacterial numbers were higher in samples adjacent to macropores

than from matrix samples (Vinther et al., 1999). Enhanced pesticide degradation activities in macropore channels and earthworm burrows have also been described and were attributed to a better oxygen and substrate supply in macropores and to a larger microbial biomass in earthworm burrows (Pivetz and Steenhuis, 1995).

In uncultivated forest soil, flow paths are particularly stable (Beven and Germann, 1982). Therefore, distinct differences in physico-chemical properties between preferential flow paths and soil matrix can be expected. As a consequence of such physico-chemical differences, the microbial biomass and the microbial community structures may be different in the two soil compartments. To our knowledge, no study has yet been conducted to investigate the microbial biomass together with the community structure in two distinct but spatially close compartments in soils. Thus, in this study we tested the hypothesis that preferential flow paths have a higher microbial biomass and different community structures than the rest of the soil and therefore exhibit characteristics of extended continuous biological 'hot spots' in soils.

## 4.3 Materials and Methods

### 4.3.1 Study site and sampling schedule

The study was conducted at a forested site with a flat topography and a moderate slope of approximately 2° near Unterehrendingen, Switzerland. The forest was planted in 1930 with Norway spruce (*Picea abies* (L.) Karst.) as the dominant tree mixed with beech (*Fagus sylvatica* L.) and some other species. Four plots of approximately 4 by 6 m were chosen at the corners of a 2-ha experimental site of a wood ash-recycling project. Plots no. 1 and 3 were mainly surrounded by spruce and had little ground vegetation, whereas plots no. 2 and 4 were framed by spruce and beech with some blackberries (*Rubus* sp. L.) in the understorey vegetation. The soil type was for all plots a typic Haplumbrept (Soil Survey Staff, 1994). However, while the parent material was Upper Marine Molasse, plot no. 3 had some influence from an near-by end-moraine and plot no. 4 showed a clay lens at 80-100 cm depth. Mean selected chemical and physical properties are given in Table 4.1.

Table 4.1: Physical and chemical properties of preferential flow paths and soil matrix.

	Depth	pH <sup>a</sup>	Water content <sup>b</sup>	Sand	Silt	Clay	N <sub>tot</sub> <sup>c</sup>	C <sub>org</sub> <sup>c</sup>	CEC <sub>eff</sub> <sup>d</sup>	BS <sub>eff</sub> <sup>e</sup>
	[cm]		[%]	[%]	[%]	[%]	[g kg <sup>-1</sup> ]	[g kg <sup>-1</sup> ]	[mmol <sub>c</sub> kg <sup>-1</sup> ]	[%]
Flow path	0-9	3.4	44	43	38	19	2.18**	34.5**	83.8**	30**
	9-20	3.7	30	38	42	20	0.98*	14.5**	65.2*	20*
	20-50	3.8	26	35	42	23	0.65*	8.2**	60.7	26
	50-100	3.8	26	26	47	27	0.47*	4.9**	80.0	45
Matrix	0-9	3.4	34	37	41	22	1.57	24.3	74.6	21
	9-20	3.6	27	36	42	22	0.88	12.9	60.7	18
	20-50	3.8	24	35	41	24	0.60	6.4	58.4	26
	50-100	3.8	24	28	44	27	0.34	2.9	80.4	43

a: pH in 10 mM CaCl<sub>2</sub>, mean of 4 control plots.

b: Gravimetric water content after the sprinkling experiments (n=20).

c: Mean of t<sub>0</sub> and t<sub>1</sub>.

d: Effective cation exchange capacity. Mean of t<sub>0</sub> and t<sub>3,control</sub>.

e: Effective base saturation in % of CEC<sub>eff</sub>. Mean of t<sub>0</sub> and t<sub>3,control</sub>.

\*\*, \* Difference between flow paths and matrix is significant at  $P < 0.01$  and  $P < 0.05$ , respectively, depths are tested independently.

Each of the four plots was divided into a “control” subplot receiving no wood ash and a “wood ash” subplot, receiving the equivalent of 8 Mg wood ash ha<sup>-1</sup> yr<sup>-1</sup> on 7 May 1998. The wood ash was spread out by hand and formed a thin film on the soil surface. It was produced in 1997 by two medium-sized wood-chip furnaces, using only pure wood chips without additives. The neutral cations Ca, K and Mg contributed most to the elemental composition of the wood ash, which had a pH of 12.5. The wood ash was easily soluble and in October 1998 no ash could be seen on the soil surface.

Soil samples taken before the wood ash application were named “t<sub>0</sub>”. One month after the wood ash application, in June 1998, we took the next set of soil samples (“t<sub>1</sub>”), and approximately 6 months after wood ash addition, in October 1998, we again repeated the sampling procedure (“t<sub>2</sub>”). In May 1999 (i.e. one year after wood ash application), we

collected samples from the control subplots (“ $t_{3,\text{control}}$ ”) and from the wood-ash subplots (“ $t_3$ ”). At each sampling occasion, soil material from all four plots was sampled.

#### 4.3.2 Sampling procedure

The food dye Brilliant Blue (C.I. 42090) was used to stain the preferential flow paths in the soil. We applied 45 mm of dye solution ( $3 \text{ g l}^{-1}$ ) over 6 h to an area of 1 by 1.5 m with a field sprinkler (Flury and Flühler, 1994a; 1994b). One day after application of the dye solution, we dug a trench in the dye application area to 1.2 m depth. A vertical soil profile of 1 by 1 m was prepared with 0.3 m spacing to the border of the sprinkled area. The blue stained areas were defined as preferential flow paths, the non stained areas as soil matrix. With a small spatula we took soil samples from the preferential flow paths and from the soil matrix. Additionally, we took mixed bulk soil samples over the whole width and depth of the individual horizons. The bulk soil is the “normal” type of soil samples that is either taken with soil cores or, as in our case, from the face of a soil profile. We took the bulk soil samples to be able to compare the results obtained for preferential flow paths and for the matrix with the sample type normally taken in soil sampling. Sampling depths were 0 to 9, 9 to 20, 20 to 50, and 50 to 100 cm.

At each trench a series of 5 consecutive soil profiles was prepared at 10 cm spacing from each other. The corresponding soil samples of all 5 profiles from each trench were pooled, resulting in approximately 1 kg fresh soil per sample type and trench. This way we obtained  $n=4$  samples for each flow region and depth at each sampling occasion.

#### 4.3.3 Soil analyses

Exchangeable cations (K, Na, Ca, Mg, Mn, Al, and Fe) were determined by ICP-OES (Perkin Elmer Optima 3000) in extracts with 1 M  $\text{NH}_4\text{NO}_3$  (Zeien and Brümmer, 1989). The effective cation exchange capacity ( $\text{CEC}_{\text{eff}}$ ) was calculated as the sum of exchangeable cations. The effective base saturation ( $\text{BS}_{\text{eff}}$ ) equals the sum of Ca, K, Mg, and Na in % of the  $\text{CEC}_{\text{eff}}$ . Total C and N were measured with a CN auto analyser (NA 1500 and 2500,

Carlo Erba Instruments, Milano, Italy). Texture was determined with the pipette method after removing soil organic matter by digestion in  $\text{H}_2\text{O}_2$  followed by ultrasonic treatment in 0.2% Calgon for 5 min (Gee and Bauder, 1986).

#### 4.3.4 Microbial analyses

Microbial carbon contents of the soil samples were determined with the fumigation-extraction method (Vance et al., 1987). Organic C in acidified  $\text{K}_2\text{SO}_4$  extracts was measured with a total organic carbon analyser (TOC-500 Shimadzu, Tokyo, Japan). The data were expressed as microbial C ( $C_{\text{mic}}$ ) and were not adjusted by conversion factors.

DNA was extracted from fresh soils (approximately 0.5 g dry weight equivalent) using a bead beating procedure. Soil was added to 1.5 ml reaction tubes together with 1 ml extraction buffer (100 mM Tris/HCl pH 7.4, 10 mM EDTA, 1.5% SDS, 1% Deoxycholate, 1% Nonidet P-40, 5 mM thiourea, 10 mM dithiothreitol) (Chatzinotas et al., 1998). Bead beating was performed for 1 min with a B. Braun bead beater (Bender and Hobein, Zürich, Switzerland). The slurry was centrifuged (1 min, 16000 x g). The supernatant was saved and extracted once with 1 volume phenol/chloroform/isoamylalcohol (25:24:1) and twice with 1 volume chloroform/ isoamylalcohol (24/1). The DNA solution was mixed with 1 volume precipitation solution (20% polyethylene glycol 6000, 2.5 M NaCl), incubated at 37°C for 1 h and centrifuged at room temperature (15 min, 16000 x g). The pellet was washed once with 70% ethanol, air dried, and resuspended in TE (10 mM Tris/HCl; 1 mM EDTA, pH 8) at 1 ml  $\text{g}^{-1}$  (dry weight equivalent) extracted soil (Widmer et al., 1996). Extracted DNA was quantified by fluorescence spectroscopy using PicoGreen (Molecular Probes, Eugene, OR, USA) according to the procedure of Sandaa et al. (1998).

For genetic fingerprinting DNA concentrations were adjusted to 2  $\mu\text{g ml}^{-1}$  and 1  $\mu\text{l}$  of these DNA solutions was used for the polymerase chain reaction (PCR) which was performed according to (Widmer et al., 1998). PCR was either performed with specific forward-primers selective for the small subunit (SSU) rRNA genes from Bacteria (EUB338), Archaea (ARCH915), and Eukarya (EUK516) in conjunction with a universal SSU-rRNA reverse primer (UNI-b-rev: GACGGGCGGTGTGT(A/G)CAA) modified from

(Amann et al., 1995) or with a primer combination selective for *Pseudomonas* sp. (Ps-for and Ps-rev) (Table 4.2). Primers were purchased from MWG Biotech (Ebersberg, Germany). PCR amplification was performed with *Taq* polymerase (Amersham, Zürich, Switzerland) with the supplied buffer (2 mM Mg) and at an annealing temperature of 65°C. PCR products were analyzed on 1.2% UltraPure agarose gels (GIBCO/BRL, Life Technologies AG, Basel, Switzerland) and fragmented using restriction endonuclease *Hae*III (Boehringer Mannheim, Rotkreuz, Switzerland) (Widmer et al., 1999). Restriction fragment length polymorphism (RFLP) patterns were analyzed by MetaPhor gel electrophoresis (FMC BioProducts, Rockland, USA) and ethidium bromide staining (Sambrook et al., 1989). Gels were photographed using Polaroid 677 films (Polaroid, Uxbridge, UK).

**Table 4.2:** PCR primers and amplification conditions.

Primer (name)	Length (bp)	Position <sup>a</sup> (bp)	PCR cycles (number)	Reference
EUB338 for	18	338-355	28	(Amann et al., 1995)
ARCH915 for	20	915-934	40	(Stahl and Amann, 1991)
EUK516 for	16	502-516	30	(Amann et al., 1995)
UNI-b-rev	18	1390-1407	var <sup>b</sup>	this study
Ps-for	20	289-308	40	(Widmer et al., 1998)
Ps-rev	18	1258-1275	40	(Widmer et al., 1998)

a: Position of primers according to standard *E. coli* 16S rRNA numbering.

b: Numbers of PCR cycles depended on the specific forward primers EUB338, ARCH915, and EUK516.

#### 4.3.5 Direct cell counts

Direct cell counts were performed with 4',6-diamidino-2'-phenylindole (DAPI; Sigma, Buchs, Switzerland) according to standard procedures (Zarda et al., 1997; Schönholzer et al., 1999). Soil samples (approximately 100 mg) were fixed in 1 ml paraformaldehyde (4%) in phosphate buffered saline (PBS: 130  $\mu$ M NaCl, 7 mM Na<sub>2</sub>HPO<sub>4</sub>, 3 mM NaH<sub>2</sub>PO<sub>4</sub>, pH 7.2) for 12 h at 4°C. Samples were centrifuged (1 min, 16000 x g), washed once with PBS, suspended in ethanol (96%), and stored at -20°C. For cell counting, fixed soil samples were thoroughly mixed and 10 to 120  $\mu$ l aliquots were suspended in sodium pyrophosphate (0.1%) to a final volume of 1 ml. After dispersing soil and cells by sonification (Sonicator b-12, 2 mm dia probe; Branson, Danbury, USA), 10  $\mu$ l to 20  $\mu$ l aliquots were added to slides coated with gelatin (0.1% gelatin, 0.01% KCr(SO<sub>4</sub>)<sub>2</sub>), air dried, and dehydrated for 3 min in each of a series of 50%, 80%, and 96% ethanol. DAPI (4 mg ml<sup>-1</sup> H<sub>2</sub>O) was applied for 10 min. After rinsing the slides with water they were incubated in water for 10 min, and then mounted with Citifluor (Citifluor UKC Laboratory, Canterbury, UK). Direct counts were determined with a Zeiss Axioplan microscope (Carl Zeiss AG, Zürich, Switzerland) fitted for epifluorescence with a high-pressure mercury bulb (50 W) and filter set 02 (G365, Ft395, LP420) at 400 x magnification (Plan-Neofluar 40x/1.30 oil).

#### 4.3.6 Calculations and statistical analyses

Mean values of organic C, C<sub>mic</sub>, DNA, cell counts were compared using analysis of variance (ANOVA, Scheffé, 1959). The statistical model used was a split-plot-model with the plot as the block-factor, the flow region as split-unit-factors, and the time of sampling as the main-unit-factor. Depths were tested independently. The residuals were checked for normality and independence using the normal-probability-plot and the Tukey-Anscombe-plot. Biomass data was transformed  $x_t = \log(x+30)$  prior to analysis. Means of single sampling dates were separated using the paired t-test or the nonparametric Wilcoxon signed rank test for paired data (Conover, 1980). All statistical analyses were performed with the software S-Plus (Version 5.0, 1998, MathSoft, Seattle).



## 4.4 Results

### 4.4.1 Physico-chemical properties of preferential flow paths and soil matrix

As an example, a picture of one of the soil profiles with stained preferential flow paths and unstained soil matrix is shown in Figure 4.1. After the sprinkling experiments the mean water content in the uppermost layer (0-9 cm) was by 10% higher in the preferential flow paths as compared to the matrix (Table 4.1). At 9-20 cm depth it was still higher in the preferential flow paths by 3%.

Initially, there was no significant pH difference (ANOVA:  $P=0.97$ ) between preferential flow paths and matrix soil (Table 4.1). The application of 8 Mg wood ash  $\text{ha}^{-1}$  increased the pH in the preferential flow paths of the uppermost horizon from 3.4 to values of 4.0, 4.3, and 3.9 after 1, 6, and 12 months after ash application. The differences between preferential flow paths and matrix were 0.4, 0.8 and 0.3 pH units, respectively. The largest increase in the pH values and the largest difference between preferential flow paths and matrix was found 6 months after ash application.

The soil organic matter content in the preferential flow paths was higher than in the matrix (Table 4.1). The organic C concentrations ( $C_{\text{org}}$ ) from top to bottom were by 42%, 12%, 28%, and 69% higher in the preferential flow paths than in the matrix. The organic N concentration was similarly enriched in the preferential flow paths (Table 4.1). Even without wood ash application the preferential flow paths had a significantly higher effective cation exchange capacity ( $\text{CEC}_{\text{eff}}$ ) and effective base saturation ( $\text{BS}_{\text{eff}}$ ) than the soil matrix down to a depth of 20 cm. At one month after wood ash application ( $t_1$ ), the  $\text{CEC}_{\text{eff}}$  changed remarkably only in the preferential flow path of the uppermost sampling depth (+12%). Even more pronounced was the increase of the base saturation of the same depth (+2.2-fold in the preferential flow path and +1.4-fold in the matrix).

### 4.4.2 Microbial biomass in preferential flow paths and soil matrix

A typical depth function of the microbial C ( $C_{\text{mic}}$ , Figure 4.1) shows a mean of 225 mg  $C_{\text{mic}}$  ( $\text{kg}^{-1}$  dry soil) in the preferential flow paths and 104 mg  $C_{\text{mic}}$   $\text{kg}^{-1}$  in the matrix of the

uppermost soil horizon, and a rapid decrease with depth. The concentrations of  $C_{\text{org}}$  and  $C_{\text{mic}}$  in the different depths was highly correlated ( $R^2=0.90$ ,  $P<0.001$ ). The  $C_{\text{mic}}$  was higher in the preferential flow paths than in the matrix (ANOVA:  $P<0.001$ , for all sampling occasions). The enrichment in the preferential flow paths as compared to the matrix was 24%, 35%, 9% and 92% top down and the difference of  $C_{\text{mic}}$  between preferential flow paths and matrix changed significantly with depth (ANOVA;  $P<0.001$ ). Soil samples from October 1998, that were used for the specific microbial analysis also displayed significant differences of  $C_{\text{mic}}$  between preferential flow paths and matrix (Wilcoxon test:  $P=0.001$ ). The differences between preferential flow paths and matrix were in the same order of magnitude as the differences between individual soil plots, the greatest difference between preferential flow paths and matrix being  $196 \text{ mg } C_{\text{mic}} \text{ kg}^{-1}$  and between plots only  $123 \text{ mg } C_{\text{mic}} \text{ kg}^{-1}$ .

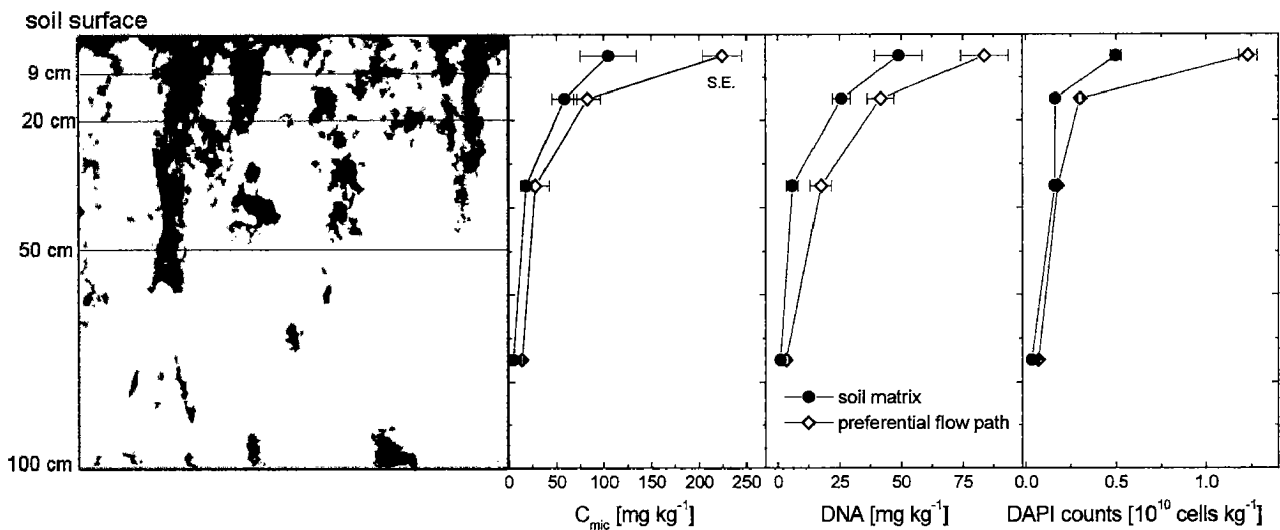


**Figure 4.1:** Processed photo of a soil profile of 1 by 1 m with stained preferential flow paths and unstained matrix. Depth profile of  $C_{\text{mic}}$  concentrations and DNA concentrations, and cell counts in preferential flow paths and matrix ( $n = 4$ ).

We measured temporal variations of  $C_{mic}$  in the uppermost horizon (Figure 4.2). However, we cannot distinguish between simple seasonal variations and changes through the wood ash addition. The  $C_{mic}$  of  $t_0$  (control) differed significantly from  $t_1$  (one month after wood ash addition,  $P=0.04$ ), which could have been attributed to a wood ash effect. However,  $t_0$  also differed significantly from  $t_{3,control}$  ( $P=0.004$ ), although both control treatments were sampled in spring (April and May) of two subsequent years. Also, the sampling program was not a significant factor for the differences of  $C_{mic}$  between preferential flow paths and matrix (ANOVA:  $P=0.55$ ), indicating that there was no temporal variation in the differences of  $C_{mic}$  between preferential flow paths and matrix.

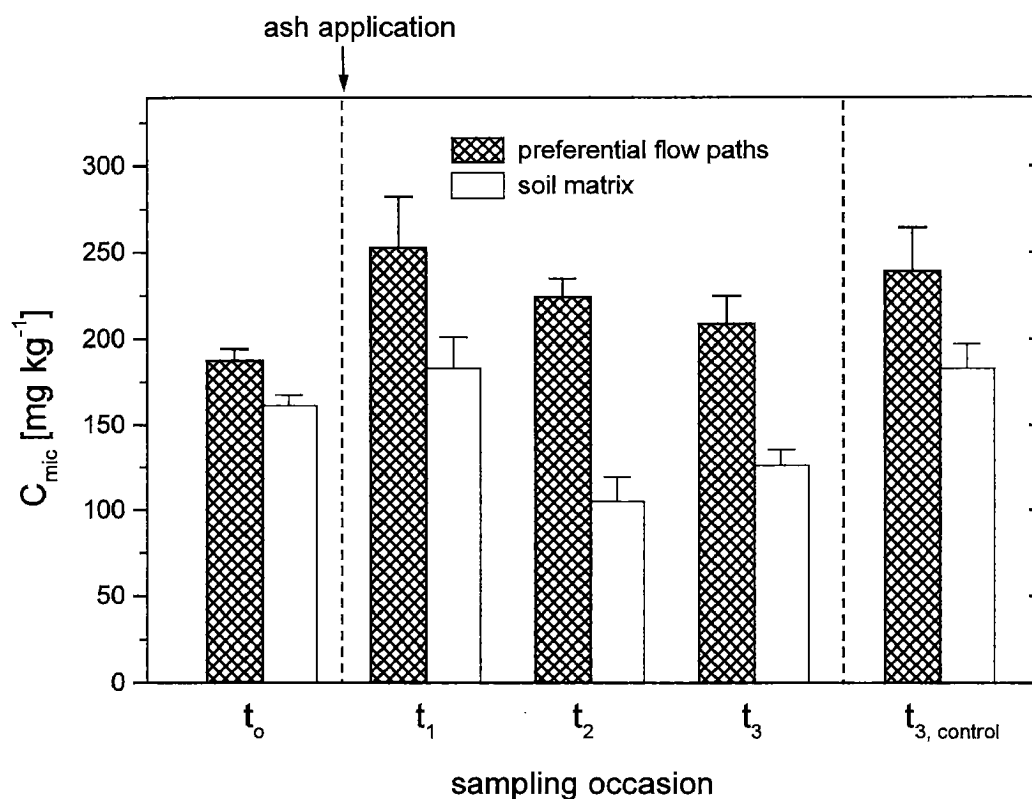


**Figure 4.2:** Mean  $C_{mic}$  concentrations ( $n=4$  plots) in preferential flow paths and soil matrix at the 5 different sampling occasions at 0-9 cm depth.

For a more detailed analysis of the microbial communities in the soils we determined total soil DNA contents and the number of microbial cells (Figure 4.1). Figure 4.3 shows the correlation between  $C_{mic}$ , extracted DNA, and direct cell counts at  $t_2$ . The linear regression revealed a good agreement between the different and independently measured microbial variables.

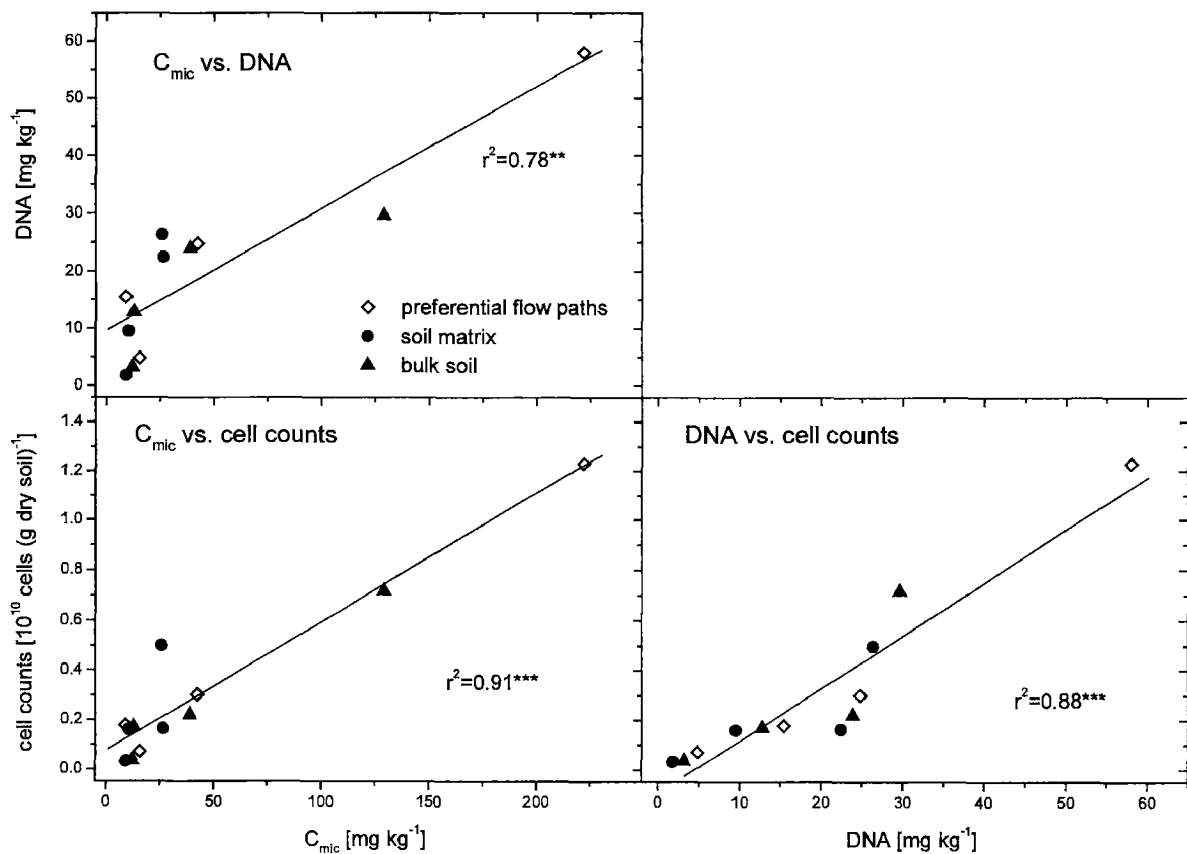


**Figure 4.3:** Correlation between  $C_{mic}$  and DNA concentrations and DAPI cell counts of all 4 depths of one plot at  $t_2$ . Clusters of the 3 different sample types (preferential flow paths, matrix, and bulk soil) are discernible for each depth.

#### 4.4.3 Ribosomal RNA gene fingerprints from preferential flow paths and matrix

For community structure analyses we applied PCR/RFLP procedures specific for ribosomal RNA genes of the domains Bacteria, Archaea, and Eukarya, and for the bacterial genus *Pseudomonas* (Figure 4.4).

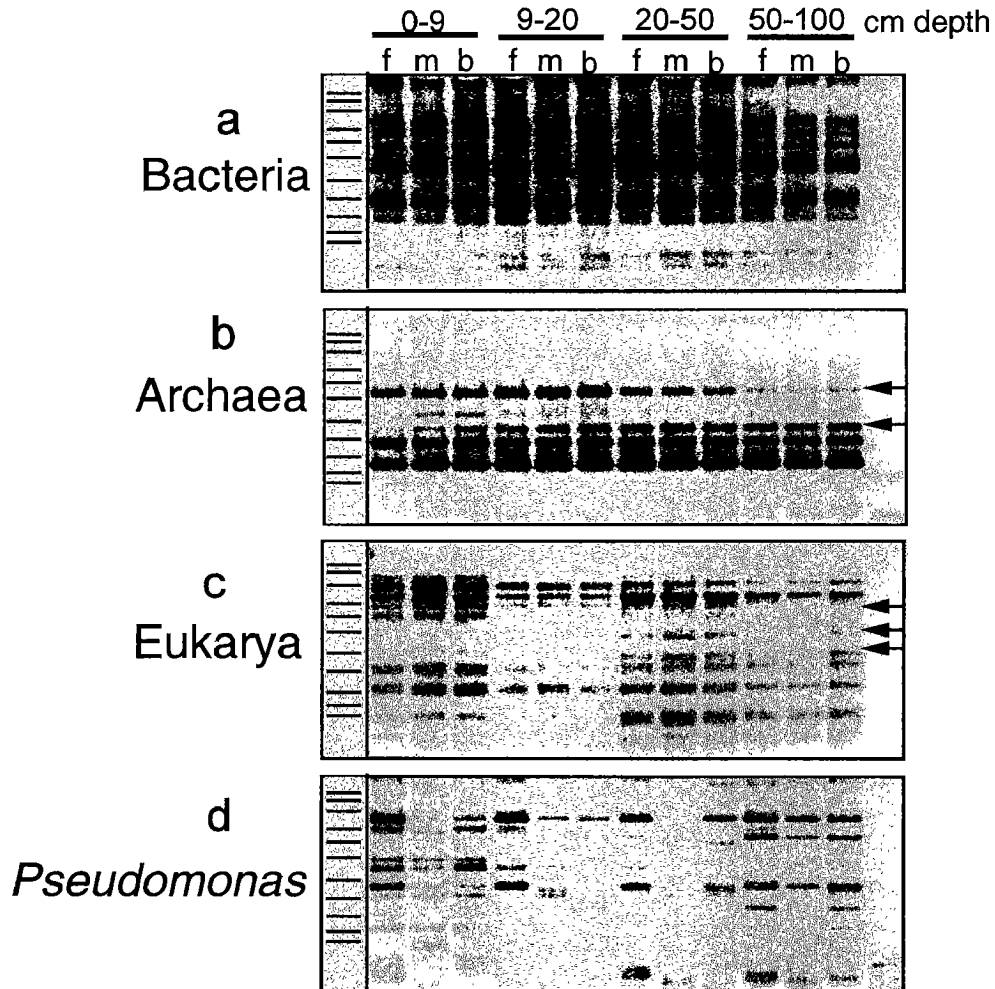


**Figure 4.4:** Photos of agarose-gels with genetic fingerprints of Bacteria (a), Archaea (b), Eukarya (c) and *Pseudomonas* sp. (d). Each picture includes the fingerprints of the preferential flow paths (f), the matrix (m), and the bulk soil (b) from left to right in the 4 sampling depths. The arrows mark bands referred to in the text. The soil material was taken in October 1998.

The bacterial fingerprints showed neither detectable differences between preferential flow paths and soil matrix, nor any change with increasing depths (Figure 4.4a). Archaeal (Figure 4.4b) and eukaryal (Figure 4.4c) fingerprints did not differ between preferential flow paths and soil matrix, but reflected the depth gradient. Fingerprints for archaea revealed a gradual increase of one band intensity and a gradual decrease of another (arrows in Figure 4.4b). Fingerprints for eukarya indicated more pronounced changes of the population structure from one depth to the next. Arrows in Figure 4.4c highlight noticeable bands. Only the fingerprints for the bacterial genus *Pseudomonas* revealed a clear difference between the preferential flow paths and the matrix samples (Figure 4.4d). However, the intensities of the amplification products differed between the sample types more than the fingerprints. The signal intensities of the *Pseudomonas*-specific PCR amplification products (data not shown) from preferential flow paths were 1.4-fold to 3.0-fold higher than the ones obtained for the matrix, indicating that relative numbers of *Pseudomonas* sp. were higher in the preferential flow paths.

## 4.5 Discussion

### 4.5.1 Physico-chemical soil properties

Preferential flow paths have physico-chemical properties that are distinct from those of the soil matrix. Gradients between preferential flow paths and soil matrix can be formed, because the preferential flow paths are persistent for decades in the studied forest soil (Bundt et al., 2000). Depending on the initial water content and the rain intensity, patterns of preferential flow paths might change, but on the whole, the same preferential flow paths are actively conducting water for long periods (Bundt et al., 2000). Some of the preferential flow paths clearly traced old root channels or living roots, but others were linked to cracks or fissures or originated from inhomogeneous infiltration at the soil surface. Therefore, the preferential flow paths that were stained by the dye application, include to some extent rhizosphere soil, but do not solely consist of rhizosphere soil.

Potentially, differences in physico-chemical properties influence the microbial biomass as well as the microbial community structures.

If we assume almost equilibrated water contents before the sprinkling experiment, the higher water contents in the preferential flow paths indicate high and rapid fluctuations of the water content in the preferential flow paths at high rainfall intensities. This causes rapidly and constantly changing environmental conditions for microorganisms in the preferential flow paths. For example, the release of microbial biomass C can be enhanced by the rewetting of relatively dry soil (Kieft et al., 1987).

One might expect a lower pH in the preferential flow paths as compared to the matrix, due to preferential percolation of rainwater and organic acids from the forest floor. Possibly, pH is not an indicator sensitive enough to detect small differences in the physico-chemical environment. Also, the pH increase after wood ash application was not high compared to other studies, where increases of 2.5 pH units were found after adding only 5 t wood ash ha<sup>-1</sup> (Bååth and Arnebrant, 1994). The small effect of wood ash application in our study may be explained by a large buffering capacity of the soil or by the leaching of much of the ash during the first heavy rain storms that occurred shortly after application without altering the soil pH (S. Zimmermann, pers. comm.).

The higher organic matter content in the preferential flow paths could be due to the greater proportion of living or decayed roots in flow paths than in the matrix (Bundt et al., 2000), or to preferential input of dissolved organic matter from the forest floor. A consequence of the organic matter distribution is the higher effective cation exchange capacity in the flow paths. Also, the effective base saturation is higher in the flow paths, pointing to external inputs of neutral cations in the preferential flow paths even before the ash treatment. The increase in base saturation after wood ash addition was probably caused by the input of easily soluble salts (mostly Ca) from the wood ash (Kahl et al., 1996). This means that preferential flow paths are important pathways for nutrient transport into the mineral soil.

In conclusion, both substrate availability and nutrient supply are higher in the preferential flow paths than in the soil matrix.

#### 4.5.2 Possible wood ash effects on microbial biomass

The effect of liming or wood ash addition on microbial biomass is mostly attributed to changes of pH (Bååth and Arnebrant, 1994; Smolander and Mälkönen, 1994). We did not detect significant effects of wood ash application on  $C_{mic}$  (Figure 4.2), which is in accordance to other studies (Fritze et al., 1994). Also, the reported effects of wood ash application on soil microbial biomass are diverse and include both stimulation (Bååth and Arnebrant, 1994) and no change (Fritze et al., 1994). The lack of microbial growth may also be explained by the unbalanced nutritional composition of wood ash. Only Ca, Mg, and K are supplied in larger quantities, whereas the growth of microorganisms is rather P and N limited (Vitousek and Howarth, 1991). However, Bååth et al. (1995) showed that wood ash addition only slightly altered the microbial community structure as determined by phospholipid fatty acid analyses.

#### 4.5.3 Microbial biomass variables

Overall, the favourable living conditions in preferential flow paths are reflected by the higher microbial biomass (Figure 4.1). Our results support those of Vinther et al. (1999), who found higher bacterial biomass, higher bacterial numbers and a higher rate of microbial processes (e.g. denitrification) in macropore material as compared to matrix soil from a forest and an agricultural site. They state that the differences were driven by increased substrate supply and transportation of bacterial cells through the macropores. Our results confirm those of Gobran et al. (1998), who reported that differences between rhizosphere and bulk soil were based on increased nutrient availability in the rhizosphere.

The results from our biomass analysis are supported by quantification of DNA concentrations and direct cell counts in the soil samples. The high correlation between  $C_{mic}$  extracted with the fumigation-extraction method and microbial biomass determined by direct microscopy is consistent with the findings of Martikainen and Palojärvi (1990).

Data from the different depths form subgroups within the plots (clusters are visible in Figure 4.3). Since fungi and bacteria have different cell-to-DNA ratios, the different ratios might be a hint towards different microbial populations at the different depths. For



example, the DNA vs. cell counts plot shows a smaller cell-to-DNA ratio for 9-20 cm depth than average, suggesting more bacteria. Although PCR/RFLP is not a quantitative technique, Figure 4.4c suggests less eukarya in the 9-20 cm depth, which points into the same direction.

The slopes of the regression lines describing the matrix, bulk soil, and flow paths for the individual depths are always slightly different. This could also be an indicator for different microbial populations in the different sample types (i.e. preferential flow paths, matrix, and bulk soil). However, the limited data did not allow for a detailed statistical analysis.

#### 4.5.4 Microbial population structures

Due to the differences in soil chemical properties and microbial variables ( $C_{mic}$ , DNA contents, and microbial cell numbers) between preferential flow paths and soil matrix we assumed that population differences might occur in the different soil compartments as well as down the depth gradient.

However, none of the domain-specific fingerprints displayed differences between preferential flow paths and soil matrix communities. Only the bacterial genus *Pseudomonas* indicated that there are specific bacterial communities adapted to the different living conditions in the two soil compartments. In the analysis of the total bacterial communities very stable major populations in the soil may obscure these differences. Our results imply that the whole community may profit from the improved growth conditions in the preferential flow paths, which results in a biomass increase of up to 92%. It is possible that only few communities with a broad acceptance for substrates and oxygen demand like *Pseudomonas* sp. specifically profit to some degree from the favourable growth conditions in the preferential flow paths.

All fingerprints but those for Bacteria showed distinct depths dependence. The fingerprints for Archaea indicated only gradual changes along the depth gradient while Eukarya displayed the most pronounced depth dependence. The high stability of bacterial fingerprints (Figure 4.4a) was to some extent unexpected. If decreasing oxygen supply along the depth gradient was assumed, anaerobic growing populations would succeed

aerobic ones, possibly having effects on the fingerprints. The lack of response found in our soil may be explained with a rather stable and homogenous bacterial community at the site in Unterehrendingen. Additionally, the soil was not anaerobic, as indicated by rather high nitrate concentrations up to 125 mg l<sup>-1</sup> in the soil solution of 75-80 cm depth (S. Zimmermann, pers.comm.).

#### 4.6 Conclusions

Preferential flow paths are more exposed to drying and wetting than the soil matrix. They permit a better nutrient and substrate supply than the soil matrix. The overall favourable living conditions in preferential flow paths are reflected by a significantly larger microbial biomass. Therefore, preferential flow paths may be interpreted as continuous 'hot spots' in soils. Microbial community structures as measured by domain-specific genetic fingerprints did not differ between preferential flow paths and soil matrix. Specialized microbial groups such as the genus *Pseudomonas* adapted to the broader spectrum of substrates and changes in environmental conditions which was reflected by a higher relative abundance of these communities in the preferential flow paths. In general, our results suggest that the whole microbial community profit from the favourable living conditions along preferential flow paths. Also, the limitations of the genetic fingerprinting technique are evident. Domain-specific as well as genera specific primers are necessary to analyse the microbial community structure. In our study the high bacterial diversity completely masked the changes between different soil compartments and with depth that were evident when we studied single genera.

#### 4.7 References

- Amann, R.L., W. Ludwig, and K.-H. Schleifer. 1995. Phylogenetic and in situ detection of individual microbial cells without cultivation. *Microbiol. Rev.* 59: 143-169.
- Bååth, E., and K. Arnebrant. 1994. Growth rate and response of bacterial communities to pH in limed and ash treated forest soils. *Soil Biol. Biochem.* 26: 995-1001.
- Bååth, E., Å. Frostegård, T. Pennanen, and H. Fritze. 1995. Microbial community structure and pH response in relation to soil organic matter quality in wood-ash fertilized, clear cut or burned coniferous forest soil. *Soil Biol. Biochem.* 27: 229-240.
- Beven, K., and P. Germann, 1982. Macropores and water flow in soils. *Water Resour. Res.* 18: 1311-1325.
- Bundt, M., A. Albrecht, P. Froidevaux, P. Blaser, and H. Flühler. 2000. Impact of preferential flow on radionuclide distribution in soil. *Environ. Sci. Technol.* 34: 3895-3899.
- Chatzinotas, A., R.-A. Sandaa, W. Schönhuber, R. Amann, F.L. Daae, V. Torsvik, J. Zeyer, and D. Hahn. 1998. Analysis of broad-scale differences in microbial community composition of two pristine forest soils. *Syst. Appl. Microbiol.* 21: 579-587.
- Conover, W.J. 1980. *Practical Nonparametric Statistics*. 2<sup>nd</sup> edn. Wiley, New York.
- Edwards, W.M., M.J. Shipitalo, L.B. Owens, and W.A. Dick. 1993. Factors affecting preferential flow of water and Atrazine through earthworm burrows under continuous no-till corn. *J. Environ. Qual.* 22: 453-457.
- Flury, M., 1996. Experimental evidence of transport of pesticides through field soils- A review. *J. Environ. Qual.* 25: 25-45.
- Flury, M., and H. Flühler. 1994a. Brilliant Blue FCF as a dye tracer for solute transport studies- A toxicological overview. *J. Environ. Qual.* 23: 1108-1112.
- Flury, M., and H. Flühler. 1994b. Susceptibility of soils to preferential flow of water: A field study. *Water Resour. Res.* 30: 1945-1954.
- Fritze, H., A. Smolander, T. Levula, V. Kitunen, and E. Mälkönen. 1994. Wood-ash fertilization and fire treatments in a Scots pine forest stand: effects on the organic layer, microbial biomass, and microbial activity. *Biol. Fert. Soils* 17: 57-63.
- Gee, G.W., and J.W. Bauder. 1986. Particle-size analysis. pp. 383-411. *In* Page, A.L., R.H. Miller, and D.R. Keeney (eds.) *Methods of Soil Analysis. Part 1: Physical and Mineralogical Methods*. American Society of Agronomy, Madison.

- Ghodrati, M., and W.A Jury. 1990. A field study using dyes to characterize preferential flow of water. *Soil Sci. Soc. Am. J.* 54: 1558-1563.
- Gobran, G.R., S. Clegg, and F. Courchesne. 1998. Rhizospheric processes influencing the biogeochemistry of forest ecosystems. *Biogeochem.* 42: 107-120.
- Hagedorn, F., J. Mohn, P. Schleppei, and H. Flühler. 1999. The role of rapid flow paths for nitrogen transformation in a forest soil- a field study with micro suction cups. *Soil Sci. Soc. Am. J.* 63: 1915-1923.
- Joergensen, R.G. 2000. Ergosterol and microbial biomass in the rhizosphere of grassland soils. *Soil Biol. Biochem.* 31: 647-652.
- Kahl, J.S., I.J. Fernandez, L.E. Rustad, and J. Peckenham. 1996. Threshold application rates of wood ash to an acidic forest soil. *J. Environ. Qual.* 25: 220-227.
- Kieft, T.L., E. Soroker, and M.K. Firestone. 1987. Microbial biomass response to a rapid increase in water potential when dry soil is wetted. *Soil Biol. Biochem.* 19: 119-1265.
- Mallawatantri, A.P., B.G. McConkey, and D.J. Mulla. 1996. Characterization of pesticide sorption and degradation in macropore linings and soil horizons of Thatuna silt loam. *J. Environ. Qual.* 25: 227-235.
- Martikainen, P.J., and A. Palojarvi. 1990. Evaluation of the fumigation-extraction method for the determination of microbial C and N in a range of forest soils. *Soil Biol. Biochem.* 22: 797-802.
- Parkin, T.B. 1987. Soil microsites as a source of denitrification variability. *Soil Sci. Soc. Am. J.* 51: 1194-1199.
- Petersen, S.O., T.H. Nielsen, Å. Frostegård, and T. Olesen. 1996. O<sub>2</sub> uptake, C metabolism and denitrification associated with manure hot-spots. *Soil Biol. Biochem.* 28: 341-349.
- Pivetz, B.E., and T.S. Steenhuis. 1995. Soil matrix and macropore biodegradation of 2,4-D. *J. Environ. Qual.* 24: 564-570.
- Sambrook, J., E.F. Fritsch, and T. Maniatis. 1989. *Molecular Cloning: A Laboratory Manual*. 2<sup>nd</sup> edn. Cold Spring Harbor Laboratory Press, Plainview.
- Sandaa, R.-A., Ø. Enger, and V. Torsvik. 1998. Rapid method for fluorometric quantification of DNA in soil. *Soil Biol. Biochem.* 30: 265-268.
- Scheffé, H. 1959. *The Analysis of Variance*. Wiley, New York.
- Schönholzer, F., D. Hahn, and J. Zeyer. 1999. Origins and fate of fungi and bacteria in the gut of *Lumbricus terrestris* L. studied by image analysis. *FEMS Microbiol. Ecol.* 28: 235-248.

- Selker, J.S., T.S. Steenhuis, and J.-Y. Parlange. 1992. Wetting front instability in homogeneous sandy soils under continuous infiltration. *Soil Sci. Soc. Am. J.* 56: 1346-1350.
- Sexstone, A.J., N.P. Revsbech, T.B. Parkin, and J.M. Tiedje. 1985. Direct measurement of oxygen profiles and denitrification rates in soil aggregates. *Soil Sci. Soc. Am. J.* 49: 645-651.
- Smolander, A., and E. Mälkönen. 1994. Microbial biomass C and N in limed soil of Norway spruce stands. *Soil Biol. Biochem.* 26: 503-509.
- Soil Survey Staff. 1994. *Keys to Soil Taxonomy*. 6<sup>th</sup> edn. Pocahontas Press, Blacksburg.
- Sollins, P., and R. Radulovich. 1988. Effects of soil physical structure on solute transport in a weathered tropical soil. *Soil Sci. Soc. Am. J.* 52: 1168-1173.
- Stagnitti, F., J.-Y. Parlange, T.S. Steenhuis, J. Boll, B. Pivetz, and D.A. Barry. 1995. Transport of moisture and solutes in the unsaturated zone by preferential flow. pp. 193-224. *In* Singh, V. P. (ed.) *Environmental Hydrology*. Kluwer Academic Publishers. Dordrecht.
- Stahl, D.A., and R.I. Amann. 1991. Development and application of nucleic acid probes. pp. 205-248. *In* Stackebrandt, E., and M. Goodfellow (eds.) *Nucleic Acid Techniques in Bacterial Systematics*. John Wiley, Chichester.
- Stamm, C., H. Flühler, R. Gächter, J. Leuenberger, and H. Wunderli. 1998. Preferential transport of phosphorus in drained grassland soils. *J. Environ. Qual.* 27: 515-522.
- van Noorwijk, M., P.C. de Ruiter, K.B. Zwart, J. Bloem, J.C. Moore, H.G. van Faassen, and S.L.G.E. Burgers. 1993. Synlocation of biological activity, roots, cracks and recent organic inputs in a sugar beet field. *Geoderma* 56: 265-276.
- Vance, E.D., P.C. Brooks, and D.S. Jenkinson. 1987. An extraction method for measuring soil microbial biomass C. *Soil Biol. Biochem.* 19: 703-707.
- Vinther, F.P., F. Eiland, A.-M. Lind, and L. Elsgaard. 1999. Microbial biomass and numbers of denitrifiers related to macropore channels in agricultural and forest soils. *Soil Biol. Biochem.* 31: 603-611.
- Vitousek, P.M., and R.W. Howarth. 1991. Nitrogen limitation on land and in the sea: How can it occur? *Biogeochem.* 13: 87-115.
- Widmer, F., R.J. Seidler, P.M. Gillevet, L.S. Watrud, and G.D. Di Giovanni. 1998. A highly selective PCR protocol for detecting 16S rRNA genes of the genus *Pseudomonas* (sensu stricto) in environmental samples. *Appl. Environ. Microbiol.* 64: 2545-2553.

- 
- Widmer, F., R.J. Seidler, and L.S. Watrud. 1996. Sensitive detection of transgenic plant marker gene persistence in soil microcosms. *Molecul. Ecol.* 5: 603-613.
- Widmer, F., B.T. Shaffer, L.A. Porteous, and R.J. Seidler. 1999. Analysis of *nifH* gene pool complexity in soil and litter at a Douglas fir forest site in the Oregon Cascade mountain range. *Appl. Environ. Microbiol.* 65: 374-380.
- Zarda, B., D. Hahn, A. Chatzinotas, W. Schoenhuber, A. Neef, R.I. Amann, and J. Zeyer. 1997. Analysis of bacterial community structure in bulk soil by in situ hybridization. *Arch. Microbiol.* 168: 185-192.
- Zeien, H., and G.W. Brümmer. 1989. Chemische Extraktionen zur Bestimmung von Schwermetallbindungsformen in Böden. *Mitteilg. Dt. Bodenkundl. Ges.* 59: 505-510.



## **CHAPTER 5**

# **Sorption characteristics of preferential flow paths and transport of reactive solutes after wood ash application**

with

STEFAN ZIMMERMANN, FRANK HAGEDORN AND PETER BLASER

Submitted to the European Journal of Soil Science



### 5.1 Abstract

As a consequence of heterogeneous transport in soils, only a small part of the soil might be responsible for sorbing incoming elemental loads. We sampled soil material of a forest soil from preferential flow paths and from the matrix after staining the preferential flow paths with a dye. We measured sorption characteristics of these two flow regions and estimated the significance of preferential flow paths for the transport of solutes leached from surface applied wood ash. In the preferential flow paths, the cation exchange capacity of was 12%, the base saturation was 217%, and the soil organic matter content was 41% higher than in the soil matrix of the uppermost 9 cm of the soil. In preferential flow paths, the sorption capacity for Cu was increased as compared to the matrix, while the sorption capacity for Sr was similar in both flow regions. The impact of the application of 8 Mg wood ash ha<sup>-1</sup> on soil chemical properties was mainly restricted to the uppermost 20 cm of the soil and was negligible in the matrix, while chemical properties of preferential flow paths significantly changed. Concentrations of exchangeable Ca in the preferential flow paths increased nearly ten-fold during the six months following the wood-ash application, those of organically bound Pb by 50%. The opposite effect was found for exchangeable Al. Our results show that only part of the whole soil volume, approximately 50% of 0 to 20 cm in our study, are involved in transporting and sorbing the elements applied with the wood ash or as tracers. This must be considered when calculating the maximal amount of any addition of fertilizer, wood ash, or liming agent.

## **5.2 Introduction**

Rising landfill costs and the environmental ethics of recycling and re-using secondary products has triggered a renewed interest in the disposal of wood ash in forests. The benefits of wood ash applications to forest soils are an input of essential basic cations, especially Ca, K, and Mg, and a rise in pH of forest soils (Eriksson, 1990; Kahl et al., 1996; Meiwes, 1995). These positive effects are often accompanied by side effects. The greatest concern is generally given to the additional loading of forest soils with heavy metals (Bramyard and Fransman, 1995). Another problem is the high reactivity and the high pH of the wood ash itself, since it may lead to a mineralization flush with additional nutrient losses, mobilization of dissolved organic matter and pollutants, and to a damage of the sensitive biological communities of the forest floor (Cervelli et al., 1987; Frostegård et al., 1993; Kahl, et al., 1996).

In almost all studies, bulk samples of the forest soils, of the organic layer, or of the soil solution are taken and analyzed when assessing the positive and negative effects of a wood ash application. Most of the common sampling methods do not take the small scale spatial heterogeneity of forest soils into account. Heterogeneities are usually considered on a large scale, or in the vertical direction along the gradients with soil depth. Small-scale heterogeneities have already been reported for soil aggregates (Hildebrand, 1991; Wilcke and Kaupenjohann, 1998) and for macropores (Pierret et al., 1999; Pivetz and Steenhuis, 1995; Turner and Steele, 1988; Vinther et al., 1999). These studies indicate that nutrients, heavy metals, sorption characteristics, and biodegradation of pesticides vary within centimeters of soil. In the mentioned studies, the heterogeneities are not randomly distributed, but are linked to the soil structure. The main cause for the formation of such heterogeneities is thought to be the preferential flow of water. Preferential flow is the rapid transport of water and solutes through the soil that bypasses a large part of the soil matrix. This also implies that only part of the soil is responsible for sorbing and buffering incoming elemental loads, such as from deposited wood ash. Therefore, it is crucial to know the transport pathways of the anthropogenic element input. Also, sorption characteristics of preferential flow paths and soil matrix might be different from each other. When studying and modeling solute transport, however, different sorption characteristics must be considered.

In this study, we tested the hypothesis that:

- (1) surface-applied substances such as wood-ash products affect only a small fraction of the soil volume, and
- (2) sorption characteristics of preferential flow paths and soil matrix are different.

## 5.3 Materials and Methods

### 5.3.1 Study site

The study was conducted at a forested site in Unterehrendingen, Switzerland (N: 47°30'34"/E: 008°20'50"). The forest was planted in 1930 with Norway spruce (*Picea abies* (L.) Karst.) as the dominant tree species mixed with beech (*Fagus sylvatica* L.) and some other species. Soil type is a fine-loamy mixed typic Haplumbrept (Soil Survey Staff, 1994). Selected properties are given in Table 5.1.

**Table 5.1:** Physical and chemical properties of preferential flow paths and soil matrix.

	Depth [cm]	pH <sup>a</sup>	Sand	Silt	Clay	f <sup>b</sup>	C <sub>org</sub> <sup>c</sup> [g kg <sup>-1</sup> ]	CEC <sub>eff</sub> <sup>d</sup> [mmol <sub>c</sub> kg <sup>-1</sup> ]	BS <sub>eff</sub> <sup>d</sup> [%]	Mn <sub>Ox</sub>	Fe <sub>Dith</sub>	Fe <sub>Ox</sub>	Fe <sub>Py</sub>
			-----[%]-----								-----[mg kg <sup>-1</sup> ]-----		
Pref. flow path	0-9	3.4	43	38	19	69	34.5	83.8	30	88	8627	3210	3087
	9-20	3.7	38	42	20	38	14.5	65.2	20	147	8800	3246	2300
	20-50	3.8	35	42	23	13	8.2	60.7	26	215	10053	3285	1736
	50-100	3.8	26	47	27	2	4.9	80.0	45	157	12867	2883	1191
Matrix	0-9	3.4	37	41	22	31	24.3	74.6	21	93	8653	3288	2977
	9-20	3.6	36	42	22	62	12.9	60.7	18	150	9240	3300	2203
	20-50	3.8	35	41	24	87	6.4	58.4	26	259	10240	3201	1482
	50-100	3.8	28	44	27	98	2.9	80.4	43	336	14013	3175	855

a: pH in 0.01 M CaCl<sub>2</sub>, mean of 4 control plots.

b: f: Volumetric fraction of preferential flow paths and matrix

c: Mean of C1 and t1.

d: Mean of control plots.

The soil samples were taken from four plots that were situated immediately outside the HARWA (wood ash recycling experiment) experimental sites (Figure 5.1), where we took the soil water samples (see below). Each of the four plots was divided into a “control” subplot receiving no wood ash and a “wood ash” subplot, receiving the equivalent of 8 Mg wood ash  $\text{ha}^{-1} \text{yr}^{-1}$  on 7 May 1998.

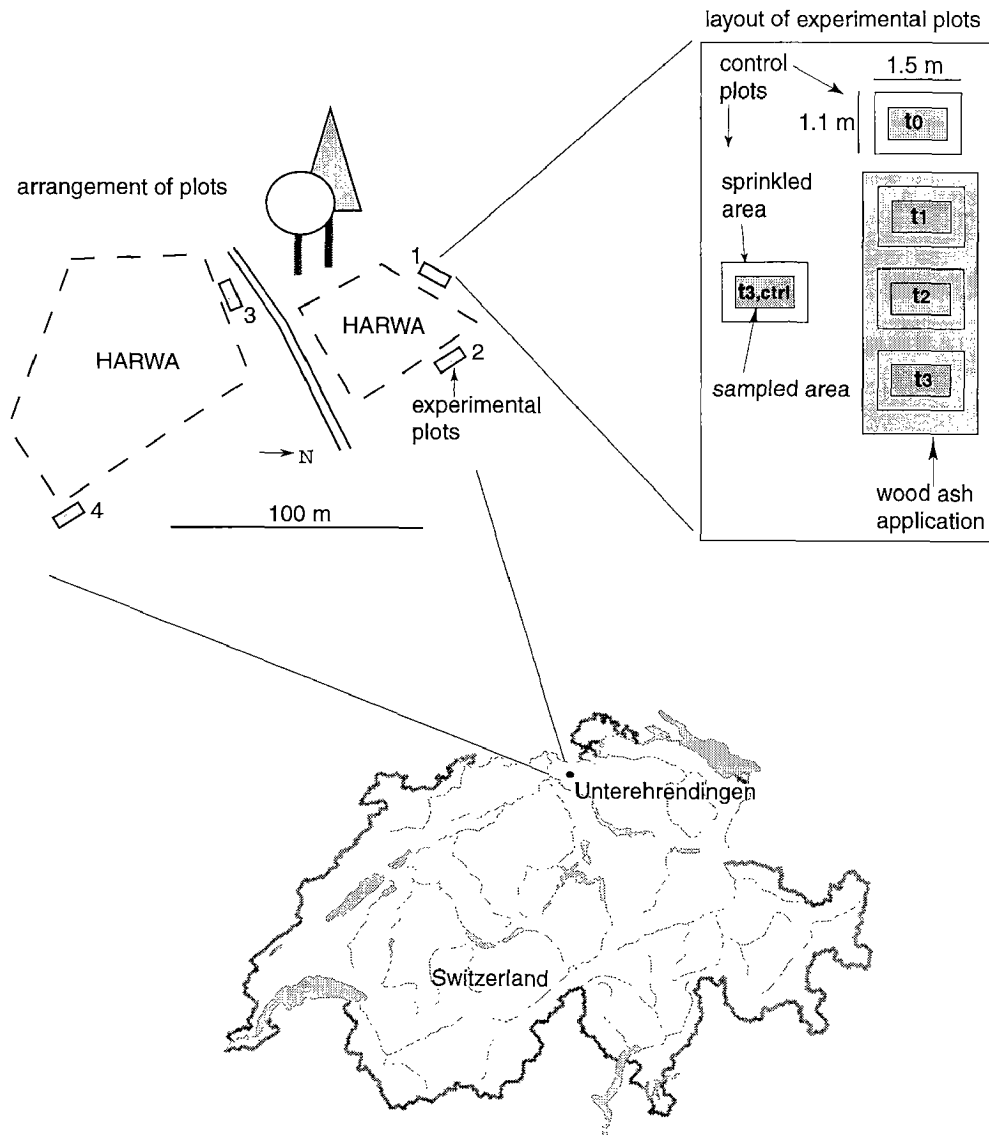


**Figure 5.1:** Location of the study site and experimental setup.

The wood ash was spread out by hand and formed a thin film on the soil surface. It was produced in 1997 by two medium-sized wood-chip furnaces, using only pure wood

chips without additives. The cations Ca, K and Mg contributed most to the elemental composition of the wood ash (Table 5.2).

**Table 5.2:** Chemical properties of the used wood ash and loads to the forest soil with the amount of 8 Mg ha<sup>-1</sup>.

	wood ash [mg kg <sup>-1</sup> ]	Input with 8 Mg ha <sup>-1</sup> [mg m <sup>-2</sup> ]	Recovery (range) <sup>a</sup> [% of input]
pH (H <sub>2</sub> O)	12.5		
Ca	285064	228051	41 to 101
K	59382	47505	45 to 81
Mg	22829	18263	94 to 196
Al	5726	4581	-1923 to 1050
Fe	2072	1658	-191 to 51
Mn	3135	2508	-672 to 193
Zn	267	213	-500 to 92
Cu	131	105	-201 to 3
Pb	14	11	536 to 5427

a: Data was used from plots 1, 2, and 4.

Immediately after spreading the ash, we applied 20.29 g Br<sub>2</sub>Sr·6H<sub>2</sub>O m<sup>-2</sup> (i.e. 5 g Sr m<sup>-2</sup>) as a tracer dissolved in 1 L of distilled water on each plot. This amount of water was sufficient to leach ash particles off the sparse ground vegetation and hence prevent loss of ash due to wind. By October 1998 the applied wood ash was completely dissolved and no longer visible at the soil surface. Soil samples taken before the wood ash application were named “t<sub>0</sub>”. One month after the wood ash application, in June 1998, we took the next set of soil samples (“t<sub>1</sub>”), and approximately 6 months after wood ash application, in October 1998, we again repeated the sampling procedure (“t<sub>2</sub>”). In May 1999 (i.e. one year after wood ash application), we collected samples from the control subplots (“t<sub>3,control</sub>”) and from the wood-ash subplots (“t<sub>3</sub>”).

### 5.3.2 Sampling procedure

At every sampling campaign, we took soil samples from each of the four plots. The sampling procedure included a dye-tracer experiment to stain the preferential flow paths in the soil. With a field sprinkler we applied 45 mm of de-ionized water containing 3 g Brilliant Blue (CI 42090) per liter at a rate of  $7.5 \text{ ml hr}^{-1}$  (Flury and Flühler, 1994a; Flury and Flühler, 1994b). This corresponds approximately to a heavy rainstorm that is not unusual for the area. One day after dye application, we opened a trench to 1.2 m depth. A vertical soil profile of 1 by 1 m was prepared 0.3 m away from the plots border. Photographs were taken to estimate the dye coverage of each profile. These were later used to determine the volumetric proportions of preferential flow paths and soil matrix. The blue stained areas were defined as preferential flow paths, the non stained areas as soil matrix. With a small spatula we took soil samples over the whole width and depth of the individual horizons from the preferential flow paths and from the soil matrix. Sampling depths were 0 to 9, 9 to 20, 20 to 50, and 50 to 100 cm.

### 5.3.3 Soil solution sampling

Soil water samples were collected from one plot within the HARWA experimental site (Figure 5.1), that received  $4 \text{ Mg wood ash ha}^{-1}$  at 28 May 1998. We installed three suction cups (Soil Moisture, California, USA) per depth at 25 cm and 80 cm depth in December 1997. The suction cups were allowed to equilibrate with the soil for four months. With a small self-regulating motor we maintained a constant suction of 600 hPa. Additionally, we installed three Plexiglas plates to sample the free draining water percolating through the organic layer (0 cm). Soil water samples were taken every week immediately before and after the wood ash application and from mid July onwards every two weeks.

### 5.3.4 Sorption experiments

The sorption experiments were conducted with soil material from preferential flow paths and matrix from 0 to 9 cm and 20 to 50 cm depth that was bulked over all four plots. We weighed 2 g dry soil material in 85 ml polycarbonat centrifuge-tubes and pre-washed the samples by shaking them twice with 50 ml  $\text{CaCl}_2$  (0.01M) for 20 h on a

head-over-head shaker. Copper and Sr were added as  $\text{CuCl}_2$  and  $\text{SrCl}_2$  in concentrations from 2 to 50 mg Cu and Sr  $\text{L}^{-1}$ , respectively. The sorption time for the sorption with Cu and Sr was 24 h. The sorption experiments were conducted in duplicates. At all stages, we monitored the pH values of the supernatant solutions. We used atomic absorption spectroscopy (Philips PU 9200, Cambridge, UK) to measure the Cu concentrations in the supernatant solution. The Sr concentrations were measured by ICP-OES (Perkin Elmer Optima 3000).

### 5.3.5 Chemical extractions and analyses

Soil samples were oven dried at  $45^\circ\text{C}$  and sieved to 2 mm. Readily soluble and exchangeable elements were determined in extracts with 1 M  $\text{NH}_4\text{NO}_3$  (Zeien and Brümmer, 1989). The effective cation exchange capacity ( $\text{CEC}_{\text{eff}}$ ) was calculated as the sum of the exchangeable cations K, Na, Ca, Mg, Mn, Al, and Fe. The effective base saturation ( $\text{BS}_{\text{eff}}$ ) equals the sum of Ca, K, Mg, and Na in % of the  $\text{CEC}_{\text{eff}}$ . Manganese oxides were determined in 0.1 M  $\text{NH}_2\text{OH}\cdot\text{HCl}$  + 1 M  $\text{NH}_4$ -acetate, and organically bound Pb in 0.025 M  $\text{NH}_4\text{EDTA}$  after removal of the exchangeable fraction. Elements in the extracts were determined by ICP-OES (Perkin Elmer Optima 3000). Iron was additionally determined in extracts (1) with oxalate in the dark to receive amorphous Fe compounds, (2) with dithionite to receive crystalline Fe oxides, and (3) with pyrophosphate to receive Fe from metal-organic complexes (Loeppert and Inskeep, 1996). Iron in the extracts was measured with atomic absorption spectroscopy (Philips PU 9200, Cambridge, UK). Total C and N were measured with a CN auto analyzer (NA 1500 and 2500, Carlo Erba Instruments, Milano, Italy). Texture was determined with the pipette method after removing soil organic matter by digestion in  $\text{H}_2\text{O}_2$  followed by ultrasonic treatment in 0.2% Calgon for 5 min (Gee and Bauder, 1986). Soil water samples were filtered ( $45\mu\text{m}$ ) and stored at  $4^\circ\text{C}$  until analysis. Elements were determined in the acidified samples with ICP-OES.

### 5.3.6 Calculations and statistical analyses

The recovery of the Sr-tracer and of the elements leached from the wood ash was calculated scaling the concentrations in preferential flow paths and soil matrix with the proportion of the respective flow region:

$$R_x = \sum_{h=1}^3 \sum_{j=1}^2 (c_{xhj}(t_2) - c_{xhj}(t_0)) \cdot \rho_h \cdot \Delta z_h \cdot f_{jh} \quad (1)$$

with  $R_x$  being the recovery of an individual element  $x$ ,  $h$  and  $j$  the indices for the soil horizon and the flow region, respectively,  $c_{xj}$  being the concentration of the element in at time  $t_2$  (i.e. six month after wood ash application) and time  $t_0$  (i.e. control treatment before wood ash application),  $\rho_h$  refers to the bulk density of the respective soil horizon  $h$ ,  $\Delta z_h$  to the thickness of the horizon, and  $f_{jh}$  to the volumetric fraction of the stained preferential flow paths and the unstained matrix in the respective soil horizon.

Mean values of elemental concentrations were compared using analysis of variance (Scheffé, 1959). The model used was a split-plot-model with the plot as the block-factor, the flow region as split-unit-factors, and the time of sampling as the main-unit-factor. Individual horizons were tested separately. Means of single sampling dates were separated using the paired t-test (Conover, 1980). All statistical analyses were performed with the software S-Plus (Version 5.0, 1998, MathSoft, Seattle).

## 5.4 Results

### 5.4.1 Sorption characteristics of preferential flow paths and matrix

Adsorption of Cu and Sr is best described with a Freundlich isotherm at both depths:

$$c_s = K \cdot c_i^n \quad (2)$$

with  $c_s$  and  $c_i$  being the concentration of Cu or Sr on the sorbent and in the water, respectively, and  $K$  and  $n$  being adjustable parameters. For Cu remarkable differences between the preferential flow paths and the soil matrix at 0-9 cm depth existed (Figure 5.2a).

While  $n$  was similar for the two flow regions (0.48 and 0.52 for preferential flow paths and matrix at 0-9 cm depth and 0.58 and 0.59 at 20-50 cm depth),  $K$  was different for preferential flow paths and matrix, especially in the topsoil horizon (260 and 78 L



$\text{kg}^{-1}$  for preferential flow paths and matrix at 0-9 cm depth and 35 and 28  $\text{L kg}^{-1}$  at 20-50 cm depth). In contrast to Cu, there was no significant difference of the sorption characteristics between preferential flow paths and soil matrix for Sr, neither at 0-9 cm nor at 20-50 cm depth (Figure 5.2b).

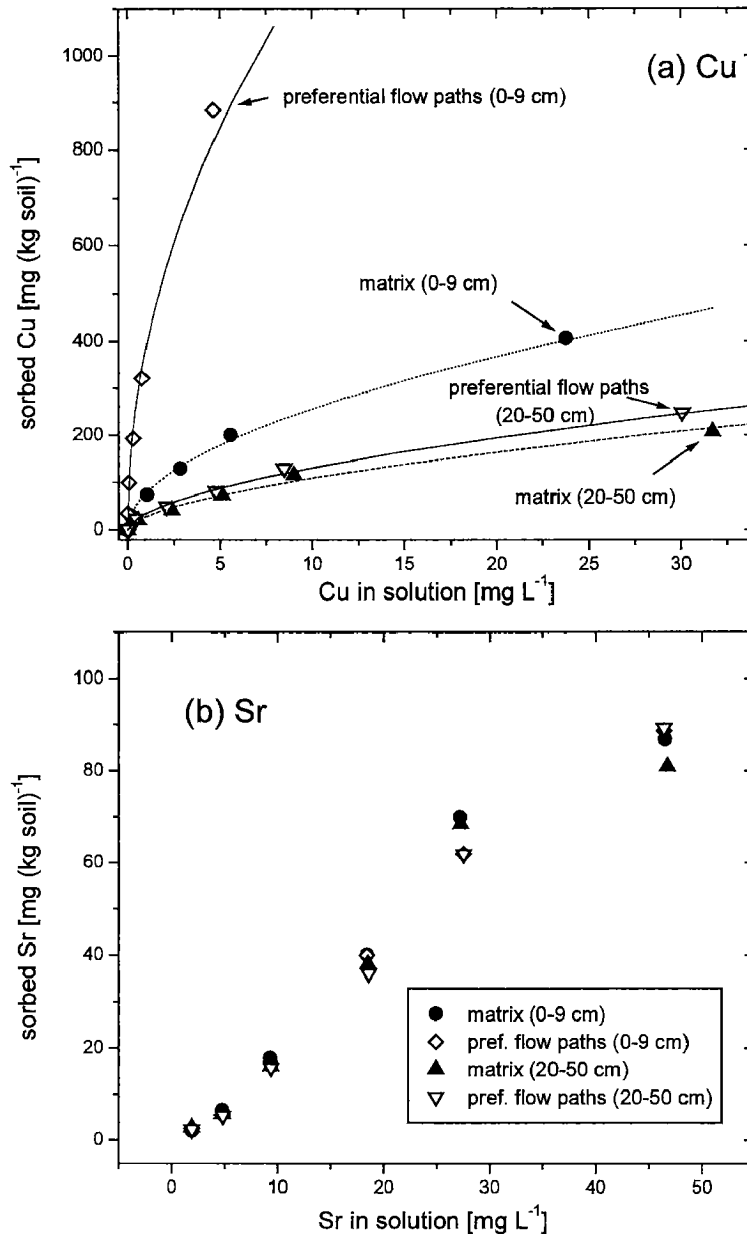


**Figure 5.2:** Sorption isotherms for Cu (a) and Sr (b) for soil material from preferential flow paths and matrix in the depth zones 0-9 cm and 20-50 cm. The curves are Freundlich fits.

We studied the physico-chemical properties that influence sorption in soil material taken from preferential flow paths and from the soil matrix (Table 5.1). In the preferential flow paths, the texture was slightly coarser compared to the matrix, where we found a higher percentage of clay sized particles. The concentration of amorphous and crystalline Fe-oxides did not differ between preferential flow paths and matrix. However, organically bound Fe was increased in the preferential flow paths as compared to the matrix. Manganese oxides were significantly increased in the matrix (ANOVA,  $p < 0.05$ ).

Initially, there was no difference in pH values between the two flow regions, although the effective base saturation was higher in the preferential flow paths at 0-20 cm depth ( $p < 0.01$  and  $p < 0.05$  for 0-9 cm and 9-20 cm, respectively). The effective cation exchange capacity was also higher in the preferential flow paths ( $p < 0.01$  and  $p < 0.05$  for 0-9 cm and 9-20 cm, respectively, Figure 5.3), as was soil organic matter ( $p < 0.01$  for 0-9 cm and  $p < 0.05$  for 9-20, 20-50, and 50-100 cm).

#### **5.4.2 Strontium tracer experiment**

The Sr recovery six months after the tracer application was between 9 and 83%. Concentrations of Sr in the uppermost 20 cm of the soil increased until 6 months after the addition and decreased subsequently (Figure 5.4). In 50 to 100 cm depth, Sr concentrations increased steadily until 12 months after the tracer application. In the preferential flow paths, concentrations of Sr showed a significantly larger response to the Sr application than in the matrix, particularly at 0-9 cm and 9-20 cm depth (Figure 5.4).

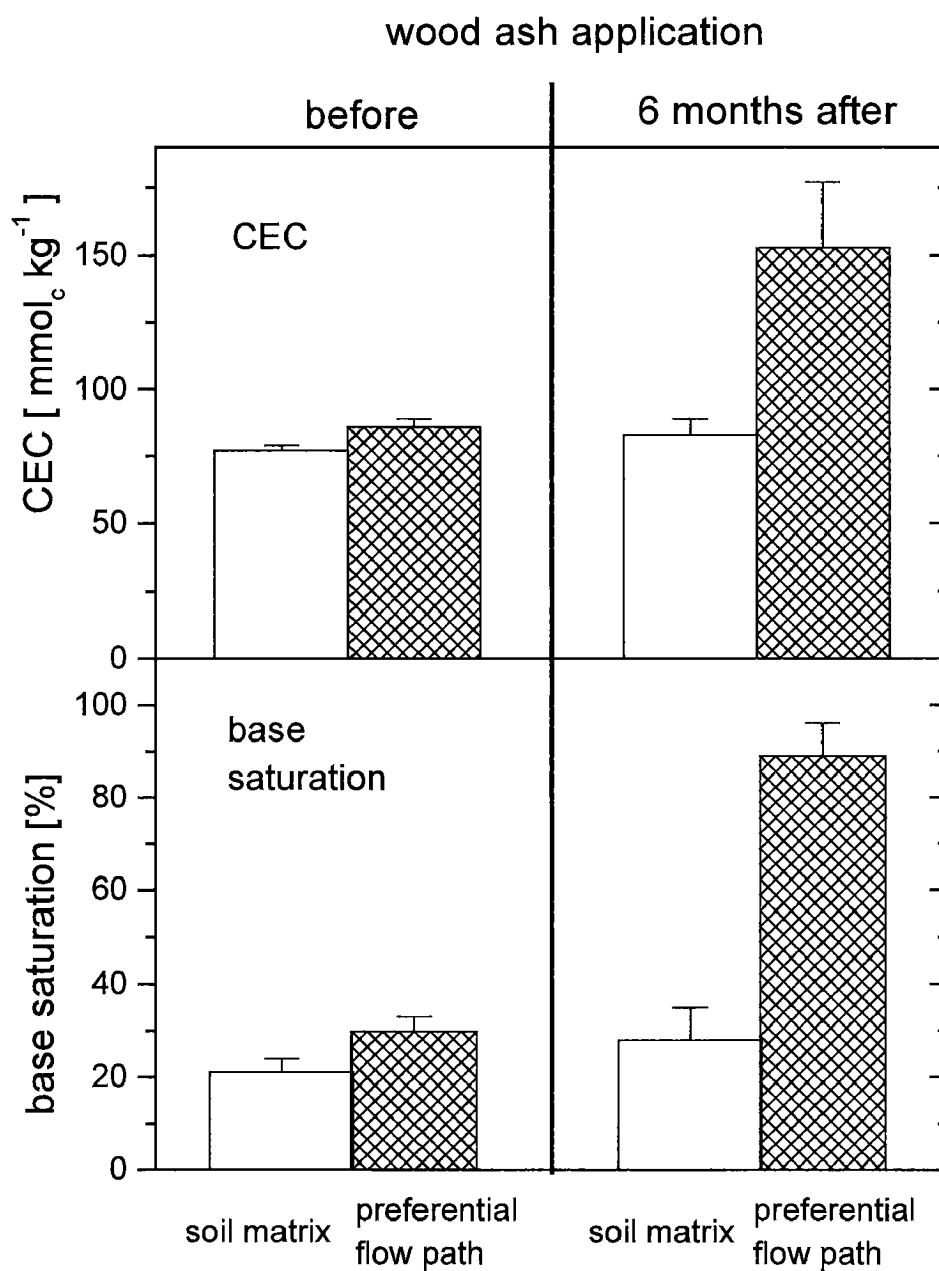


**Figure 5.3:** Effective cation exchange capacity (CEC) and base saturation in soil material from preferential flow paths and matrix at 0-9 cm depth before and six months after the wood ash application.

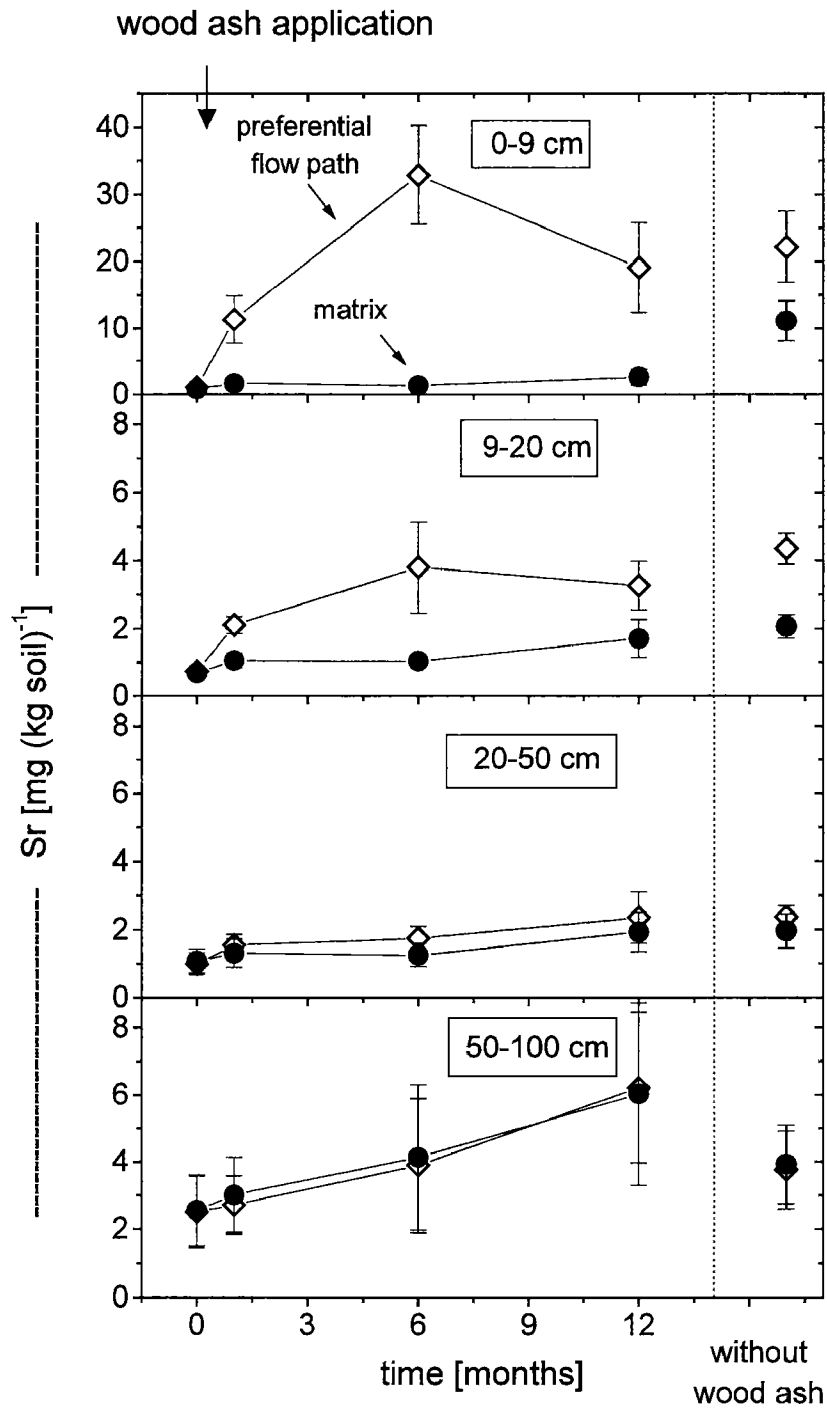


**Figure 5.4:** Strontium concentrations in preferential flow paths and matrix in four different depth zones. The first and the last sampling campaigns represent control plots, the three campaigns in between one, six, and twelve months after tracer addition. All data are means of four plots. Standard errors are shown as error bars. Mind the different scaling of the axes.

### 5.4.3 Effects of wood ash application

After the wood ash application, the pH values increased mainly in the preferential flow paths of 0-9 cm depth. Here, the pH rose from 3.5 before the wood ash application ( $t_0$ ) to 4.3 six month after the wood ash application ( $t_2$ ), but decreased to 3.9 already one year after the wood ash application ( $t_3$ ). In the matrix, the pH remained rather stable at all depths and changed by not more than 0.2 pH units. The wood ash application increased the  $CEC_{eff}$  and the base saturation significantly in the preferential flow paths of 0-9 cm depth ( $p < 0.05$ , Figure 5.3). In the matrix, however, the increase was only small and statistically not significant.

To show the impact of the wood ash application on extractable element concentrations, we exhibit the results of Ca, Al, and Pb (Figures 5.5 to 5.7). Data for Mg and K are not shown, because they were very similar to those for Ca. The effect of the wood ash application on exchangeable Ca concentrations in the preferential flow paths and in the soil matrix in the course of one year resembled those of Sr (Figure 5.5). The differences of Ca concentrations between preferential flow paths and matrix were statistically significant for 0-9 cm ( $p < 0.01$ ) and 9-20 cm ( $p < 0.01$ ). The wood ash application significantly influenced the Ca concentrations in the preferential flow paths ( $p < 0.01$  at 0-9 cm,  $p < 0.05$  at 9-20), but did not affect Ca concentrations in the matrix. The recovery of Ca ranged from 41 to 101% (Table 5.2).

In contrast to Ca, concentrations of exchangeable Al showed an inverse pattern (Figure 5.6). Despite an Al input with the wood ash of  $4.6 \text{ g m}^{-2}$ , the exchangeable Al was reduced by approximately  $63 \text{ g m}^{-2}$  when calculated with Equation 1. The difference of exchangeable Al concentrations between preferential flow paths and matrix were, as in case of Ca, significant for 0-9 and 9-20 cm depth and additionally for 50-100 cm depth ( $p < 0.01$ ,  $< 0.01$ , and  $< 0.05$ , respectively).

The organically bound Pb concentrations at 0-9 cm depth were significantly increased only 6 month after wood ash application ( $p < 0.05$ ) and then decreased again (Figure 5.7). The differences in Pb concentrations of preferential flow paths and soil matrix were statistically significant at 0-9, 9-20, and 50-100 cm depth. The increase of Pb after the wood ash application was larger in the uppermost horizon than the input with the wood ash (Table 5.2).

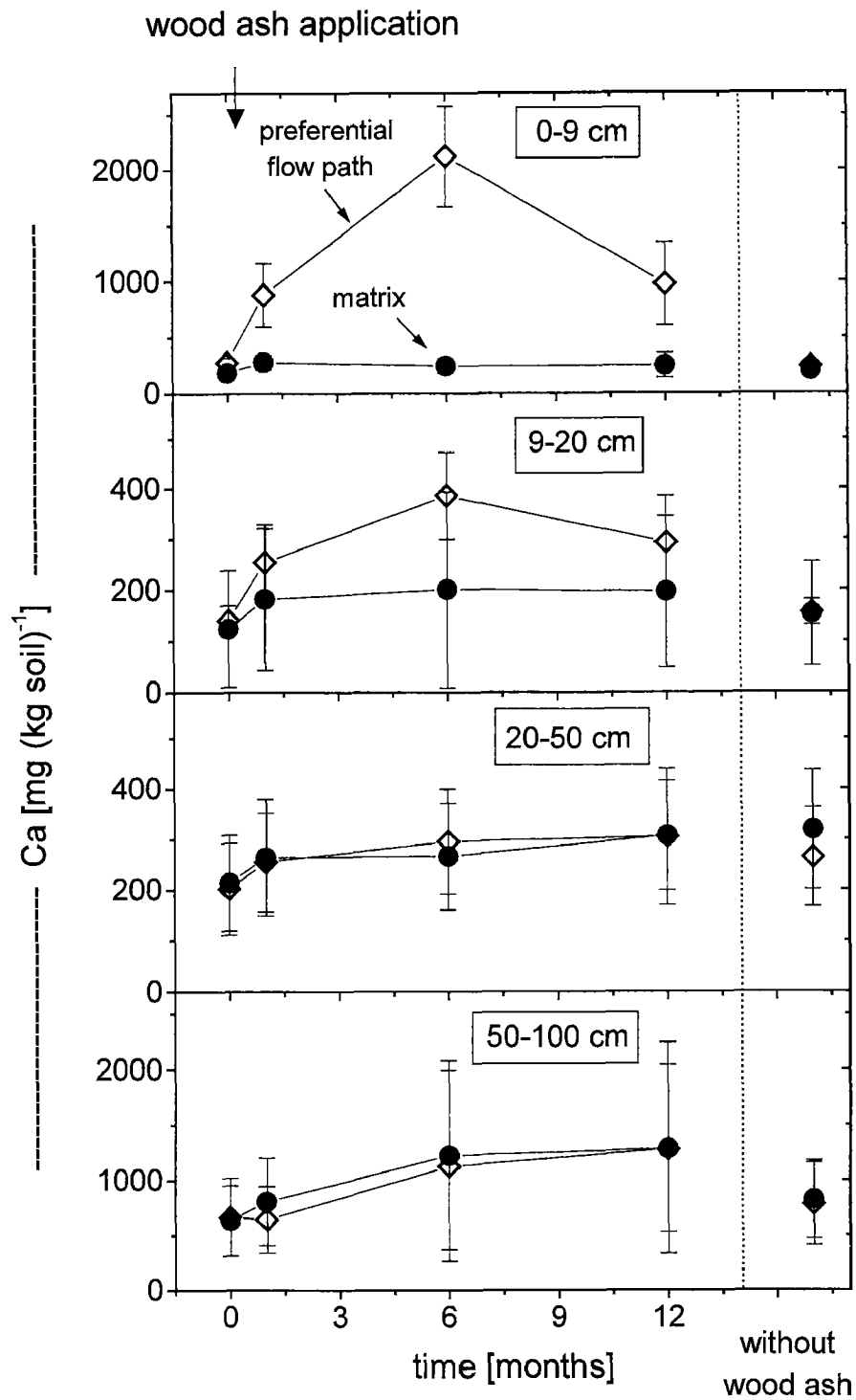


**Figure 5.5:** Exchangeable Ca concentrations in preferential flow paths and matrix in four different depth zones. The first and the last sampling campaign represent control plots, the three campaigns in between one, six, and twelve months after wood ash application. All data are means of four plots. Standard errors are shown as error bars. Mind the different scaling of the axes.

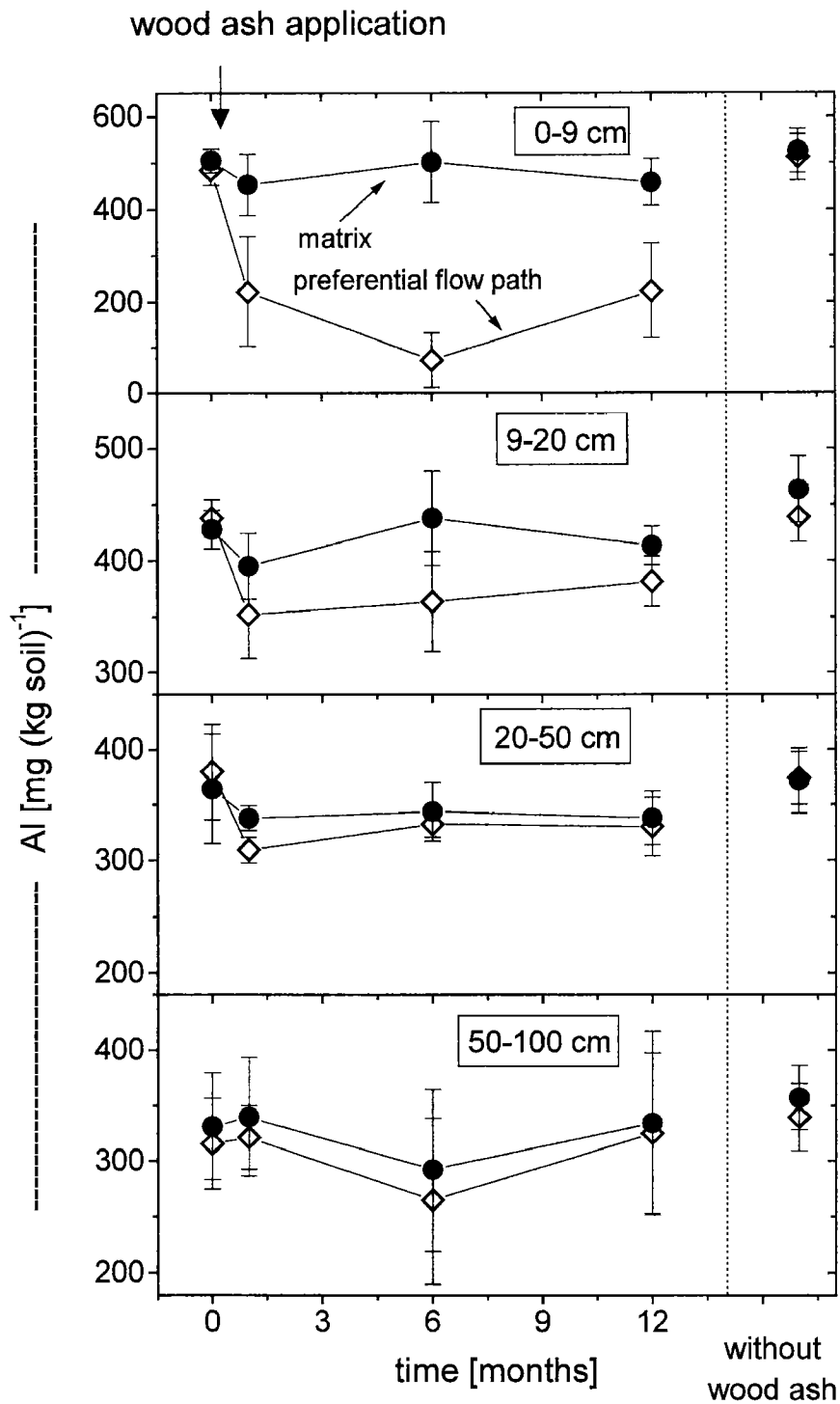


**Figure 5.6:** Exchangeable Al concentrations in preferential flow paths and matrix in four different depth zones. The first and the last sampling campaign represent control plots, the three campaigns in between one, six, and twelve months after wood ash application. All data are means of four plots. Standard errors are shown as error bars. Mind the different scaling of the axes.

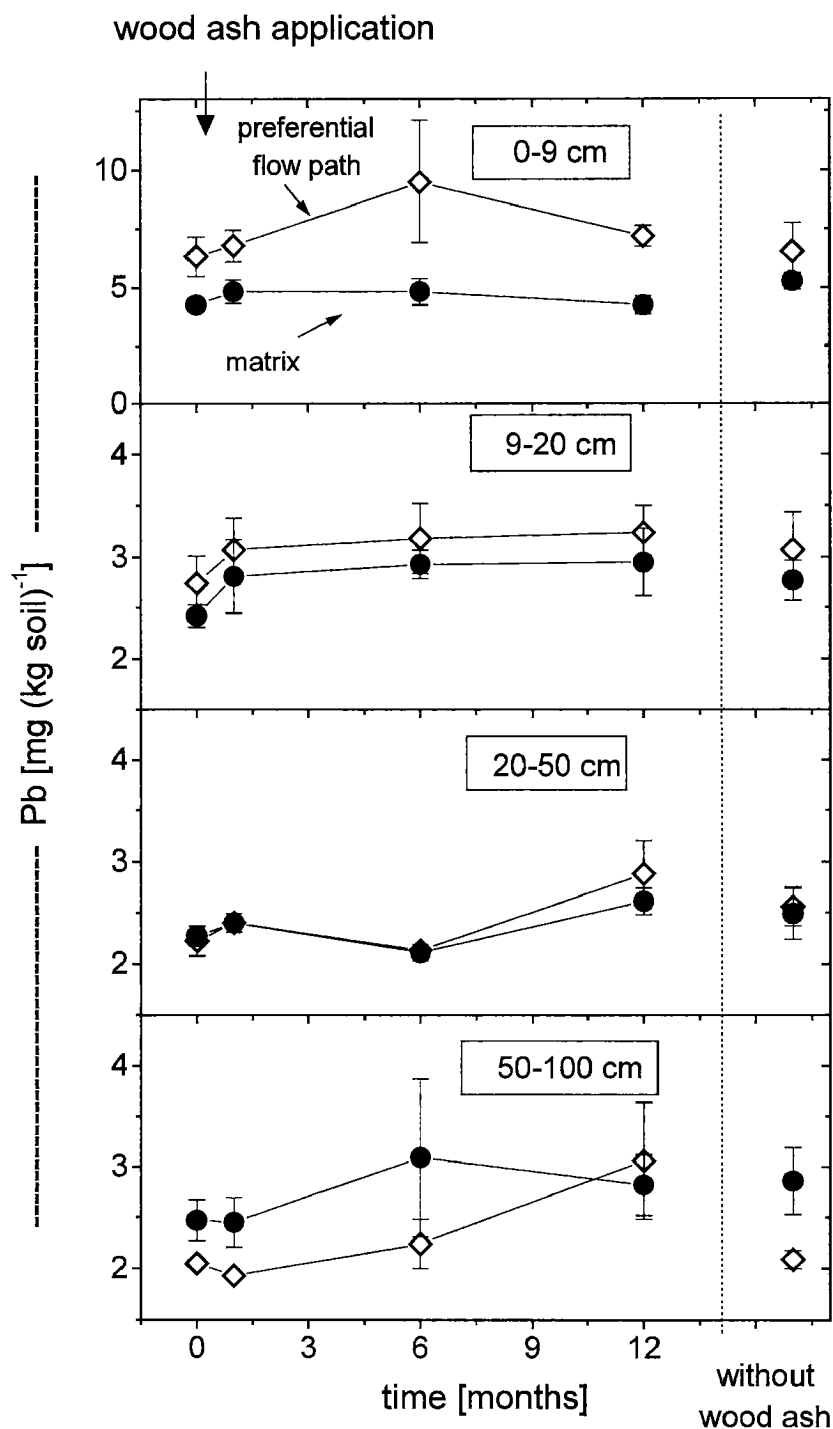


**Figure 5.7:** Organically bound Pb concentrations in preferential flow paths and matrix in four different depth zones. The first and the last sampling campaign represent control plots, the three campaigns in between one, six, and twelve months after wood ash application. All data are means of four plots. Standard errors are shown as error bars. Mind the different scaling of the axes.



#### 5.4.4 Soil solution

Concentrations of Al, Ca, and dissolved organic carbon (DOC) in the soil solution increased immediately after the wood ash application at all depths down to 25 cm (Figure 5.8). Subsequently, concentrations of Ca decreased slowly at the mineral soil surface (0 cm depth), while concentrations of DOC dropped rapidly.

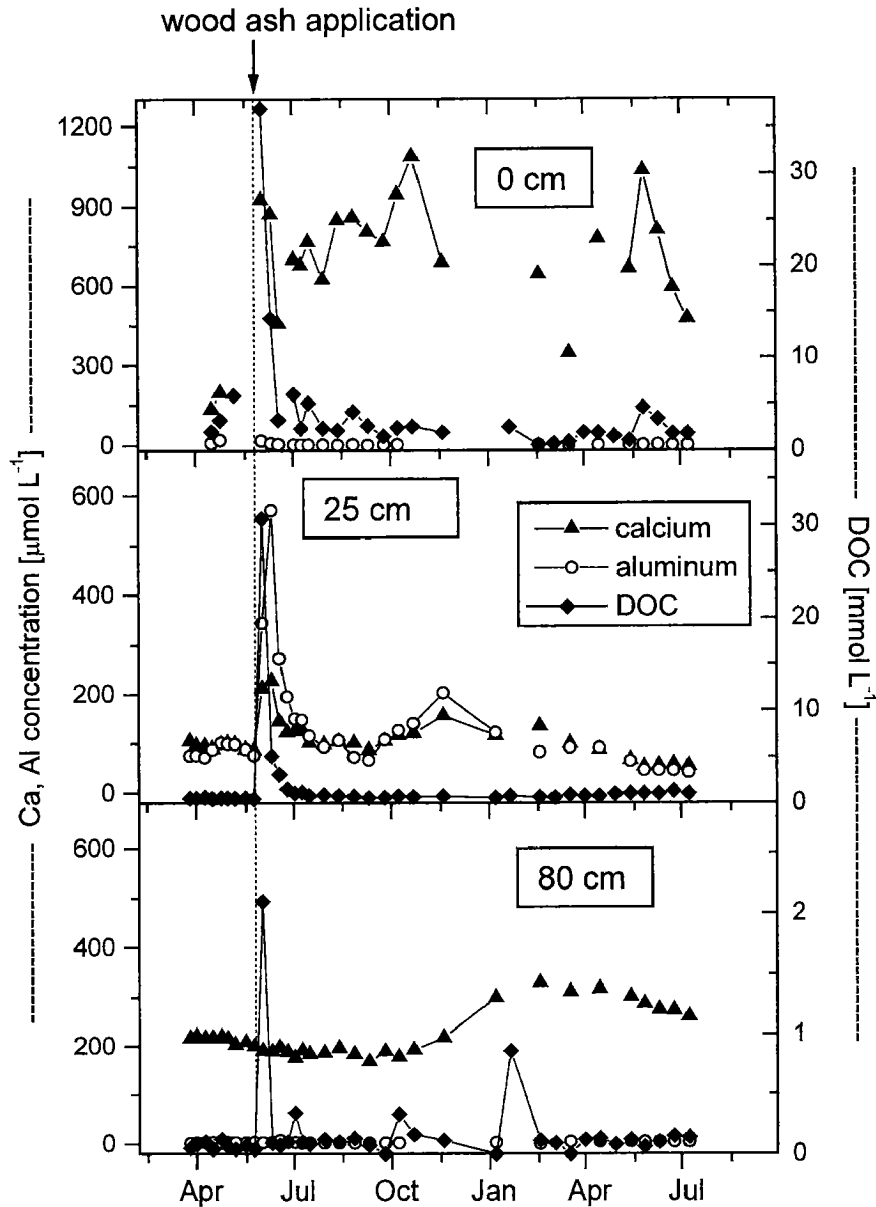


**Figure 5.8:** Concentrations of Ca, Al, and DOC in the soil solution before and after the wood ash application in three different depth zones. Mind the different scaling of the axes.

At 25 cm depth, concentrations of Ca and Al decreased within one month after the first flush, but showed a second lower peak 6 months later. In the subsoil, at 80 cm depth, Ca concentrations started to increase 6 months after the wood ash application and approximately doubled. Here, concentrations of Al remained below  $5 \mu\text{mol Al L}^{-1}$ . Concentrations of Pb (and other heavy metals) followed closely the temporal pattern of DOC (data not shown).

## 5.5 Discussion

### 5.5.1 Sorption characteristics of preferential flow paths and matrix

To test the hypothesis whether preferential flow paths and soil matrix have different sorption characteristics, sorption batch experiments were conducted with Cu and Sr. We chose Cu as a probe for heavy metals that are strongly sorbed by soil organic matter. Strontium, being like Ca and Mg an element of the Group IIA of the periodic chart, is often used as a probe for Ca in plant sciences.

Since the contents of sorbents of the mineral phase such as clay and Fe oxides are similar in preferential flow paths and soil matrix, the stronger sorption of Cu to the soil material from the preferential flow paths probably stems from the higher soil organic matter (SOM) concentrations (Table 5.1). The higher SOM concentrations in the preferential flow paths as compared to the matrix are probably due to an enhanced C input by roots and to a preferential input of dissolved organic matter in these flow regions (Bundt et al. 2000, submitted). Chelating and complexing are the key reactions governing Cu behavior in most soils, giving SOM the leading role in controlling the fate of Cu in soils (Kabata-Pendias and Pendias, 1992). A similar preferred sorption can be expected in case of other heavy metals and hydrophobic organic compounds. This is confirmed by the higher concentrations of organically bound iron in the preferential flow paths as compared to the matrix. Strontium, however, was not preferentially sorbed by the soil from the preferential flow paths. Geochemical characteristics of Sr are similar to those of Ca, thus Sr is mainly sorbed to general cation exchange sites (Kabata-Pendias and Pendias, 1992). In contrast to organic sorption sites, inorganic

sorption sites might be more numerous in the matrix than in the preferential flow paths. The concentrations of Mn oxides are significantly higher in the matrix as compared to the preferential flow paths. This can be a result of the higher microbial activity, reducing Mn oxides to soluble Mn ions, and the faster transport of solutes in the preferential flow paths, removing the mobile Mn efficiently. Also, the clay content is slightly, but statistically not significantly higher in the matrix than in the preferential flow paths and thus, might provide more permanently negative exchange sites for cations.

The finding of an increased Cu sorption in preferential flow paths shows that the preferred transport of pollutants can be counterbalanced by a stronger sorption to soil material from preferential flow paths, in particular of pollutants with a high affinity to SOM.

#### **5.5.2 Effects of wood ash application on exchangeable elements and soil solution**

The wood ash we used had similar elemental concentrations as ashes used in other studies (Bramyard and Fransman, 1995; Unger and Fernandez, 1990). The effects of the wood ash application on the soil solid phase and on the soil solution were more or less restricted to the uppermost 20 cm of the soil. At deeper depths, all effects were still discernible but small compared to the effects in the topsoil. Also, they were temporally retarded. This was consistent with the results of Kahl et al. (1996) who found only moderate changes in the B horizon after the application of 6 t wood ash ha<sup>-1</sup>. The increase of 0.8 pH units in the preferential flow paths of 0-9 cm depth resulting from the wood ash application was approximately similar to the increase measured by Unger and Fernandez (1990), but smaller than the increase found by Bååth and Arnebrant (1994). As expected, CEC and base saturation increased after wood ash application, due to the rise in pH and the input of neutral cations. The decrease in exchangeable Al concentrations was probably not only due to a simple pH effect, but also to a displacement of acid cations by neutral cations (Matzner et al., 1995; Unger and Fernandez, 1990). This was supported by the increase of Al concentrations in the soil solution after the wood ash application (Figure 5.8). The increase of EDTA-extractable Pb concentrations at 0-9 cm depth (Figure 5.7) and the finding, that more Pb was recovered in that depth than was added with the wood ash points to remobilization

processes in the organic layer. As Pb concentrations at the mineral soil surface (0 cm depth) were closely correlated to those of DOC in the soil solution ( $R^2=0.95$ ), it is likely that Pb was transported as a metal-organo complex with DOC. Due to the high sorption capacity of aerobic forest soils for DOC (Guggenberger and Zech, 1993), the remobilized Pb did not reach deeper depths.

### 5.5.3 Transport

Solute transport was investigated for Ca, applied as Ca oxides with the wood ash, and for Sr, which has a small background concentration in the wood ash and in the soil. Since both elements showed a similar fate in the soil (Figures 5.4 and 5.5), it seems that the temporal and spatial distribution in the soil was not governed by the solubility of the wood ash, but by transport processes in the soil.

Within one year after their application, virtually no Sr, Ca or Mg penetrated the matrix at 0-20 cm depth. This implies that 48% of the soil volume at 0-20 cm depth did not contribute to the sorption and buffering of elements imported by the wood ash. This is especially important, since 88% of the fine roots were located in this depth zone (Bundt et al., 2000). Another conclusion from this distribution is, that advective transport and diffusion between the flow regions can be neglected in the two uppermost depths, since these two processes did not reduce the large concentration gradients between preferential flow paths and soil matrix over the period of one year.

The elemental concentrations of the matrix below 20 cm depth were increased, while those above 20 cm were not. There are two possible explanations how the solutes reached the matrix at the 20-50 and 50-100 cm: (1) The solutes were rapidly transported in the preferential flow paths. Passages of higher flow resistance may have led to local and temporal "ponding" in the subsoil and to a lateral movement of water and solutes into the matrix.

(2) More preferential flow paths were active at 20-100 cm in the course of the year than were actually stained during our experiments in October 1998 and May 1999. This

way, we would have sampled both former preferential flow paths and matrix when ostensibly sampling matrix.

The effectiveness of preferential flow through the uppermost soil is supported by the temporal pattern of the Ca and Al concentration in the soil solution, which is typical for two flow regimes. The first fast breakthrough with a sharp peak was due to preferential flow. This means that the suction cups are located in close vicinity to preferential flow paths, or that a possible interception of the flow paths led to lateral dispersion into the matrix. The second, broader and smaller peak likely stems from "matrix flow".

## **5.6 Conclusions**

Preferential flow paths and matrix are chemically different. The sorption capacity for specifically organically bound heavy metals is higher in the preferential flow path due to higher organic matter contents as compared to the matrix. This is important when assessing leaching and the risk of groundwater contamination.

Soil chemical properties were distinctly altered by the wood ash application. In the solid phase, the full effect of the wood ash application on pH and exchangeable elements was reached six month after adding the wood ash. One year after wood ash application, these effects already decreased and concentrations approach initial values. Therefore, the effects are not persistent. The soil solution reacted much faster and elemental concentrations reached peak values only two weeks after wood ash application. The application of 8 Mg wood ash ha<sup>-1</sup> led to a re-mobilization of Al or heavy metals such as Pb. Thus, disposal of wood ash to contaminated forest soils represents a potential risk to the environment.

At our study site, only about half the soil volume in the upper soil horizons was affected by the wood ash application. Therefore, only about half the soil volume was available to sorb and buffer incoming elements and acted as a storage compartment for the additional nutrients applied with the wood ash. This must be considered when calculating the maximal amount of any addition of fertilizer, wood ash, or liming agent.

## 5.7 References

- Bååth, E., and K. Arnebrant. 1994. Growth rate and response of bacterial communities to pH in limed and ash treated forest soils. *Soil Biol. Biochem.* 26: 995-1001.
- Bramyard, T., and B. Fransman. 1995. Sylvicultural use of wood ashes- Effects on the nutrient and heavy metal balance in a pine (*Pinus sylvestris* L.) forest soil. *Water Air Soil Pollut.* 85: 1039-1044.
- Bundt, M., A. Albrecht, P. Froidevaux, P. Blaser, and H. Flühler, 2000. Impact of preferential flow on radionuclide distribution in soil. *Environ. Sci. Technol.*, in press.
- Cervelli, S., G. Petruzzelli, and A. Perna. 1987. Fly ash as an amendment in cultivated soils. I. Effect on Mineralization and Nitrification. *Water Air Soil Pollut.* 33: 331-338.
- Conover, W. J. 1980. *Practical Nonparametric Statistics*. 2<sup>nd</sup> edn. Wiley, New York.
- Eriksson, H. 1990. Early results from a wood ash application experiment in central Sweden. *In* Tham, A. (ed.) *Changes to forest management and silvicultural techniques necessitated by forest energy production*. Sveriges Lantbruksuniversitet Garpenberg, Garpenberg.
- Flury, M., and H. Flühler. 1994a. Brilliant Blue FCF as a dye tracer for solute transport studies- A toxicological overview. *J. Environ. Qual.* 23: 1108-1112.
- Flury, M., and H. Flühler. 1994b. Susceptibility of soils to preferential flow of water: A field study. *Water Resour. Res.* 30: 1945-1954.
- Frostegård, Å., E. Bååth, and A. Tunlid. 1993. Shifts in the structure of soil microbial communities in limed forests as revealed by phospholipid fatty acid analysis. *Soil Biol. Biochem.* 25: 723-730.
- Gee, G.W., and J.W. Bauder. 1986. Particle-size analysis. *In* . Page, A. L., R. H. Miller, and D. R. Keeney (eds.) *Methods of soil analysis. Part1: Physical and Mineralogical Methods*. 2<sup>nd</sup> edn, pp. 383-411. American Society of Agronomy, Madison.
- Guggenberger, G., and W. Zech. 1993. Dissolved organic carbon controls in acid forest soils of the Fichtelgebirge (Germany) as revealed by distribution patterns and structural composition analyses. *Geoderma* 59: 109-129.
- Hildebrand, E.E. 1991. *Die chemische Untersuchung ungestört gelagerter Waldbodenproben- Methoden und Informationsgewinn*. KfK-PEF 85. Kernforschungszentrum Karlsruhe, Karlsruhe.
- Kabata-Pendias, A., and H. Pendias. 1992. *Trace elements in soils and plants*. 2<sup>nd</sup> edn. CRC Press. Boca Raton.
- Kahl, J.S., I.J. Fernandez, L.E. Rustad, and J. Peckenham. 1996. Threshold application rates of wood ash to an acidic forest soil. *J. Environ. Qual.* 25: 220-227.

- Loeppert, R.H., and W.P. Inskeep. 1996. Iron. pp.639-664. *In* Sparks, D. L. (ed.) *Methods of Soil Analysis. Part 3. Chemical Methods.* Soil Science Society of America, Madison.
- Matzner, E., P.K. Khanna, K.J. Meiwes, and B. Ulrich. 1995. Effects of fertilization and liming on the chemical soil conditions and element distribution in forest soil. *Plant Soil* 7: 405.
- Meiwes, K.J. 1995. Application of lime and wood ash to decrease acidification of forest soils. *Water Air Soil Pollut.* 85: 143-152.
- Pierret, A., C.J. Moran, and C.E. Pankhurst. 1999. Differentiation of soil properties related to the spatial association of wheat roots and soil macropores. *Plant Soil* 211: 51-58.
- Pivetz, B.E., and T.S. Steenhuis. 1995. Soil matrix and macropore biodegradation of 2,4-D. *J. Environ. Qual.* 24: 564-570.
- Scheffé, H. 1959. *The Analysis of Variance.* Wiley, New York.
- Turner, R.R., and K.F. Steele. 1988. Cadmium and Manganese sorption by soil macropore linings and fillings. *Soil Sci.* 145: 79-86.
- Unger, Y., and I.I. Fernandez. 1990. The short-term effect of wood-ash amendment on forest soil. *Water Air Soil Pollut.* 49: 299-314.
- Vinther, F.P., F. Eiland, A.-M Lind, and L. Elsgaard. 1999. Microbial biomass and numbers of denitrifiers related to macropore channels in agricultural and forest soils. *Soil Biol. Biochem.* 31: 603-611.
- Wilcke, W., and M. Kaupenjohann. 1998. Heavy metal distribution between soil aggregate core and surface fractions along gradients of deposition from the atmosphere. *Geoderma* 83: 55-66.
- Zeien, H., and G.W. Brümmer. 1989. Chemische Extraktionen zur Bestimmung von Schwermetallbindungsformen in Böden. *Mitteilg. Dt. Bodenkund. Ges.* 59: 505-510.

## CHAPTER 6

# **Forest fertilization with wood ash: impact on the distribution and storage of organic contaminants**

with

MARTIN KRAUSS, PETER BLASER AND WOLFGANG WILCKE

Submitted to the Journal of Environmental Quality



## 6.1 Abstract

Before wood ash can be safely used as a fertilizer in forests, possible negative effects such as input of organic contaminants or re-mobilization of contaminants already stored in the soil must be investigated. The objective of this study was to examine the effects of wood ash application on concentrations, storage and distribution of polycyclic aromatic hydrocarbons (PAHs) and polychlorinated biphenyls (PCBs) in a Swiss forest soil. In May 1998, we added 8 Mg wood ash ha<sup>-1</sup> to a forest soil. We determined 20 PAHs and 14 PCBs in the organic layer, in the bulk mineral soil, and in soil material taken from preferential flow paths and from the matrix before and after the wood ash application. In the control plots, the concentrations of PAHs in the organic layer indicated moderate pollution (sum of 20 PAHs: 0.8 – 1.6 mg kg<sup>-1</sup>), but sum of PCB concentrations was high (21 – 48 µg kg<sup>-1</sup>). The wood ash had high concentrations of PAHs (sum of 20 PAHs: 16.8 mg kg<sup>-1</sup>), but low concentrations of PCBs (sum of 14 PCBs: 3.4 µg kg<sup>-1</sup>). The wood ash application increased the PAH concentrations in the organic horizons up to sixfold. In contrast, PCB concentrations did not change in the Oa horizon and decreased up to one third in the Oi and Oe horizons. The decrease was probably caused by the mobilization of stored PCBs because of the pH effect of the wood ash. This probably results in a higher mobility of dissolved organic matter, acting as PCB carrier. In the mineral soil, the preferential flow paths of the A horizon contained more PAHs and PCBs (+20 ±15% and +43 ±60%, respectively) than the matrix. This was particularly true for higher molecular compounds (molecular weight > 200 g mol<sup>-1</sup>). Below 50 cm depth, concentrations of PAHs and PCBs were smaller in the preferential flow paths, suggesting that processes acting as sinks dominated over inputs.

## 6.2 Introduction

In many countries, wood ash is used as a fertilizer in forests (Vance, 1996). However, wood ash can only be safely used in forests, if negative effects are small in comparison to benefits (Noger et al., 1996; Zollner et al., 1997). Wood ash is known to contain significant concentrations of heavy metals, but little is known about the concentrations of organic contaminants such as polycyclic aromatic hydrocarbons (PAHs) and polychlorinated biphenyls (PCBs) and their fate after addition to the soil. Furthermore, PAHs and PCBs are already present in most soils, because they are ubiquitously distributed and are persistent in different ecosystems (Sims and Overcash, 1983; Harrad et al., 1994; Wild and Jones, 1995). Due to high rates of interception deposition, forest soils receive particularly high inputs of organic contaminants from the atmosphere that mainly accumulate in the organic layer (Matzner, 1984; Berteigne et al., 1988; Wilcke et al., 1996b). After applying wood ash onto a forest soil, the increase in pH might lead to an increased solubility of dissolved organic matter (DOM) and to an enhanced mineralization (Lamersdorf, 1985; Schierl et al., 1986; Marschner, 1995). This might result in a mobilization of already accumulated organic contaminants and in a redistribution of PAHs and PCBs due to DOM-facilitated transport (Chiou et al., 1986; McCarthy and Zachara, 1989; Marschner, 1999).

In most studies on PAH and PCB concentrations in soil, the homogenized bulk soil was analyzed. However, in soils organic contaminants are heterogeneously distributed. Wilcke and Zech (1997) reported higher PAH concentrations in soil samples taken from the stem foot area of beech trees (*Fagus sylvatica* L.) as compared with samples taken between trees and attributed this to increased inputs with stem flow. On a smaller scale, Wilcke et al. (1996a, b) found higher PAH concentrations at the surfaces of soil aggregates than in their cores. The authors explain their findings with preferential water movement along the aggregate surfaces leading to an increased sorption of the PAHs at the aggregate surfaces.

Preferential flow of water and solutes has been shown for a large variety of soils (Sollins and Radulovich, 1988; Ghodrati and Jury, 1992; Flury and Flühler, 1994b). The rapid water movement through a small fraction of the soil volume leads to a faster transport of solutes, particles, and contaminants. There is evidence that preferential flow

paths are not only regions of increased transport, but also of enhanced root growths and microbial activity (Pierret et al., 1999; Vinther et al., 1999). Therefore, organic contaminants stored in or near preferential flow paths might represent an "active" pool, whereas contaminants stored in the matrix regions might have slower turnover rates.

The objective of this study was to examine the effects of an experimental application of wood ash on the concentrations, storage and distribution of PAHs and PCBs in a Swiss forest soil. Special consideration was dedicated to the distribution of these contaminants between soil material from preferential flow paths and from the soil matrix.

## 6.3 Materials and Methods

### 6.3.1 Study site and experimental setup

The study was conducted at a forested site in Unterehrendingen, Switzerland (N: 47°30'34"/E: 008°20'50", Figure 6.1). The forest was planted in 1930 with Norway spruce (*Picea abies* (L.) Karst.) as the dominant tree species mixed with beech (*Fagus sylvatica* L.) and some other species. Soil type was a fine-loamy mixed typic Haplumbrept (Soil Survey Staff, 1994). The soil was covered by a approximately 2 cm deep moder type organic layer. The parent material was upper sea molasse. Selected properties are given in Table 6.1.

**Table 6.1:** Selected physical and chemical soil properties at the study site.

Depth [cm]	Bulk density [g cm <sup>-3</sup> ]	pH	C <sub>org</sub>	N <sub>tot</sub>	C <sub>org</sub>	
					Flow path	Matrix
0-9	1.1	3.4	27	1.7	35	24
9-20	1.3	3.7	12	0.8	15	13
20-50	1.4	3.8	6	0.5	8	6
50-100	1.6	3.8	3	0.3	5	3

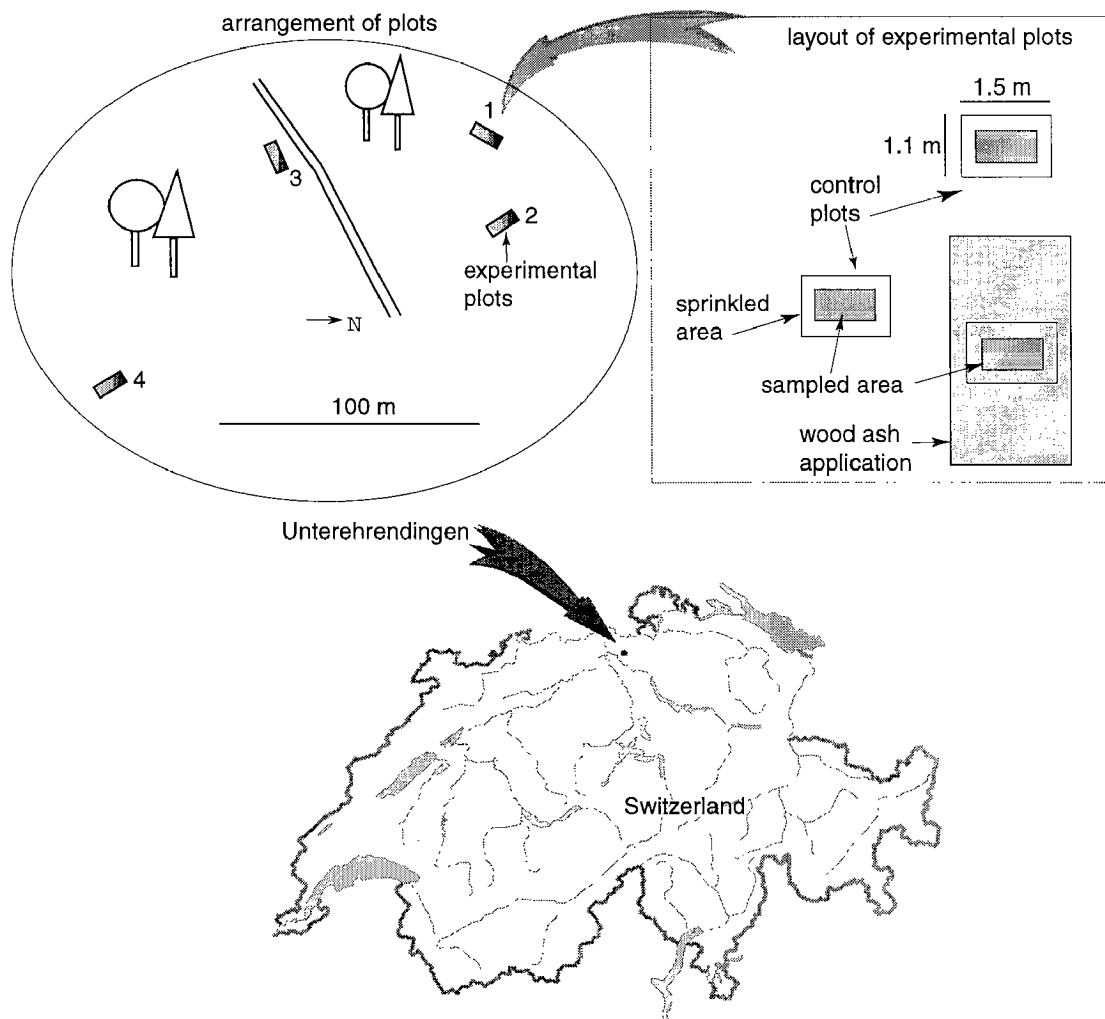


**Figure 6.1:** Location and layout of the experimental site.

The samples were taken from four plots, that were divided into “control” subplots receiving no wood ash and “wood ash” subplots, receiving the equivalent of 8 Mg wood ash  $\text{ha}^{-1}$  on 7 May 1998 (Figure 6.1). The wood ash was spread out by hand and formed a thin film on the soil surface. It consisted mainly of Ca-oxides and had completely disappeared from the soil surface by October 1998. Soil and organic layer samples were taken from all plots before the wood ash application in April 1998. In May 1999 (i.e. one year after wood ash application), we again collected mineral soil and organic layer

samples from the control subplots and the wood-ash subplots. To determine the depth distribution of organic contaminant concentrations, soil samples from one control subplot were used.

### 6.3.2 Sampling procedure

The sampling procedure included an experiment to stain the preferential flow paths in the soil. With a field sprinkler we applied 45 mm of de-ionized water containing 3 g of the food dye Brilliant Blue (CI 42090) per liter in 6 h (Flury and Flühler, 1994a, b). One day after dye application, we opened a trench to 1.2 m depth. A vertical soil profile of 1 by 1 m was prepared 0.3 m away from the plot's border. Photos were taken to estimate the dye coverage of each profile. These were used to determine the volumetric proportions of preferential flow paths and soil matrix. The blue stained areas were defined as preferential flow paths, the non stained areas as soil matrix. As a mean of 40 profile photos, we calculated the volumetric proportions of preferential flow paths as 74, 34, 9, and 1% in 0 to 9, 9 to 20, 20 to 50, and 50 to 100 cm depth, respectively. With a small spatula we took samples of the preferential flow paths and of the matrix at various locations distributed over the whole width and depth of the horizon (0-9 cm). Additionally, we took representative bulk soil samples. For the depth distribution of PAHs and PCBs, soil material from 0 to 9, 9 to 20, 20 to 50, and 50 to 100 cm depths was sampled. In April 1998, we sampled the total organic layer ("bulk organic layer") and in May 1999 we sampled Oi, Oe, and Oa horizons separately.

### 6.3.3 Sample preparation and analyses

Soil samples were oven-dried (45°C), sieved (2 mm) and stored in closed polythene bags until analysis. Minor sorption of PAHs and PCBs to the plastic may have occurred but is considered negligible. Total C and N concentrations were measured with a CN auto analyzer (NA 1500 and 2500, Carlo Erba Instruments, Milano, Italy).

We quantified 20 PAHs and 14 PCBs: naphthalene (NP), acenaphthylene (ACY), acenaphthene (ACE), fluorene (FLU), phenanthrene (PHE), anthracene (ANT), fluoranthene (FLA), pyrene (PYR), benz(a)anthracene (BAA), chrysene+triphenylene (CT), benzo(b+j+k)fluoranthenes (BBJK), benzo(a)pyrene (BAP), benzo(e)pyrene

(BEP), perylene (PER), indeno(1,2,3-cd)pyrene (IND), dibenz(a,h)anthracene (DBAH), benzo(ghi)perylene (BGHI), and the PCB congeners 1, 8, 20, 28, 52, 35, 101, 118, 138, 153, 180, 199, 206, and 209 (numbers according to Ballschmiter and Zell, 1980).

The air-dried and homogenized samples were extracted with hexane/acetone 2:1 in an Accelerated Solvent Extractor (Dionex ASE 200, Dionex Co., Sunnyvale, USA) as described in Krauss et al. (2000). All samples were purified with a column filled with aluminum oxide and silica. Details of the purification procedure are found in Wilcke et al. (1999a). Extracts containing a high amount of waxes, which interfered with PER and IND signals in mass-selective detection, were further purified using columns filled with 1 g HR-P resin (polystyrene-divinylbenzene copolymer, Macherey-Nagel, Dueren, Germany). Aliphatic compounds were eluted with 10 mL hexane, PAHs were eluted with 20 mL toluene. For the determination of PCBs, the extracts were additionally purified with an acid-base-silica column (Wilcke et al., 1999b).

A Hewlett-Packard 5890 Series II gas chromatograph equipped with a Hewlett-Packard 5-MS fused silica capillary column (30 m x 0.25 mm x 0.25  $\mu$ m) was used with He as carrier gas (constant pressure mode 80 kPa) and splitless injection. Compounds were detected with a Hewlett Packard 5971 A mass selective detector with electron impact ionization in selected ion monitoring mode. Details of the GC program are given in Wilcke et al. (1999a) for PAHs and in Wilcke et al. (1999b) for PCBs.

Eight deuterated PAHs (NP-D<sub>8</sub>, ACE-D<sub>10</sub>, FLU-D<sub>10</sub>, ANT-D<sub>10</sub>, PYR-D<sub>10</sub>, chrysene-D<sub>12</sub>, PER-D<sub>12</sub>, BGHI-D<sub>12</sub>) and seven <sup>13</sup>C-labelled PCBs (congeners 28, 52, 101, 138, 153, 180, 209) were used as internal standard for quantification and spiked to the soil samples prior to extraction. To check the recovery of the internal standards and thus the quality of the analytical procedure, fluoranthene-D<sub>10</sub> was spiked to the extracts prior to injection into the gas chromatograph. The average recoveries and standard deviations of the internal standards ranged from 74±18 % to 93±16 % (n= 94, silica-alox cleanup) and 48±17 % to 85±10 % (n= 36, HR-P cleanup) for the PAHs and from 83±13 % to 91±11 % (n=125) for PCBs. Details on the principle of the quantification method are e.g. found in Kjeller (1998). The influence of background contamination as determined with seven blanks was negligible.

### 6.3.4 Calculations and statistical analyses

The increase/ decrease in storage of PAHs and PCBs was calculated using the following equation

$$\Delta storage_x = \sum_{h=1}^n (C_{h,ash} - C_{h,control}) \cdot \Delta z_h \cdot \rho_h \quad (1)$$

with  $\Delta storage_x$  being the increase/decrease in storage of  $x$ = PAHs or PCBs,  $h$  being the number of horizons, for which the storage was calculated,  $c_h$  the concentration of organic contaminants in the respective horizon one year after the wood ash application (“ash”) and without wood ash (“control”),  $\Delta z_h$  the thickness of the horizon  $h$ , and  $\rho_h$  its bulk density.

The differences in PAH and PCB concentrations between preferential flow paths and soil matrix and between the control and the wood ash treatments were tested with Analysis of variance (Conover, 1980) using the software S+ (Version 3.0, MathSoft, Seattle).

## 6.4 Results and Discussion

### 6.4.1 Concentrations of PAHs and PCBs before the wood ash application

Before the wood ash application, the concentrations of PAHs in the bulk organic layer ranged between 815 and 1640  $\mu\text{g kg}^{-1}$  with a mean of 1230  $\mu\text{g kg}^{-1}$ . The PAH concentrations in the control plots did not change significantly during the experimental period of one year. The PAH concentrations are comparable to those of other temperate forests in Europe (Wilcke, 2000). Within the organic layer, PAH concentrations showed a slight increase (approximately 10%) from the Oi to the Oe and the Oa horizon (Table 6.2). In the mineral soil, the sum of 20 PAH ( $\Sigma 20$  PAH) concentrations was lower than in the organic layer. The fraction of low molecular PAHs (LMPAH: NP, ACY, ACE, FLU, PHE, ANT) decreased from the Oi-horizon to the Oa-horizon and increased slightly in the A horizon (Table 6.2), which is consistent with other studies (Pichler et

al., 1996; Wilcke and Zech, 1997; Krauss et al., 2000). The increase of PAH concentrations and decrease of the fraction of LMPAHs with depth in the organic layer is explained by the faster mineralization of organic matter than of PAHs and by preferential degradation and leaching of the LMPAHs.

**Table 6.2:** Mean concentrations  $\pm$  standard errors of  $C_{org}$ ,  $\Sigma 20$  PAHs, and  $\Sigma 14$  PCBs in the organic layer and the A horizons one year after application of  $8 \text{ Mg ha}^{-1}$  wood ash and of the control plots ( $n=4$ ). In parenthesis the percentage of low-molecular weight PAHs (LMPAHs) and lower chlorinated PCBs (LCPCBs) is given.

Horizon	depth [cm]	$C_{org}$ [g kg <sup>-1</sup> ]	$\Sigma 20$ PAH [ $\mu\text{g kg}^{-1}$ ]		$\Sigma 14$ PCB [ $\mu\text{g kg}^{-1}$ ]	
			control	wood ash	control	wood ash
Oi	+2.2	425	1250 $\pm$ 330 (49)	1390 $\pm$ 270 (46)	25.4 $\pm$ 5 (47)	21.1 $\pm$ 5 (43)
Oe	+1.7	368	1350 $\pm$ 120 (42)	7660 $\pm$ 2960 (30)	33.1 $\pm$ 3 (31)	21.3 $\pm$ 4 (40)
Oa	+0.5	212	1390 $\pm$ 220 (38)	8050 $\pm$ 4120 (29)	32.5 $\pm$ 8 (27)	33.7 $\pm$ 5 (26)
A	0-9	27	527 $\pm$ 81 (40) <sup>a</sup>	492 $\pm$ 97 (47)	5.5 $\pm$ 0.5 (29) <sup>a</sup>	6.0 $\pm$ 1 (18)

a: Data are from April 1998, before the wood ash application.

Before the wood ash application, the sum of 14 PCB ( $\Sigma 14$  PCB) concentrations in the bulk organic layer ranged between 21.7 and 48.8  $\mu\text{g kg}^{-1}$  with a mean of 35.3  $\mu\text{g kg}^{-1}$ . This is considerably higher than values in forest soils in southern Germany (Krauss et al., 2000). The increase in the  $\Sigma 14$  PCB concentrations from the Oi to the Oe and Oa horizon was approximately 30% (Table 6.2). Similarly to the PAH concentrations, the PCB concentrations in the mineral soil were substantially lower than in the organic layer. As for LMPAHs, there was a decrease of the fraction of lower chlorinated PCBs (LCPCBs: PCB congeners 1, 8, 20, 28, 52, 35) in the order Oi>Oe>Oa horizon. Lower chlorinated PCBs are more easily degradable, more volatile and more water-soluble than the higher chlorinated PCBs, which can hardly be degraded by microorganisms (Hankin and Sawheney, 1984; Mackay et al., 1992). Therefore, higher chlorinated PCBs become relatively enriched with increasing degradation of soil organic matter.



#### 6.4.2 PAHs and PCBs in the wood ash

There is little information in the literature about concentrations of PAHs and PCBs in wood ash. Although PAHs are formed during the combustion process and high concentrations were measured in fumes and particles emitted from wood fires (Freeman and Cattell, 1990; Baek et al., 1991), the ash itself was seldom studied. In the wood ash used in our experiment, the  $\Sigma 20$  PAH concentration was  $16.8 \text{ mg kg}^{-1}$ . This was rather high and nearly reached the proposed threshold value of  $20 \text{ mg kg}^{-1}$  for the application of secondary materials to agricultural field soils (Zollner, et al., 1997). It was also high compared with the concentrations in the forest soil (Table 6.2, Figure 6.2), and with annual deposition rates. These were estimated to be  $2$  to  $4 \text{ mg m}^{-2} \text{ yr}^{-1}$  for Germany and approximately  $0.8 \text{ mg m}^{-2} \text{ yr}^{-1}$  for the UK (Führ et al., 1986; Wild and Jones, 1995). Therefore, the PAH input with  $8 \text{ Mg wood ash ha}^{-1}$  (Table 6.3) equals approximately 3 to 16 times the annual deposition rate.

**Table 6.3:** Range and mean storage, input with wood ash, and increase/ decrease ( $\Delta$  storage) after wood ash application of  $\Sigma 20$  PAHs and  $\Sigma 14$  PCBs in the organic layer and in the A horizon ( $n=4$ ).

	$\Sigma 20$ PAHs (range)	$\Sigma 20$ PAHs (mean)	$\Sigma 14$ PCBs (range)	$\Sigma 14$ PCBs (mean)
	[ $\text{mg m}^{-2}$ ]		[ $\mu\text{g m}^{-2}$ ]	
Storage in org. layer	5.1 to 7.6	6.3	125 to 183	146
Storage in A horizon	39.8 to 74.5	53.6	464 to 696	563
Input with wood ash		13.4		3
$\Delta$ storage in organic layer	11.8 to 49.8	24.9	-92 to +10	-34
$\Delta$ storage in A horizon	-13.4 to +4.5	-3.6	-120 to +395	+45

The concentrations of  $\Sigma 14$  PCBs in the wood ash of  $3.4 \mu\text{g kg}^{-1}$  were low compared with other soil amendments such as sewage sludge and compost with concentrations of  $1200$  to  $1600 \mu\text{g kg}^{-1}$  and  $260 \mu\text{g kg}^{-1}$ , respectively (Fiedler, 1993). They were in the same order of magnitude as the mineral topsoil (Table 6.2). The PCBs 199, 206, and 209 could not be detected in the wood ash. Annual deposition rates for rural soils in the

UK were estimated to be  $14 \mu\text{g m}^{-2} \text{yr}^{-1}$  as the  $\Sigma 8$  PCBs and  $48 \mu\text{g m}^{-2} \text{yr}^{-1}$  as the  $\Sigma 44$  PCBs (Harrad, et al., 1994). Thus, the input of  $3 \mu\text{g m}^{-2}$  with the wood ash (Table 6.3) was small in comparison with annual deposition rates in rural areas.

#### 6.4.3 Effects of wood ash application

In the organic layer, the PAH concentrations were significantly increased ( $P < 0.05$ ) one year after wood ash application in all of the four plots (Table 6.2, Figure 6.2). The increase was most pronounced in the Oe and Oa horizon. The small change in the Oi horizon is not astonishing, since most of the leaves, twigs, and needles of the Oi horizon sampled in May 1999 reached the forest floor in autumn 1998, half a year after the wood ash application.

The PAH spectra of the three organic layers of the control plots were dominated by PHE and to a slightly smaller extent by FLA, BBJK, NP, PYR, and CT (Figure 6.2). One year after the wood ash application, the spectra were still similar as before in the Oi horizon, but in the Oe and Oa horizon, they approached the wood ash spectrum (Figure 6.2). The total input of PAHs with the wood ash was  $13.4 \text{ mg m}^{-2}$ , while the increase in storage of the organic layer was  $24.9 \text{ mg m}^{-2}$  (Table 6.3). This large increase, however, was mainly due to the high storage increase of one of the four plots, which we cannot explain. Possibly, the plot was contaminated with PAHs from other sources than the experimental wood ash application. Omitting this plot, the increase in PAH storage in the organic layer was  $12.5 \text{ mg m}^{-2}$ , corresponding well to the wood ash input. The input of individual PAHs with the wood ash significantly correlated with the increase in storage in the organic horizons (Figure 6.3). This strongly suggests that the PAHs, which were applied to the forest soil with the wood ash, were stored efficiently in the organic layer without much alteration in the course of one year. Consistently, total PAH concentrations in the A horizon were not significantly ( $P = 0.15$ ) affected by the wood ash application (Table 6.2). Our findings agree well with those of Deschauer (1995), who found that two years after compost application to a forest soil, the added PAHs were mainly retained in the organic layer and were not recovered in the soil solution or in mineral soil horizons.

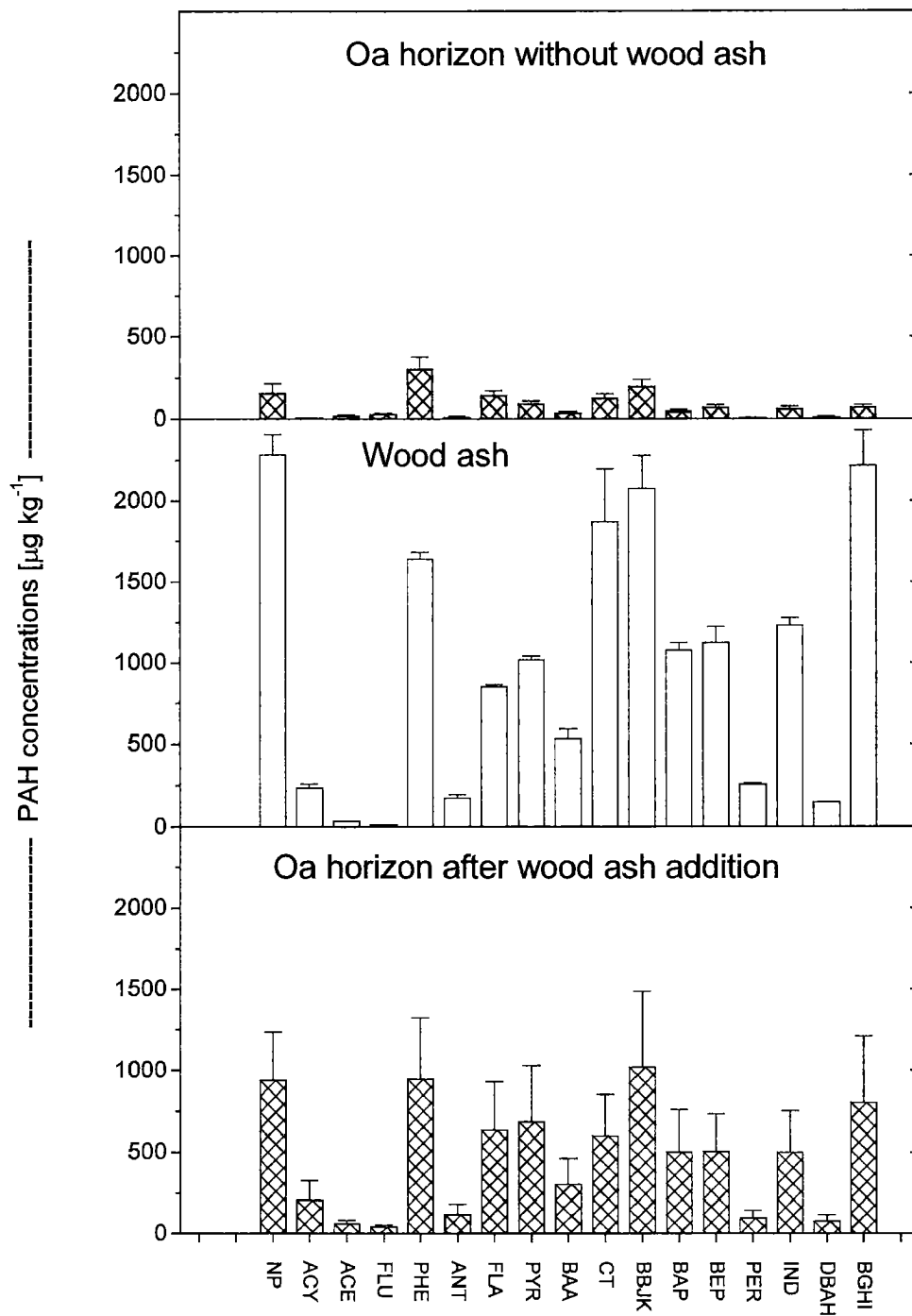


**Figure 6.2:** PAH spectra of the Oa horizon from the control plots, of the wood ash, and of the Oa horizon one year after the wood ash application.

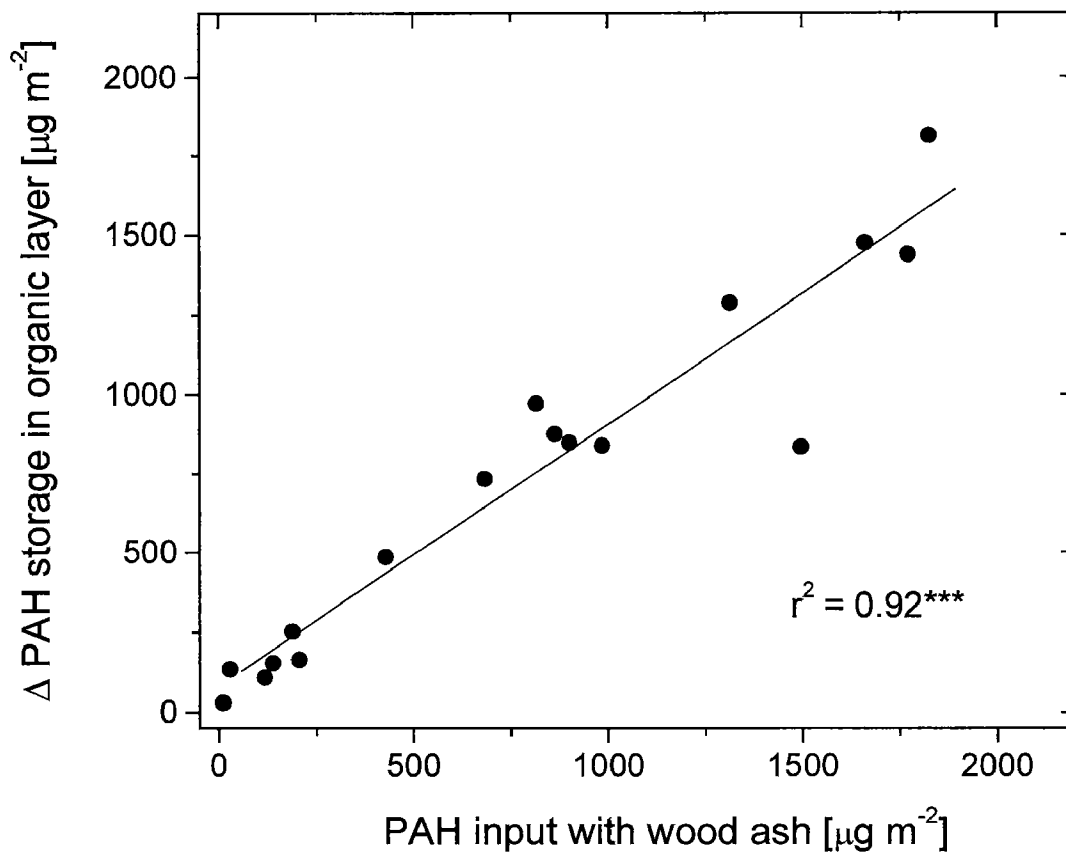


**Figure 6.3:** Correlation between the input rates of individual PAHs with the wood ash and the increase in storage ( $\Delta$ storage) in the organic layer without the outlier plot (see text).

Although the  $\Sigma 20$  PAH concentrations remained almost constant, the fraction of LMPAH increased in the A horizon after wood ash application. This was mainly due to naphthalene, which contributed the largest proportion (14 %) of all individual PAHs to the  $\Sigma 20$  PAH concentrations in the wood ash. Naphthalene is rather mobile in the soil and was probably leached through the organic layer into the mineral topsoil. At 0-9 cm depth, PHE, FLA, and BBJK showed the strongest decrease after the wood ash

application. This might be due to facilitated transport with dissolved organic matter into deeper soil layers (McCarthy and Zachara, 1989).

In contrast to PAHs, PCB concentrations were decreased in the organic layer of the wood ash plots (1 y after wood ash application) compared with the control plots (Table 6.2). Despite an input of  $3 \mu\text{g PCBs m}^{-2}$ , the  $\Sigma 14$  PCB storage in the organic layer decreased by  $34 \mu\text{g m}^{-2}$  or by  $3 \mu\text{g m}^{-2}$  when omitting the same plot as above for PAHs from the calculation (Table 6.3). The data are quite variable, but the decrease was consistent for all plots in the Oe horizon. Of particular interest was the decrease of higher chlorinated PCBs in the Oe horizon. These compounds are hardly degradable by microorganisms under aerobic conditions and are not volatile (Hankin and Sawheney, 1984; Dmochewitz and Ballschmiter, 1988; Abramowicz, 1990). Therefore, the decrease was probably due to transport into the mineral soil. Since the concentration of PCBs in the wood ash was small in comparison to the concentrations already stored in the organic layer, the spectrum of the PCBs changed only in the Oe horizon slightly after the wood ash application (Figure 6.4).

In the mineral soil, changes of PCB concentrations due to the wood ash application were not detectable. Even under the assumption that all PCBs imported with the wood ash ( $3 \mu\text{g m}^{-2}$ ) and the total PCB loss in the organic layer ( $-34 \mu\text{g m}^{-2}$ ) were retained in the Ah horizon, these potential inputs are small compared to the PCB storage of  $560 \mu\text{g m}^{-2}$ .

While adding wood ash to the forest soil increased the storage of PAHs in the organic layer without much alteration during one year, PCBs, which were stored in the organic layer of the forest soil, were mobilized and transported to deeper depths, or degraded. This was probably due to the enhanced mineralization after the wood ash application and/or due to a pH effect. The alkaline wood ash increased the pH in percolating water below the organic layer to above 9 two weeks after the wood ash application and increased concentrations of dissolved organic matter (S. Zimmermann, WSL, pers. comm.). However, the effects on PCBs were mostly restricted to the organic layer, and were not detectable in the mineral soil.

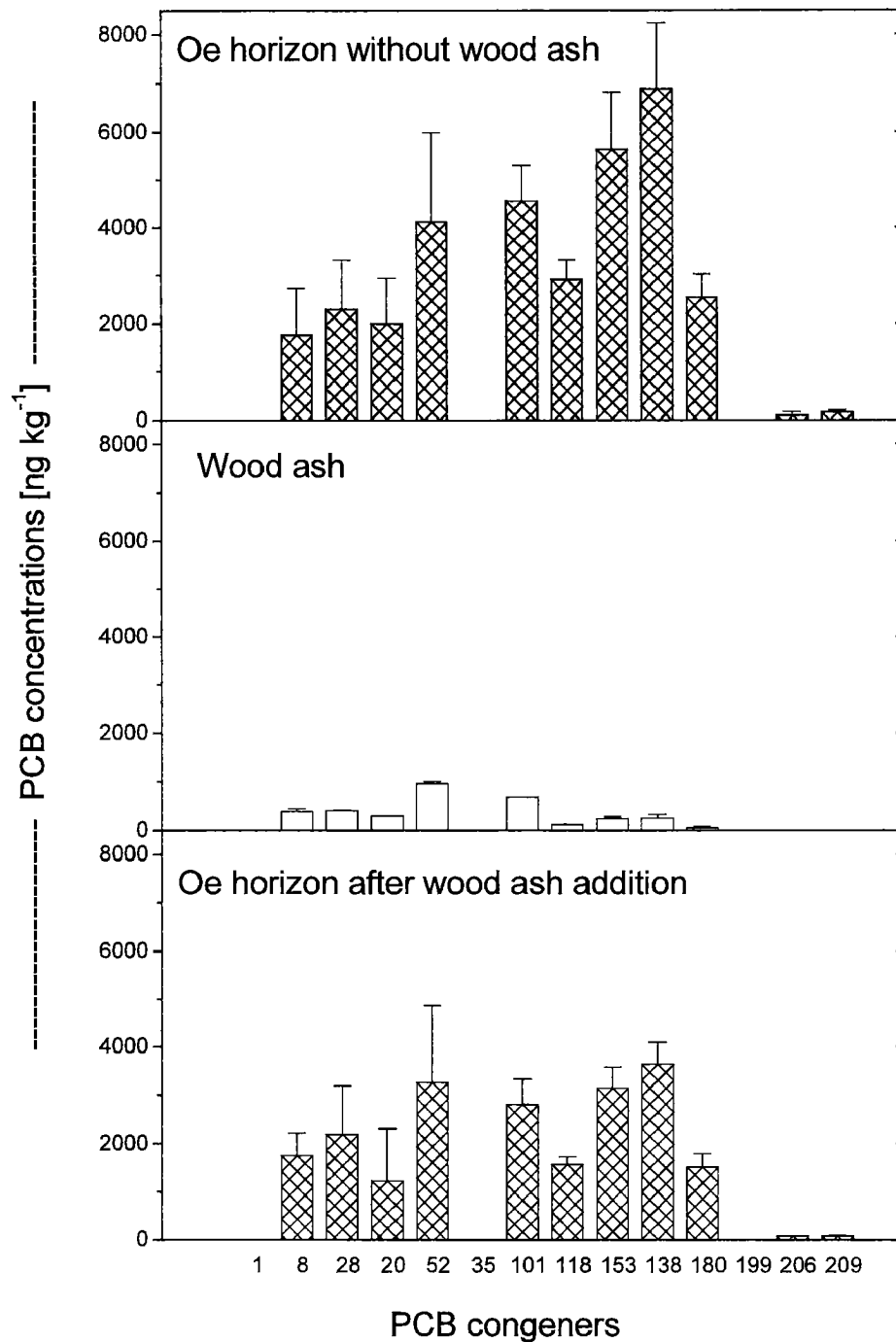


**Figure 6.4:** PCB spectra of the Oe horizon from the control plots, of the wood ash, and of the Oe horizon one year after the wood ash application.

#### 6.4.4 Distribution and dynamics

In the mineral soil, the  $\Sigma 20$  PAH concentrations was higher in the preferential flow paths than in the matrix at all of the studied depths, except for the 50 to 100 cm layer (Table 6.4). The higher PAH concentrations in the preferential flow paths down to 50 cm were most likely due to the higher input into these zones. However, preferential flow paths are also zones of preferential leaching and degradation, which limits the size of the concentration gradient between preferential flow paths and matrix. The preferential degradation can be attributed to a higher microbial biomass in the preferential flow paths than in the soil matrix of the studied forest soil (Chapter 4). Consistently, other authors also reported enhanced degradation of organic substances such as pesticides in macropores as compared to the soil matrix (Pivetz and Steenhuis, 1995; Mallawatantri et al., 1996). The lower  $\Sigma 20$  PAH concentrations in the preferential flow paths than in the matrix of the subsoil (50 to 100 cm) may be the result of higher degradation than input rates. This assumption is supported by the overall low mobility of PAHs in soils (Jones et al., 1989; Guggenberger et al., 1996; Krauss, et al., 2000).

**Table 6.4:** Concentrations of  $\Sigma 20$  PAHs and concentrations of  $\Sigma 14$  PCBs in the preferential flow paths and in the matrix of the mineral soil of one of the control plots. In parenthesis the percentage of low-molecular weight PAHs (LMPAHs) and lower chlorinated PCBs (LCPCBs) is given.

depth [cm]	$\Sigma 20$ PAH [ $\mu\text{g kg}^{-1}$ ]		$\Sigma 14$ PCB [ $\text{ng kg}^{-1}$ ]	
	flow paths	matrix	flow paths	matrix
0-9	918 (52)	818 (54)	5196 (23)	3552 (21)
9-20	492 (81)	476 (81)	1614 (54)	1599 (49)
20-50	428 (92)	385 (86)	1040 (64)	1052 (65)
50-100	230 (92)	680 (93)	936 (65)	1237 (58)

The difference between the two flow regions was for all individual PAHs and for the  $\Sigma 20$  PAH concentrations significant ( $P < 0.05$ ), except for perylene. The distribution of PAHs between preferential flow paths and matrix was controlled by the octanol-water

partition coefficient ( $K_{ow}$ ). This was indicated by the increasing ratio of individual PAH concentrations in the preferential flow paths to those in the matrix at 0-9 cm depth with increasing  $K_{ow}$  of the compounds (Figure 6.5a). After wood ash application, the slope of the regression line between  $K_{ow}$  and the ratio of PAH concentrations between preferential flow paths and matrix increased. This was due to higher concentration ratios for the higher molecular weight PAHs with high  $K_{ow}$  values, while the concentration ratios for the LMPAHs with lower  $K_{ow}$  values remained rather stable. There may be three reasons for our finding: (1) the leaching of the more mobile LMPAHs to greater depths, (2) the enhanced degradation of LMPAHs in preferential flow paths, and (3) the preferential sorption of PAHs with a higher affinity to soil organic matter in the preferential flow paths, since SOM is enriched in these flow regions (Table 6.1).

The concentrations of PCBs at 0-9 cm depth were higher in preferential flow paths as compared to the soil matrix (Table 6.4). At 9-50 cm depth, no differences in PCB concentrations between preferential flow paths and soil matrix were observed, while at 50-100 cm depth, the matrix had higher PCB concentrations than the preferential flow paths. Thus, in the upper part of the mineral soil, PCB input rates in the preferential flow paths were higher than leaching and degradation rates, while in the subsoil the opposite was true. This can be due to the transport pathways being blocked at that depth and organic contaminants being laterally dispersed into the matrix, or due to higher degradation rates in the preferential flow paths at 50-100 cm depth. Similar to the PAHs, the ratio of PCB concentrations in preferential flow paths and in the matrix increased linearly with the  $\log K_{ow}$  of the compounds (Figure 6.5b). However, unlike the PAHs, the slope of the regression line did not change one year after the wood ash application. This may be explained by the negligible input of PCBs into the mineral soil after the wood ash application compared with the PCB storage.



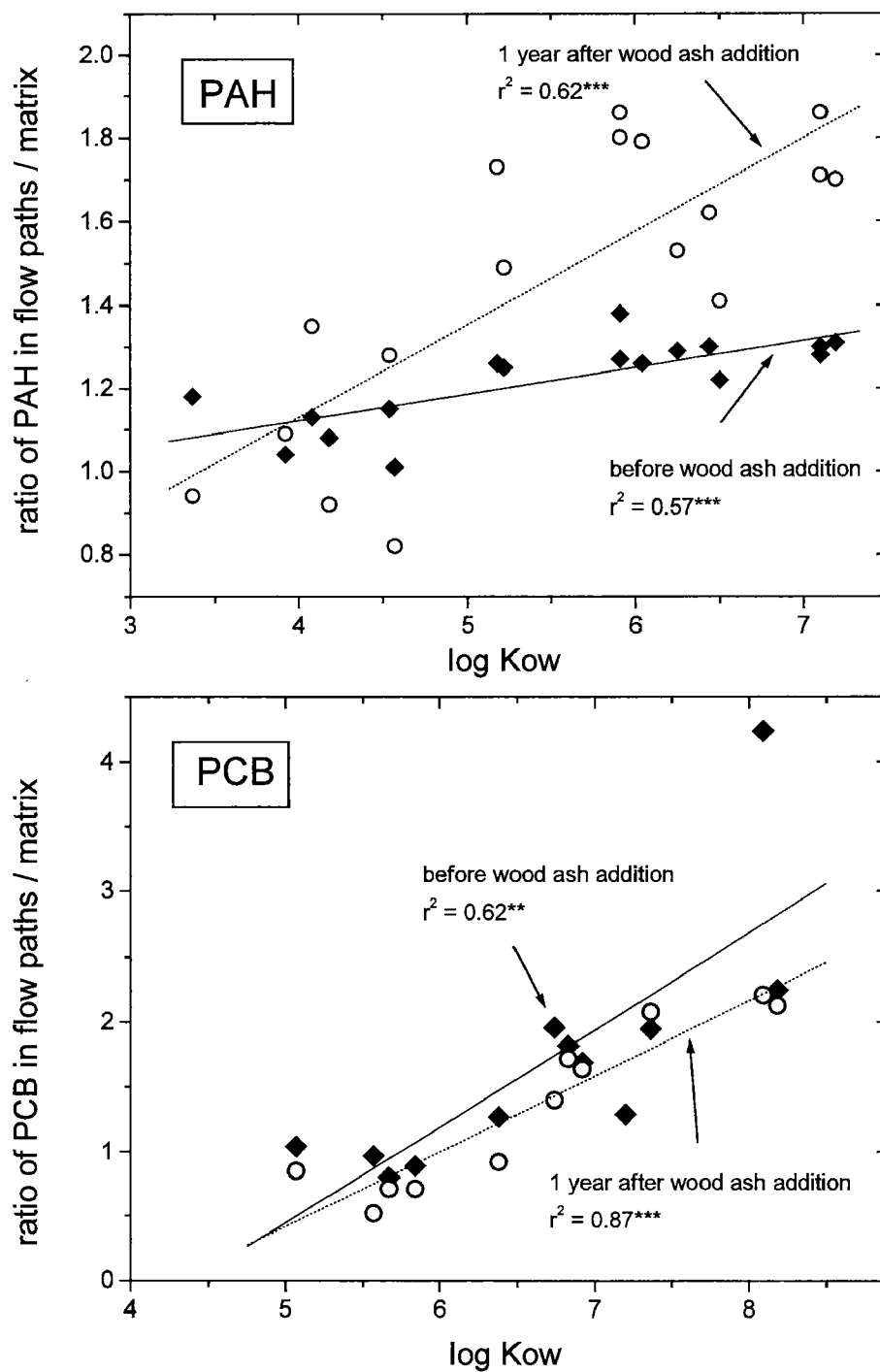


**Figure 6.5:** Relationship between the octanol-water partition coefficient ( $\log K_{ow}$ ) value of the compounds (Mackay et al., 1992; Hawker and Connell, 1988) and the concentration ratio between the individual PAHs and PCBs in the preferential flow paths and in the matrix of the A horizon (0 to 9 cm).

## 6.5 Conclusions

Prior to the experiment, the studied forest soil had moderate PAH concentrations and high PCB concentrations when compared with the literature. Wood ash application to the forest soil resulted in considerable inputs of organic contaminants, particularly of PAHs. The effects of the wood ash application however were not only confined to the direct inputs, but also to a re-mobilization and re-translocation of PAHs and PCBs after the wood ash application. While PAHs were effectively retained in the organic layer and infiltrated only to a small extent into the mineral soil, PCB concentrations even decreased in the organic layer after wood ash application, probably due to mobilization and leaching of stored compounds into the mineral soil.

Both contaminant classes, in particular their high molecular weight representatives, were accumulated in the preferential flow paths of the A horizon compared with the soil matrix. The enrichment resulted from the higher input into the preferential flow regions and was present in spite of the higher leaching rates in the preferential flow paths and most likely also higher degradation rates. At greater soil depth, degradation or leaching became increasingly more important than accumulation in the preferential flow paths, resulting in lower concentrations in the preferential flow paths than in the matrix in the 50 to 100 cm depth layer. Our results strongly suggest that in the mineral soil, preferential flow paths represent the “active” and accessible regions for contaminants, whereas organic contaminants stored in the soil matrix probably exhibit slower transport and turnover rates.

## 6.6 References

- Abramowicz, D.A. 1990. Aerobic and anaerobic biodegradation of PCBs - a review. *Biotech.*: 241-251.
- Baek, S.O., R.A. Field, M.E. Goldstone, P.W. Kirk, J.N. Lester, and R. Perry. 1991. A review of atmospheric polycyclic aromatic hydrocarbons: sources, fate, and behavior. *Water Air Soil Pollut.* 60: 279-300.
- Ballschmiter, K., and M. Zell. 1980. Analysis of polychlorinated biphenyls (PCB) by glass capillary gas chromatography. *Fresenius Z. Anal. Chem.* 302: 20-31.
- Berteigne, M., Y. Lefèvre, and C. Rose. 1988. Accumulation de polluants organiques (H.P.A.) dans le horizons humifères des sols. *Eur. J. For. Path.* 18: 310-318.
- Chiou, C.T., R. Malcolm, L., T.I. Brinton, and D.E. Kile. 1986. Water solubility enhancement of some organic pollutants and pesticides by dissolved humic and fulvic acids. *Environ. Sci. Technol.* 20: 502-508.
- Conover, W.J. 1980. *Practical nonparametric statistics*. Wiley, New York.
- Deschauer, H. 1995. Eignung von Bioabfallkompost als Düngung im Wald. *Bayreuther Bodenkundliche Berichte* 43, Bayreuth.
- Dmochewitz, S., and K. Ballschmiter. 1988. *Chemosphere* 17: 111-121.
- Fiedler, H. 1993. PCDD/PCDF und PCB: Quellen, Vorkommen in der Umwelt. pp. 7-38. *In* Hutzinger O., and H. Fiedler (eds.) *Organohalogen compounds* 16. ECOINFORMA-press, Nürnberg.
- Flury, M., and H. Flühler. 1994a. Brilliant Blue FCF as a dye tracer for solute transport studies- A toxicological overview. *J. Environ. Qual.* 23: 1108-1112.
- Flury, M., and H. Flühler. 1994b. Susceptibility of soils to preferential flow of water: A field study. *Water Resour. Res.* 30: 1945-1954.
- Freeman, D.J., and F.C.R. Cattell. 1990. Woodburning as a source of atmospheric polycyclic aromatic hydrocarbons. *Environ. Sci. Technol.* 24: 1581-1585.
- Führ, F., H. Scheele, and G. Kloster. 1986. Schadstoffeinträge in den Boden durch Industrie, Besiedlung, Verkehr und Landwirtschaft (organische Stoffe). *VDLUFA-Schriftenreihe* 16: 73-84.
- Ghodrati, M., and W.A. Jury. 1992. A field study of the effects of soil structure and irrigation method on preferential flow of pesticides in unsaturated soil. *J. Contam. Hydrol.* 11: 101-125.
- Guggenberger, G., M. Pichler, R. Hartmann, and W. Zech. 1996. Polycyclic aromatic hydrocarbons in different forest soils: Mineral horizons. *Z. Pflanzenernähr. Bodenk.* 159: 565-573.
- Hankin, L., and B.L. Sawheney. 1984. Microbial degradation of polychlorinated biphenyls in soil. *Soil Sci.* 137: 401-407.
- Harrad, S.J., A.P. Sewart, R. Alcock, R. Boumphrey, V. Burnett, R. Duarte-Davidson, C. Halsall, G. Sanders, K. Waterhouse, S.R. Wild, and K.C. Jones. 1994.

- Polychlorinated biphenyls (PCBs) in the British environment: sinks, sources and temporal trends. *Environ. Pollut.* 85: 131-146.
- Hawker, D.W., and D.W. Connell. 1988. Octanol-water partition coefficients of polychlorinated biphenyls congeners. *Environ. Sci. Tech.* 22: 382-387
- Jones, K.C., J.A. Stratford, K.S. Waterhouse, and N.B. Vogt. 1989. Organic contaminants in Welsh soils: Polynuclear aromatic hydrocarbons. *Environ. Sci. Technol.* 23: 540-550.
- Kjeller, L.-O. 1998. Addition of internal standards to particulate sample matrices for routine trace analyses of semivolatile organic compounds; a source of systematic and random errors. *Fresenius J. Anal. Chem.* 361: 791-796.
- Krauss, M., W. Wilcke, and W. Zech. 2000. Polycyclic aromatic hydrocarbons and polychlorinated biphenyls in forest soils: depth distribution as indicator of different fate. *Environ. Pollut.* 110: 79-88.
- Lamersdorf, N. 1985. Der Einfluß von Düngungsmaßnahmen in einem Buchen- und einem Fichtenökosystem des Sollings. *Allg. Forst Z.* 43: 1155-1158.
- Mackay, D., W.Y. Shiu, and K.C. Ma. 1992. Illustrated handbook of physical-chemical properties and environmental fate for organic chemicals, Vol I: Monoaromatic hydrocarbons, chlorobenzenes, and PCBs. Lewis Publishers, Boca Raton.
- Mallawatantri, A.P., B.G. McConkey, and D.J. Mulla. 1996. Characterization of pesticide sorption and degradation in macropore linings and soil horizons of Thatuna silt loam. *J. Environ. Qual.* 25: 227-235.
- Marschner, B. 1995. Wirkungen von Kalkungen auf Bodenchemismus und Stoffausträge. *Allg. Forst Z.* 17: 932-935.
- Marschner, B. 1999. Sorption von polycyclischen aromatischen Kohlenwasserstoffen (PAK) und polychlorierten Biphenylen (PCB) im Boden. *J. Plant Nutr. Soil Sci.* 162: 1-14.
- Matzner, E. 1984. Annual rates of deposition of polycyclic aromatic hydrocarbons in different forest ecosystems. *Water Air Soil Pollut.* 21: 425-434.
- McCarthy, J.F., and J.M. Zachara. 1989. Subsurface transport of contaminants. *Environ. Sci. Technol.* 23: 496-502.
- Noger, D., H. Felber, and E. Pletscher. 1996. Verwertung und Beseitigung von Holzaschen. Schriftenreihe Umwelt 269. Bundesamt für Umwelt, Wald und Landschaft, Bern.
- Pichler, M., G. Guggenberger, R. Hartmann, and W. Zech. 1996. Polycyclic aromatic hydrocarbons (PAH) in different forest humus types. *Environ. Sci. Pollut. Res.* 3: 24-31.
- Pierret, A., C.J. Moran, and C.E. Pankhurst. 1999. Differentiation of soil properties related to the spatial association of wheat roots and soil macropores. *Plant Soil* 211: 51-58.
- Pivetz, B.E., and T.S. Steenhuis. 1995. Soil matrix and macropore biodegradation of 2,4-D. *J. Environ. Qual.* 24: 564-570.

- Schierl, R., A. Göttlein, E. Hohmann, D. Trübenbach, and K. Kreutzer. 1986. Einfluß von saurer Beregnung und Kalkung auf Humusstoffe sowie die Aluminium- und Schwermetалldynamik in wässrigen Bodenextrakten. *Forstwiss. Zbl.* 105: 309-313.
- Sims, R.C., and M.R. Overcash. 1983. Fate of polynuclear aromatic compounds (PNAs) in soil-plant systems. *Res. Rev.* 88: 1-68.
- Soil Survey Staff. 1994. *Keys to Soil Taxonomy*. 6<sup>th</sup> edn. US Department of Agriculture. Pocahontas Press, Pittsburgh.
- Sollins, P., and R. Radulovich. 1988. Effects of soil physical structure on solute transport in a weathered tropical soil. *Soil Sci. Soc. Am. J.* 52: 1168-1173.
- Vance, E.D. 1996. Land application of wood-fired and combination boiler ashes: An overview. *J. Environ. Qual.* 25: 937-944.
- Vinther, F.P., F. Eiland, A.-M. Lind, and L. Elsgaard. 1999. Microbial biomass and numbers of denitrifiers related to macropore channels in agricultural and forest soils. *Soil Biol. Biochem.* 31: 603-611.
- Wilcke, W. 2000. Polycyclic aromatic hydrocarbons (PAHs) in soil - a review. *J. Plant Nutr. Soil Sci.* 163: 1-20.
- Wilcke, W., R. Bäumler, H. Deschauer, M. Kaupenjohann, and W. Zech. 1996a. Small scale distribution of Al, heavy metals and PAHs in an aggregated Alpine Podzol. *Geoderma* 71: 19-31.
- Wilcke, W., W. Zech, and J. Kobza. 1996b. PAH-pools in soils along a PAH-deposition gradient. *Environ. Pollut.* 92: 307-313.
- Wilcke, W., S. Müller, N. Kanachanakool, C. Niamskul, and W. Zech. 1999a. Polycyclic aromatic hydrocarbons (PAHs) in hydromorphic soils of the tropical metropolis Bangkok. *Geoderma* 91: 297-309.
- Wilcke, W., S. Müller, N. Kanachanakool, C. Niamskul, and W. Zech. 1999b. Urban soil contamination in Bangkok: concentrations and patterns of polychlorinated biphenyls (PCBs) in topsoils. *Aust. J. Soil Res.* 37: 245-254.
- Wilcke, W., and W. Zech. 1997. Polycyclic aromatic hydrocarbons (PAHs) in forest floors of the northern Czech mountains. *Z. Pflanzenernähr. Bodenk.* 160: 573-579.
- Wild, S.R., and K.C. Jones. 1995. Polynuclear aromatic hydrocarbons in the United Kingdom environment: A preliminary source inventory and budget. *Environ. Pollut.* 88: 91-108.
- Zollner, A., N. Remler, and H.-P. Dietrich. 1997. Eigenschaften von Holzaschen und Möglichkeiten der Wiederverwertung im Wald. *Berichte aus der Bayerischen Landesanstalt für Wald und Forstwirtschaft* 14, Freising.

## CHAPTER 7

### Synthesis

This study was conducted (1) to investigate biogeochemical aspects of preferential flow, (2) to observe the impact of an experimental wood ash application on a forest soil, and (3) to analyze the role of preferential flow for enhanced accessibility of nutrients and contaminants and accelerated leaching.

The study was conducted in a forest in Unterehrendingen, Switzerland. An infiltration experiment with a dye tracer identified the preferential flow paths in the soil. One day after the sprinkling, a soil profile was prepared and soil material from the stained preferential flow paths and from the unstained soil matrix was sampled and then analyzed.

#### 7.1 Persistence

The persistence of preferential flow paths is important for the generation of biological and chemical gradients between preferential flow paths and soil matrix and for solute transport and its mathematical modeling. However, since the visualization of preferential flow paths by dye infiltration experiments is destructive, it is difficult to assess the stability of preferential flow paths in the soil. Here, the experimental approach was to measure activities of atmospherically deposited radionuclides with a known deposition history, and to infer the age or stability of the preferential flow paths from the radionuclide distribution in the soil (Chapter 2).

Most of the  $^{137}\text{Cs}$  in the soil originates from the Chernobyl accident on 28 April 1986 and was deposited mainly as a single pulse input. In contrast,  $^{210}\text{Pb}$  input was continuous and more or less uniform, whereas Pu deposition stems from the global bomb fall out in the 1950's and 1960's.

The activities of the radionuclides  $^{137}\text{Cs}$ ,  $^{210}\text{Pb}$ ,  $^{239,240}\text{Pu}$ ,  $^{238}\text{Pu}$ , and  $^{241}\text{Am}$  were enriched in the preferential flow paths by a factor of up to 3.5. The similarity in their distributions in the soil in relation to the preferential flow paths suggests that the flow paths that were actively conducting water during the time of sampling in 1998 and 1999, were largely the same ones that were “active” over the course of decades. The  $^{137}\text{Cs}$  activities tracing the recent preferential flow paths point to their temporal stability of at least 13 y and the increased  $^{239,240}\text{Pu}$ ,  $^{238}\text{Pu}$ , and  $^{241}\text{Am}$  to their stability for over 40 y.

The enrichment of radionuclides in the preferential flow paths is consistent with the higher soil organic carbon (SOC) concentrations in these flow regions (Chapter 3). The enrichment of 800 to 1000 g C m<sup>-2</sup> was much larger than the annual contribution from potential sources like accelerated input of root-derived C and an increased illuviation of dissolved organic carbon (DOC). Calculations suggest that accumulation of SOC in the identified preferential flow paths lasted for periods of at least 10 years.

These findings indicate that preferential flow paths in the forest soil are temporally and spatially stable for decades. This implies (1) that biological and chemical gradients are likely to form and (2) that preferential flow of water and solutes must be incorporated into transport models.

## 7.2 Soil organic matter

Soil organic matter (SOM) plays a key role for the fertility, nutrient cycling, sorption properties, and microbial processes of forest soils. The results of Chapter 3 show that within a given soil horizon, organic matter concentrations were not evenly distributed. Preferential flow paths had higher organic C and total N concentrations compared to the rest of the soil.

Preferential flow paths were significantly depleted in  $^{13}\text{C}$  and  $^{15}\text{N}$  compared to the rest of the soil. This suggests that SOC from preferential flow paths was 'younger' than SOC from the soil matrix, pointing to an increased carbon input in the preferential flow paths.

The fate of an added  $^{15}\text{N}$ -tracer indicated that preferential flow paths are more strongly affected by external N inputs and that the turnover of N is more rapid in preferential flow paths than in the matrix.

### 7.3 Physico-chemical characteristics

The physico-chemical properties of the soil solid phase influence almost all biological or chemical processes, like plant uptake, microbial degradation, and mobilization or fixation of nutrients or pollutants. Preferential flow paths are chemically different from the soil matrix. They have a higher effective cation exchange capacity than the matrix and a higher effective base saturation, which can be attributed to the higher concentrations of SOM and to preferential inputs of neutral cations in these flow regions. No differences were found for pH, amorphous and crystalline Fe oxides, whereas Mn oxides and clay contents were higher in the matrix than in the preferential flow paths (Chapters 4 and 5). Concentrations of heavy metals and organic contaminants (polycyclic aromatic hydrocarbons and polychlorinated biphenyls) were enriched in the preferential flow paths as compared to the matrix. The enrichment stems from the higher input in the preferential flow paths and is present in spite of the higher leaching rates and most likely higher degradation rates.

### 7.4 Sorption

Sorption properties of the soil solid phase have severe implications for the transport of reactive solutes through the soil and for the storage of elements. While inorganic sorbents such as clay minerals or Fe oxides did not vary fundamentally between preferential flow paths and soil matrix (Chapter 5), the SOM enrichment along preferential flow paths was rather pronounced. Soil organic matter represents a particularly strong sorbent for many organic contaminants and heavy metals. In fact, an increased Cu sorption in the preferential flow paths was found, whereas the sorption of Sr was not greatly affected. One implication of the higher sorption capacity in the preferential flow paths is that the preferred transport of pollutants is counterbalanced by



an increased sorption. This is important when assessing leaching and the risk of groundwater contamination.

### **7.5 Microbial characteristics**

Preferential flow paths are more exposed to drying and wetting than the rest of the soil. Furthermore, they provide a better nutrient and substrate supply than the soil matrix. The overall favorable living conditions in preferential flow paths are reflected by a significantly higher microbial biomass (Chapter 4). Therefore, the turnover rates in the preferential flow paths are probably higher than in the soil matrix, which was directly shown for the added  $^{15}\text{N}$ -tracer (Chapter 3). Microbial community structures as measured by domain-specific genetic fingerprints did not differ between preferential flow paths and soil matrix. Only single genera such as *Pseudomonas* sp. developed specialized communities and adapted to the broader spectrum of substrates and changes in the environmental conditions. In general, our results suggest that the whole microbial community profit from the favorable living conditions along preferential flow paths.

### **7.6 Relevance for plant uptake**

The enrichment of nutrients, radionuclides, heavy metals, and organic contaminants in preferential flow paths have some direct implications for plant uptake, because the root biomass was also increased in the preferential flow paths (Chapters 2 and 3). In Switzerland, Germany, and Austria, soil-to-plant transfer models are widely used to estimate the plant activities after soil contamination with radionuclides. These models virtually mix the radionuclide deposition to a fixed depth, leading to extremely differing plant activities depending on the mixing depth. The heterogeneous radionuclide distribution in the soil and the more intense rooting in the preferential flow paths can be incorporated into soil-to-plant transfer models. This approach is more strongly based on physical and biological evidence than transfer models that use average bulk soil activities.

The increased plant uptake from the preferential flow paths as compared to the soil matrix was also directly shown for  $^{15}\text{N}$  (Chapter 3). After addition of a  $^{15}\text{N}$  tracer to the soil surface, the concentrations of  $^{15}\text{N}$  in the fine roots located in preferential flow paths was higher than in the fine roots taken from the soil matrix.

### 7.7 Effects of wood ash application

Wood ash application to a forest soil might be a suitable measure to replace nutrients exported with tree harvest and to dispose the wood ash cost-efficiently. Before wood ash can be safely used as a fertilizer in forests, effects of wood ash application on chemical properties of forest soils and negative effects such as input of organic contaminants or re-mobilization of already stored contaminants must be investigated.

Soil chemical properties were distinctly altered by the wood ash application of  $8 \text{ Mg ha}^{-1}$ . In the solid phase, the full effect of the wood ash application on pH and exchangeable elements was reached six months after adding the wood ash. One year after wood ash application, these effects already decreased and concentrations approached initial values. Therefore, the effects were not persistent. The soil solution reacted much faster and elemental concentrations reached peak values only two weeks after wood ash application. The application of  $8 \text{ Mg wood ash ha}^{-1}$  led to a re-mobilization of Al or heavy metals such as Pb. Thus, disposal of wood ash to contaminated forest soils represents a potential risk to the environment.

The studied forest soil exhibited a basic contamination with organic compounds that was moderate for polycyclic aromatic hydrocarbons (PAHs) and high for polychlorinated biphenyls (PCBs). Wood ash application to the forest soil was a further source of organic contaminants. The concentrations of PAHs in the wood ash were high, those of PCBs rather low. However, effects of the wood ash application were not only confined to the direct inputs, but also to a re-mobilization and re-translocation after the wood ash application. Here, PAHs and PCBs showed different fates in the soil. While PAHs were effectively retained in the organic layer, PCB concentrations decreased in the organic layer, probably due to mobilization and leaching of stored compounds into the mineral soil.

At our study site, only about half the soil volume in the upper soil horizons, i.e. the identified preferential flow paths, was affected by the wood ash application. Therefore,

only about half the soil volume was available to sorb and buffer incoming elements and acted as a storage compartment for the additional nutrients and contaminants applied with the wood ash. This must be considered when calculating the maximal amount of any addition of fertilizer, wood ash, or liming agent.

### **7.8 Future research and some open questions**

Although this thesis answers a few questions about preferential flow paths, it also opens a treasure chest full of interesting and important questions related to it. There are several points that would justify further investigations:

1. The stability and time invariance of preferential flow paths is one of the key issues, because it governs the formation of chemical and biological gradients and possibly justifies to consider flow patterns as site-specific features. Therefore, it is important to investigate this issue further.
2. Concerning the environmental impact of the findings presented here, root distribution in relation to soil structure and/or preferential flow paths is relevant and should be investigated further.
3. This study was designed to integrate over all causes for preferential flow and did not distinguish between preferential flow paths caused by different mechanisms. However, a more detailed study would yield additional information about the differences and similarities in biogeochemical processes in the different preferential flow paths, such as biopores, cracks or zones with continuously higher infiltration rates.
4. Also, it would be important to investigate the observed gradients at a smaller scale to obtain information about the conditions for and about their rate of formation.
5. In Chapter 4, it was shown, that the microbial community structure did not vary on the domain scale, but that a more in-depth analysis is necessary to detect differences between different flow regions within the same soil depths.
6. Last but not least, modeling the data might be an approach, to produce or extract information about exchange processes between preferential flow paths and the surrounding matrix, about the mean quantity of water flow in preferential flow paths, or yield better predictions about solute leaching in risk assessment models.

## CURRICULUM VITAE

MAYA BUNDT

- 1971            Born 25 January in San Francisco, USA
- 1977-1981     Primary School in Westerhof (Germany)
- 1981-1983     Pre-Gymnasium in Kalefeld (Germany)
- 1983-1990     Gymnasium Corvinianum Northeim (Germany)
- 1991-1996     Geoecology at the University of Bayreuth
- 1994           Research assistant at the Instituto de Café (ICAPE, Costa Rica)
- 1996           Diploma in Geoecology
- 1997-2000     PhD student at the Swiss Federal Institute of Technology (ETH) Zürich  
and research assistant at the Swiss Federal Institute for Forest, Snow, and  
Landscape Research (WSL) in Birmensdorf (Switzerland)